Antibiotic Interactions, Collateral Sensitivity, and the Evolution of Multidrug Resistance in *E. faecalis*

by

Ziah Dean

A dissertation submitted in partial fulfillment
of the requirements for the degree of
Doctor of Philosophy
(Biophysics)
in the University of Michigan
2018

Doctoral Committee:

Assistant Professor Kevin Wood, Chair
Associate Professor Julie S. Biteen
Professor Charles R. Doering
Professor Michal R. Zochowski

Ziah Dean

ziahdean@umich.edu

ORCID iD: 0000-0002-2288-5802

Dedication

This work is dedicated to my childhood friend Seyyid Kareem, who lost his life to land mines at a very young age, and to all children affected by war that is caused by the human desire for power and dominance. Although the specific details of this work are not related to this cause, the small attempt to contribute towards saving lives and gaining knowledge that could be of benefit to humanity is nevertheless relevant. The pen is indeed mightier than the sword and it is by the pen that peace can be spread.

Acknowledgements

I would like to first began by thanking God the source of Truth and Knowledge who allowed me the opportunity to explore a spec of the world that is before me. Although I could have been a more deserving student of knowledge, I intended to put forth my best effort. It is nonetheless our teachers who carry us through the fog and allow us to experience and gain new light. I am thus indebted to my academic advisor, Dr. Kevin Wood for his immense support, guidance and patience to bring my doctoral studies to a completion. It has been a great blessing and privilege to have been able to work with Dr. Wood and I will truly miss working closely with him.

I would also like to thank my fellow lab-mates Dr. Anupama Sharma, Dr. Wen Yu, Jeff Maltas, Jason Karslake, Kelsey Hallinen, Max De Jong, Keanu Guardiola, Kevin Liu Rodrigues, and Jiaming Zhang for all their companionship, feedback and support in the lab. I would especially like to thank two wonderful undergraduate interns Naji Kabbani and Zahra Arabzada who provided me excellent assistance in performing experiments and collecting data for parts of this dissertation. I am also grateful to my colleague on the journey Dr. Kristin Schimert who stood by me through many struggles along the way and with whom I am honored to have arrived at the completion of our PhD journey.

I would not have achieved any of this work without the tireless effort, care and love of my parents Salahuddin and Aziza Dean, and my siblings, Fardin, Sharaz and Dibah Dean who provided endless support and encouragement to pursue my passions and seek knowledge. I am

also very blessed with a large extended family who have all been a buttress to my educational journey.

Finally, I would like to express my sincere gratitude to my teachers of the heart, Imam Fode Drame and Ustadh Robert Abdul Hayy Darr, along with their gracious communities, for their endless prayers, love, and encouragement on my path to completing my PhD. I am also indebted to my dear friend Dr. Nisar Amin, who has selflessly supported me, opening his home and fridge to my leisure while I wrote this dissertation. There have been many wonderful family and friends who have supported me all throughout my studies whom I may have not been able to include here but to whom I am immensely grateful.

Table of Contents

List of Tables

List of Figures

(collateral resistance, yellow arrow), or resistance to one drug and increased sensitivity to the other (green arrows). The effect of a given mutation on growth will depend on both the magnitude of the rescaling (in each direction) as well as the interaction between drugs (the shape of the isobole contours). 15

Figure 1.6: Measurement of Evolutionary Growth Rates and Resistance Characterization to Each Drug for a Single Mutant on a Drug Combination Surface. a. Cartoon depiction of antagonistic interaction with colors representing per capita growth rate as a function of two drug concentrations and white line highlighting a particular contour, here selected at 30% inhibition. Four white dots correspond to mutants selected along the white contour line with four different conditions, two single drug conditions (Drug 1 and Drug 2) and two combination drug conditions. Pink arrow indicates evolution of mutants in one of the four conditions over 3 days with N=24 mutants per condition, in 96 well plates. Mutants are diluted 1:100 per well (see methods for details). **b.** Growth rate (g) is estimated each day by fitting OD time series to a simple exponential function. **c.** Growth rate adaptation over multiple days is given by the slope of the best-fit line through the growth evolution data. **d.** Dose response curves were measured in triplicate for each population to estimate each drug's IC_{50}, the half-maximal inhibitory concentration. The curve is fit to a hill function, where K is the concentration of drug at which 50% growth inhibition is obtained (IC_{50}). 19

Figure 2.1: Ceftriaxone and Ampicillin Combination Gives Rise to Synergistic Interaction in *E. faecalis*. a. Interaction with colors representing per capita growth rate as a function of two drug concentrations space. Four dots correspond to mutants selected with the same selective pressure at ~30% inhibition of growth with four different drug conditions. The first condition (in red) corresponds to [CRO] = 48.51ug/mL and [AMP]=0, the second condition (in magenta) corresponds to [CRO] = 2.59ug/mL, and [AMP]=0.051ug/m, the third condition (in cyan) corresponds to [CRO] = 1.29ug/mL, and [AMP]=0.102ug/mL, and the fourth condition (in blue) correspond to [CRO] = 0, and [AMP]=0.431ug/mL. Each condition is evolved over 4 days with N=24 mutants per condition, in 96 well plates. **b.** Smoothed version of interaction. See methods for smoothing details. Note that in both plots, the red point actually lies far above the axis, at the point where ceftriaxone inhibition first reaches approximately 70%. For visualization purposes, however, we have zoomed in on the primary region of interest but keep the red point as a reminder of the CRO-only point. Colors from blue to yellow represent growth rates. 26

Figure 2.2: Growth Curves of Day 1 and Day 4 for All Mutants Indicate Resistance at a Glance. Optical density time series measured in liquid cultures of *E. faecalis* on the first (blue) and last (red) day of laboratory evolution. Plots are arranged in 4 groups of 24 (three rows) corresponding to the four different conditions in Figure 2.1. Rows 1-3: ([CRO],[AMP])=(48.51, 0) (red axes); Rows 4-6: ([CRO],[AMP])=(2.59, 0.051) (magenta axes); Rows 7-9: ([CRO],[AMP])=(1.29, 0.102) (cyan axes); Rows 9-12: ([CRO],[AMP])=(0, 0.43) (blue axes). All concentrations are given in micrograms per mL. 27

Figure 2.3: Growth Rate Adaptation Over 4 days of Evolution for All Mutants. Per capita growth rate of *E. faecalis* cultures over 4 consecutive days of laboratory evolution.

Abstract

Antibiotic resistance is a growing threat to public health, as modern medicine relies heavily on effective drugs for combatting bacterial infections. The emergence of multi-drug resistant pathogens combined with the sluggish pace of drug discovery underscore the need for new treatment strategies that balance short-term drug efficacy with long-term evolutionary considerations. Drug combinations are one potential solution to minimize or reverse antibiotic resistance, but multi-drug treatments are difficult to systematically design because drugs frequently interact, strengthening or weakening the overall effect of a drug cocktail in counterintuitive ways. Recent studies suggest that drug interactions can have a significant impact on the evolution of resistance, though predicting evolution in multi-drug environments remains a challenge, in part because resistance to one drug is often correlated with altered sensitivity to other drugs.

Drug combinations are particularly important for successful treatment of *E. faecalis*, an opportunistic pathogen that contributes to multiple human infections, including endocarditis, bacteremia, urinary tract infections, and medical device infections. While numerous synergistic drug combinations for *E. faecalis* have been identified—and several are commonly used in clinical practice—much less is known about how these combinations impact the rate of resistance evolution. In this work, we use high-throughput laboratory evolution experiments to quantify adaptation in growth rate and drug resistance of *E. faecalis* exposed to clinically relevant drug combinations exhibiting different classes of interactions, ranging from synergistic

to suppressive. We identify a wide range of evolutionary behavior, including both increased and decreased rates of adaptation, depending on the specific interplay between drug interaction and collateral drug sensitivity. To disentangle these effects, we generalized previous quantitative models based on drug concentration rescaling to account for collateral sensitivity between drugs. Our results highlight trade-offs between drug interactions and collateral effects during the evolution of multi-drug resistance and, more specifically, emphasize unappreciated evolutionary benefits of particular drug pairs in targeting aminoglycoside-resistant enterococcus. Overall, the results represent a quantitative case study in the evolution of multidrug resistance in an opportunistic human pathogen and provide a general framework for evaluating and predicting resistance evolution in multi-stress environments.

Chapter 1: Introduction

The word *antibiotic* literally means 'opposing life', a reference to the drugs' powerful impact on the survival of microbes, many of which cause life-threatening infections in humans. The discovery of antibiotics was a watershed moment in modern medicine, and one that has saved countless lives and reduced suffering for people around the world. The study of antibiotics has also generated significant advances in the fields of chemical biology, genetics and cell physiology (Davies and Davies 2010), leading to the discovery of other therapeutics, including antiviral, antitumor, or anticancer agents, whose utility has sometimes matched or even exceeded that of antibiotics (Demain and Sanchez 2009).

Unfortunately, microbes have a remarkable ability to adapt to antibiotics, and the evolution of drug resistance has been recognized as a serious challenge since the earliest days of antibiotic research (Abraham et al. 1941). Due to the rise of drug-resistant bacteria, some early-stage antibiotics are now almost completely ineffective as therapeutic agents (CDC 2013), and resistance is taking an increasingly large toll on public health. Recent figures have shown that resistance evolution takes 23,000 lives in the United States and 25,000 lives in Europe on an yearly basis (CDC 2013; WHO 2014a).

1.1 Antibiotic Resistance

Antibiotic resistance threatens to usher in a "post-antibiotic" era, leading experts to warn of an impending large scale "reversal to all of modern medicine" (Michael Baym, Stone, and

Kishony 2016). Effective antibiotics are central to successful treatment of many human diseases, as chronic bacterial infections can be associated with conditions ranging from viral infections, such as human immune deficiency virus (HIV), hepatitis B virus (HBV), and hepatitis C virus (HCV), to human cancers, particularly when treatments involve immunotherapies (Chernish and Aaron 2003; Gupta et al. 2012; Tana, Michele M., Ghany 2013; Pawlotsky 2011; Zumla et al. 2012; Holohan et al. 2013; Bozic et al. 2013; Moreno-Gamez et al. 2015).

In 2016, the CDC listed antibiotic resistance at the top of its list of public health threats facing the nation (Becker's Clinical Leadership & Infection Control 2016). The discovery of new antibiotics, along with modification of existing antibiotics, have so far prevented widespread failure of antibiotic therapy; however the recent rapid rise in resistance appears to be a tipping point, and the pace of new developments is insufficient to counter the rapidly growing resistance threat (Neu 1992; Golan et al. 2012; Davies and Davies 2010; Hede 2014; Laxminarayan 2014). In response to this threat, significant national and international efforts have been devoted to discovering new drugs, particularly by the United States and European Union (Donadio et al. 2010; Boucher et al. 2013; Cooper and Shlaes 2011; Lewis 2013). Despite these efforts, however, the discovery of new drugs has been excruciatingly slow, and resistance remains an evolutionary reality even for new drugs (Davies and Davies 2010; Hede 2014).

The slow pace of drug discovery and the rapid rise of resistance underscore the need for new strategies that prolong the efficacy of current drugs (McClure and Day 2014; Bush et al. 2011). The last decade, in particular, has seen an increased focus on understanding and systematically designing evolutionarily sound strategies that balance short-term drug efficacy with long-term potential to develop resistance (M Baym, Stone, and Kishony 2016). Despite the promise of this approach, the molecular and physiological diversity of microbes—along with the

stochastic nature of evolution—make it difficult to extract general features of successful therapies, even in simplified *in vitro* scenarios.

1.2 Drug Combinations to Slow Resistance

Bacteria develop resistance to antibiotics by acquiring spontaneous mutations that, for example, decrease binding of the drug to its target or up-regulate expression of native defense systems—such as efflux pumps or enzymes—to reduce the effective concentration of drug. (Blair et al. 2011; Wright 2011; A C Palmer and Kishony 2014). These genetic changes confer a fitness advantage to the mutant cells, allowing them to outcompete sensitive cells and eventually dominate the population. One promising strategy for slowing resistance is combination therapy, wherein multiple drugs are deployed at the same time to enhance the effect of treatment while forcing the cells to simultaneously solve potentially conflicting evolutionary challenges (M Baym, Stone, and Kishony 2016; Adam C. Palmer and Kishony 2013). In fact, combination therapy has been endorsed by the World Health Organization (WHO) as a first-line of treatment against a number of major diseases, including HIV, malaria, and tuberculosis (World Health Organisation 2013; World Health Organization (WHO) 2015; WHO 2014b).

Combinations therapies have multiple advantages over single-drug therapies. First, simultaneous resistance to two drugs often requires two independent genetic events, each of which, on its own, occurs with low probability. In addition, drug combinations can sometimes be used to restore the efficacy of a particular drug, essentially reversing the impact of previously acquired resistance mechanisms. For example, ampicillin and an aminoglycoside are often used in combination to combat infections due to enterococcus (Murray 2018; Kak and Chow 2002; Sahm et al. 1989). Aminoglycosides exhibit poor intracellular penetration in many enterococcus isolates, yet by adding ampicillin—a cell well degrading antibiotic—intracellular penetration of

aminoglycosides is effectively increased, thereby enhancing aminoglycoside activity and yielding a powerful combined effect (Murray 2018; Kristich, Rice, and Arias 2014; Miller, Munita, and Arias 2014). On the other hand, these combined effects are often counterintuitive and unexpected, making it difficult to systematically design multidrug cocktails.

1.3 Drug Interactions Are Complex And The Underlying Mechanisms Are Not Always Known

The difficulty in designing multi-drug therapies arises because drugs in a combination can 'interact', leading to behavior that is not easily predicted based on the individual effects of the drugs. Consider, as a simple example, the effects of salicylate (an analgesic) and chloramphenicol (an antibiotic that inhibits protein synthesis (Cohen et al. 1993; Berlanga and Viñas 2000)) on the per capita growth of liquid cultures of *E. coli*. Figure 1.1 shows a heat map of per capita growth rate in the 2D space of drug concentrations (data modified from Wood et al. 2012). Increasing the concentration of either drug, in isolation, leads to a monotonic decrease in the growth rate of the population (Figure 1.1, bottom panels; blue and pink box outline). On the other hand, consider what happens when salicylate is added to cells initially exposed to 1.5 ug/mL of chloramphenicol (Figure 1.1, black box). In this regime, adding low concentrations of salicylate—up to approximately 0.5 mM—will actually *increase* the population growth, despite the fact that the drug inhibits growth when administered on its own. This type of drug interaction, a strong type of antagonisms known as suppression, indicates that the joint effect of the combination is significantly lower than one would anticipate based on single drug effects. Stated simply, the addition of an otherwise inhibitory drug (salicylate) can actually promote growth in the presence of chloramphenicol.

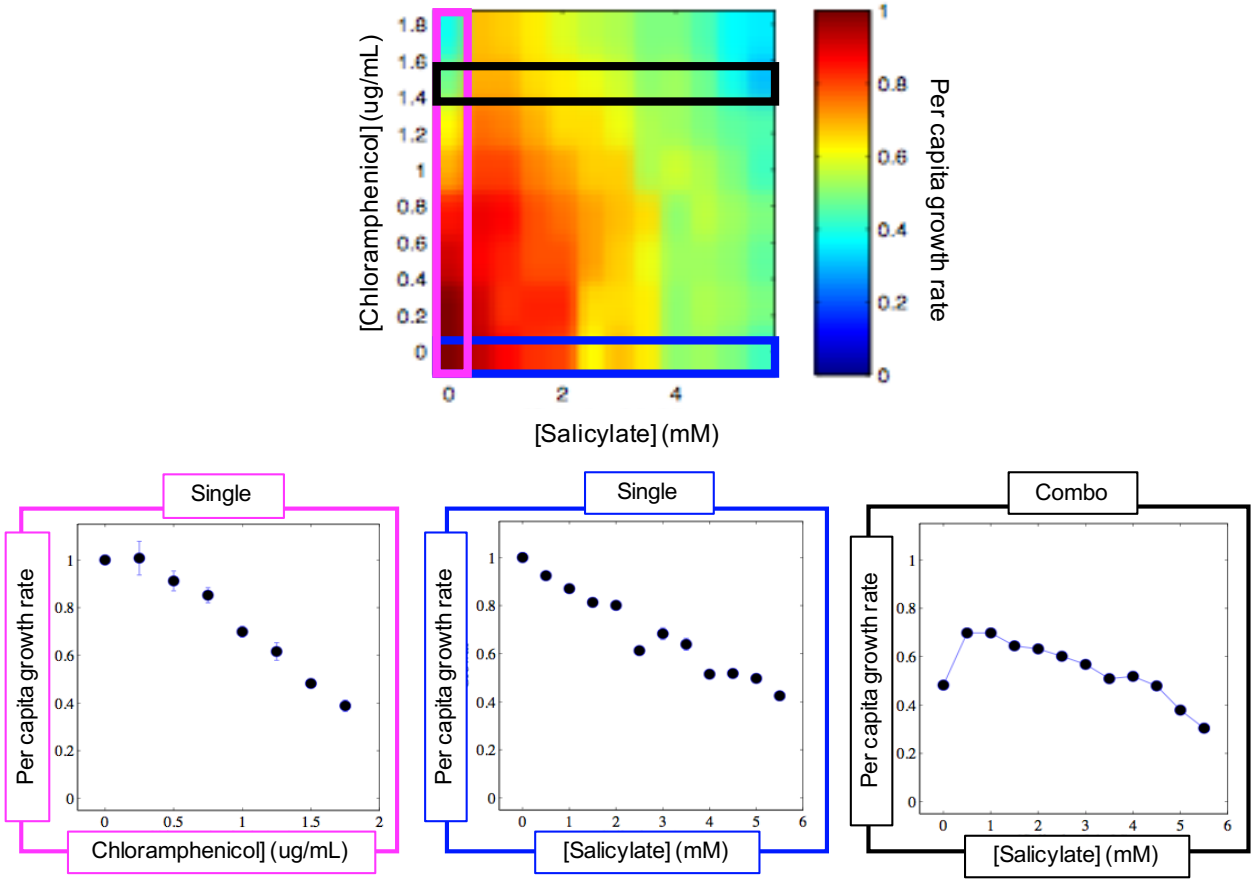

Figure 1.1: Growth Costs with Single and Combined Drugs. Top panel shows a heat map of *E. Coli* cells grown in concentration space of chloramphenicol and salicylate drug combinations, indicating suppressive interaction. Bottom panel shows dosage response curves of cells grown in the presence of single and combination drugs. Magenta and blue boxes show growth response to individual drugs, chloramphenicol and salicylate, respectively, and black box demonstrates growth response to salicylate combined with a constant 1.5ug/mL chloramphenicol. Growth in the absence of drug is normalized to 1. (Adapted from Wood et al. 2012)

This combination represents a relatively rare example where the mechanism of drug interaction is largely understood (Wood et al. 2014). Salicylate is a membrane permeating weak acid and, more importantly, is a known inducer of the multiple antibiotic resistant (MAR) regulon, which up-regulates the expression of multidrug efflux-pumps that expel from the cell a number of toxic small molecules, including chloramphenicol (Cohen et al. 1993; Wood et al. 2014). Salicylate alone inhibits cell growth, in part due to metabolic costs associated with

unnecessary expression of efflux pumps. On the other hand, it can also provide enormous benefit to the cell in the presence of high levels of a drug, like chloramphenicol, that can be rendered ineffective by the efflux pumps. Loosely speaking, the beneficial effects of added efflux more than compensate for the fitness costs of salicylate exposure. Note that like many drug interactions, the combined effect is not due to direct chemical interactions between the drugs, but arises instead because one drug modifies bacterial physiology in a way that alters the impact of the other drug.

Drug interactions are classified into three main types: synergistic, additive and antagonistic (Figure 1.2) (LOEWE 1953; Greco, Bravo, and Parsons 1995; P. J. Yeh et al. 2009; Michel et al. 2008). These interactions signify whether the combined effects of the drugs are, respectively, greater than, equal to, or less than what is expected based on their individual effects (Keith, Borisy, and Stockwell 2005; LOEWE 1953). The definition of an interaction requires the establishment of a "null model"—that is, a careful definition of what is "expected" when non-interacting drugs are combined. Multiple null models exist in the literature (Greco, Bravo, and Parsons 1995), some phenomenological and some based on molecular level models in simplified enzyme systems. In this thesis, we adopt the Loewe definition of drug interactions (Figure 1.2), which—we will see—is convenient because it allows one to link drug interactions to changes in growth adaptation rate in evolving bacterial lineages.

According to the Loewe paradigm, drug interactions are characterized by the shape of contours of constant population growth in drug concentration space. Contours of constant growth, also known as isoboles, are perfectly linear when the drugs combine additively (i.e. without interacting). The intuition behind this null model comes from a simple thought experiment. Consider taking one drug and dividing into two volumes. If we treat each volume

as a separate drug, we would expect to see linear isoboles for this artificial "combination", and since a drug should not interact with itself, combinations exhibiting linear isoboles are defined as additive (non-interacting). More specifically, the effect of 1 unit of drug 1 is the same as 1 unit of drug 2, or ½ unit of each drug, or ¾ unit of drug 1 combined with ¼ unit of drug 2, etc. On the other hand, a drug combination would be considered synergistic if the contours of constant growth appear concave (up), as the drugs mutually strengthen one another and exhibit combined efficacy at considerably reduced doses (Figure 1.2, left panel). Similarly, convex (concave down) contours of growth indicate antagonism, where the drugs counteract one another (Figure 1.2, right panel). A particularly strong version of antagonism, called suppression, occurs when the marginal effects of a second drug are not only weaker than expected, but actually reverse the effects of the first drug (e.g. Figure 1.1).

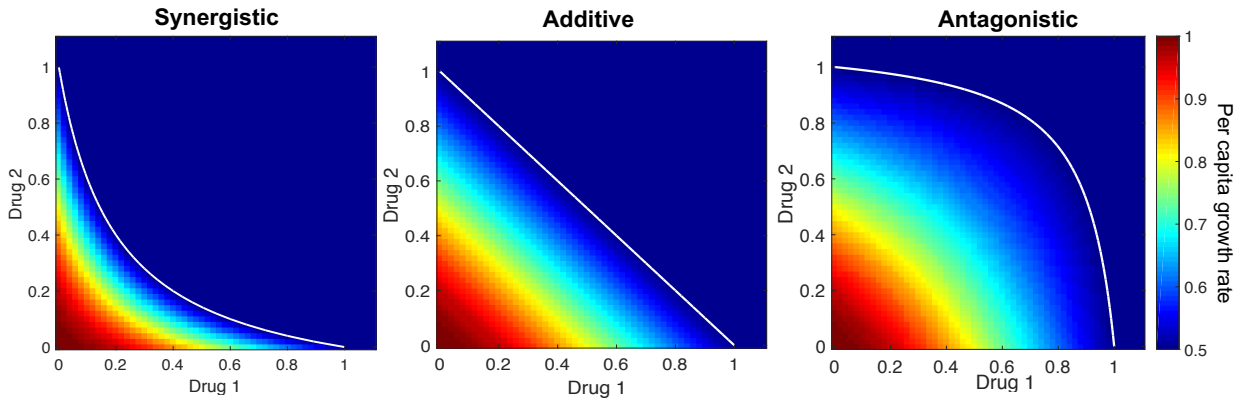

Figure 1.2: Drug Interactions Defined by Shape of Constant Contours of Growth. Cartoon depiction of three classes of drug interaction plots, demonstrating synergistic, additive and antagonistic, from left to right. Color represents per capita growth rate as a function of two drug concentrations space. White line highlights a particular contour, here selected at 25% inhibition.

From a clinical perspective, synergistic interactions have long been considered the goal of therapy, while antagonistic interactions have been traditionally avoided due to lower efficacy (Greco, Bravo, and Parsons 1995; Pillai S. K., Moellering R. C., Jr. 2005). However, a

groundbreaking collection of recent studies have challenged this conventional wisdom by demonstrating that synergistic interactions have a potentially serious drawback: they may accelerate the evolution of resistance (R Chait, Craney, and Kishony 2007; Hegreness et al. 2008; Michel et al. 2008; Michael Baym, Stone, and Kishony 2016; Barbosa et al. 2018). Similarly, antagonistic and suppressive drug interactions can slow or even reverse the evolution of resistance (R Chait, Craney, and Kishony 2007; Hegreness et al. 2008). These seminal results indicate that drug interactions underlie a natural trade-off between short-term efficacy and long-term evolutionary stability.

1.4 Drug Interactions Modulate Evolution of Resistance

The connection between the rate of resistance evolution and drug interaction arises because many mutations decrease the "effective" concentration of the drug (R Chait, Craney, and Kishony 2007; Wood et al. 2014). In some cases, such as enzyme-mediated drug degradation or drug efflux, this reduction in effective concentration corresponds to a true decrease in intracellular drug concentration; in other cases—such as the modification of a drug's molecular target to reduce binding affinity—the intracellular concentration may remain unchanged but the functional concentration is reduced. Mathematically, these and other mutations approximately correspond to a rescaling of drug concentration, with resistant mutants experiencing a lower effective drug concentration than their wild-type counterparts. In the presence of only one drug, the effect of this rescaling is simple: the growth rate of resistant cells increases relative to that of their drug sensitive ancestors. However, when mutations occur in the presence of more than one drug, the fitness effects of these mutations—specifically, the resulting change in growth rate due to concentration rescaling—depends not merely on the magnitude of the concentration rescaling, but also on the shape of the multi-drug landscape (Chait, Craney, and Kishony 2007; Hegreness

et al. 2008). In other words, translating changes in effective drug concentration into growth effects depends on the specific shapes of the growth rate contours, which directly define the drug interaction.

Using this approach, one can quantitatively predict the rate of evolution by imagining evolutionary trajectories on "isobole" plots, which show contours of constant growth in the 2d space of drug concentrations (R Chait, Craney, and Kishony 2007; Hegreness et al. 2008). For instance, Figure 1.3 shows schematic examples of synergistic (left) and antagonistic (right) drug interactions. Consider a thought experiment where one takes a single population of drug sensitive cells, divides it into two vials, and exposes one vial to the synergistic combination and one to the antagonistic combination. In both cases, the drug concentrations (cyan and magenta dots) are chosen so that 1) the concentration of drug 1 is the same in both cases, and 2) the concentration of the second drug ensures an identical level of inhibition in both experiments. Both populations are then allowed to evolve for several days, and the rate of growth adaptation is measured as the cells become increasingly resistant to drug 1.

If the mutations underlying growth adaptation change the effective concentration of drug 1, the mutant experiences an effective drug concentration corresponding to a different point in drug concentration space, as indicated by the vertical arrows. Even if the rescaling of drug 1 concentration is identical—for example, the concentration of drug 1 is effectively reduced by 50 percent in both cases—the increase in growth for the population grown in the synergistic combination will be considerably larger, as the arrow crosses more growth contours. In general, the density of contour lines (i.e. the steepness of the growth surface) depends strongly on the drug interaction type. Synergistic plots have more densely packed contours, so reducing the concentration of drug 1 by a given amount will yield a bigger growth effect than in antagonistic

plots, leading to more rapid growth adaptation (Figure 1.3, middle panel). This framework—originally introduced by the Kishony group (P. Yeh, Tschumi, and Kishony 2006; Remy Chait, Craney, and Kishony 2007) and applied to *E. coli*—is powerful because it links evolutionary behavior of resistant mutants to growth measurements (specifically, two-drug response surfaces) made in ancestral populations that have not yet developed resistance.

The rescaling approach has also been extended to link drug interaction surfaces of drug sensitive and drug resistant populations, potentially simplifying the design of evolution-proof drug combinations (Wood et al. 2014). Nevertheless, applications to date have focused primarily on simplified, proof-of-principle experiments dominated by evolutionary trajectories largely driven by resistance to a single drug. It is not clear whether this approach could be successfully applied to more complex evolutionary scenarios where, for example, mutants exhibit pervasive correlations between resistance levels to different drugs.

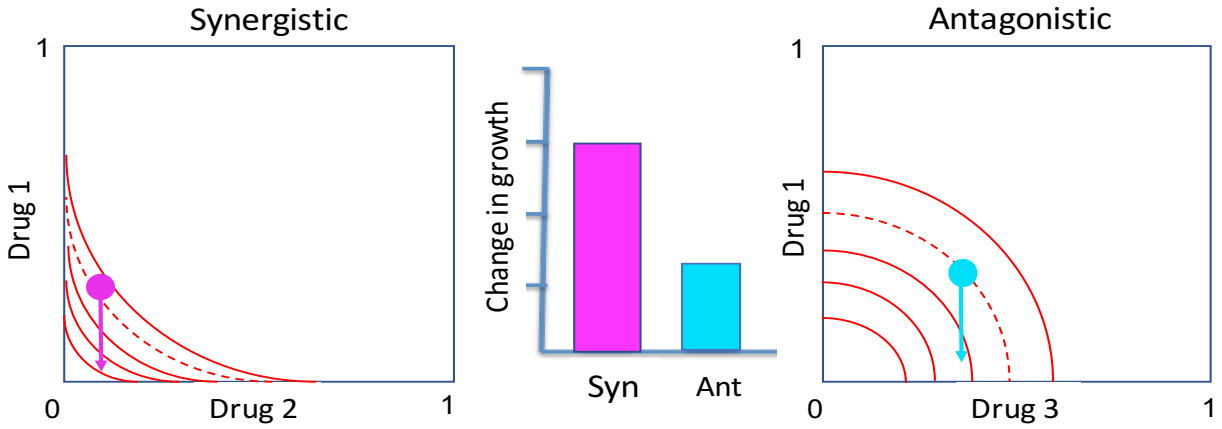

Figure 1.3: Geometric Argument Predicting Accelerated Growth Adaptation for Synergistic Combinations. Contours of constant growth in the space of two drug concentrations, indicating synergistic (left) and antagonistic (right) interactions. Dotted contour lines represent the same selection pressure in both synergistic and antagonistic interactions, and pink dots indicate the dosage combination used to evolve resistant mutants. Within this framework mutations are represented by effective changes in drug concentration (arrows). The arrows associated with each dot (pink and cyan) depict the effects of an identical mutation in both synergistic and antagonistic combinations. The bar plot at the center depicts the increased growth rate change (adaptation) in a synergistic interaction (pink bar) compared to an antagonistic (cyan bar) interaction.

1.5 Resistance To One Drug Can Lead To Collateral Changes In Sensitivity To Other Drugs

The evolutionary argument for drug combinations says that it should be more difficult to simultaneously evolve resistance to multiple agents because such multidrug resistance likely requires multiple genetic events. However, recent studies complicate this narrative by demonstrating widespread occurrence of so-called collateral effects, where a mutation conferring resistance to one drug may simultaneously confer increased resistance (cross-resistance) or increased sensitivity (collateral sensitivity) to other drugs (Figure 1.4) (S Kim, Lieberman, and Kishony 2014; C Munck et al. 2014; Barbosa et al. 2018; Imamovic and Sommer 2013; Lázár et al. 2013). Collateral effects were initially observed in the 1950s by Szybalski and Bryson (SZYBALSKI and BRYSON 1952), though until recent systematic studies in *E. coli* and *S. aureus* (Dragosits et al. 2013; Imamovic and Sommer 2013), the prospect of using collateral effects to fine-tune therapies has been largely overlooked.

Negative cross-resistance (collateral sensitivity) has been of particular interest in the field because of its potential to slow down or even reverse resistance evolution (Rodriguez De Evgrafov et al. 2015; Oz et al. 2014; Lázár et al. 2013, 2014; C Munck et al. 2014). While systematic understanding of collateral sensitivity is far from complete, the approach has proven promising in laboratory and even clinical settings (Imamovic et al. 2018) as it opens up the possibility of judiciously choosing drug cycles to steer evolution away from high-level resistance. Recent work in *E. coli* has demonstrated cycling between drugs exhibiting mutual collateral sensitivity can slow drug resistance in laboratory populations (Imamovic and Sommer 2013, (C Munck et al. 2014)).

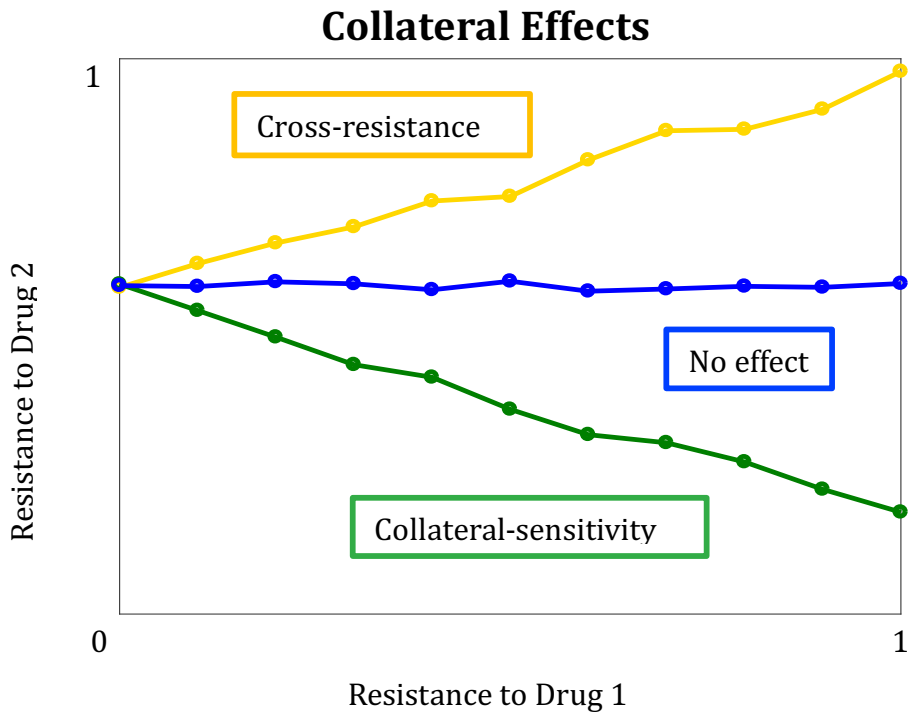

Figure 1.4: Resistance to One Drug Can Lead to Collateral Sensitivity or Resistance with Another Drug. Cartoon depiction of collateral effects between two drugs, where resistance to one drug (Drug 1) is associated with collateral-sensitivity (green line) or cross-resistance (yellow line) to a second drug (Drug 2).

Other works have investigated alternating drugs to constrain resistance evolution in *Staphylococcus aureus,* and have also concluded an overall advantage to utilizing collateral-sensitivity effects to minimizing resistance evolution (Seungsoo Kim, Lieberman, and Kishony 2014). Collateral-sensitivity strategies have also been studied in cancer drug therapy and proven useful when drug cycling or drug holidays strategies are applied (Dhawan et al. 2017). Despite this promise, there are numerous unresolved challenges of designing candidate therapies based on collateral sensitivity, including the presence of high-levels of heterogeneity (Barbosa et al. 2017; Dhawan et al. 2017) and non-repeatability (Nichol et al. 2017). Overall, these studies underscore the notion that unforeseen correlations between the fitness effects of a mutation in

different environments significantly complicate the prediction of evolutionary outcomes. On the other hand, they also provide an additional evolutionary knob that can be potentially tuned to limit resistance. These factors are important to take into consideration when aiming to design successful treatment strategies with combinations of drugs.

1.6 Collateral Sensitivity in Multi-Drug Environments

As discussed in section 1.4, drug interactions have been shown to either speed up or slow down resistance evolution when drugs are used simultaneously (Chait, Craney, and Kishony 2007; Michel et al. 2008; Hegreness et al. 2008). On the other hand, collateral resistance and sensitivity can shape evolution when multiple drugs are used in sequence (Section 1.5). However, much less is known about how these two modulatory effects—drug interactions and collateral sensitivity—combine to influence evolution of resistance in multi-drug environments. The first studies on drug interactions and resistance suggested that evolutionary acceleration was primarily due to drug synergy (Michel et al. 2008). Recent studies, by contrast, suggest that collateral effects may dominate (Yeh et al. 2009; Rodriguez De Evgrafov et al. 2015; Imamovic and Sommer 2013; C Munck et al. 2014; Barbosa et al. 2018). For instance, one group used evolution and genome analysis to identify mutations that drive resistance levels in drug combinations, allowing the prediction of collateral-sensitive or resistance between drug components. *E. coli* cells were engineered with mutations selecting for collateral-sensitivity and demonstrated suppression of sensitive cells and limiting resistance evolution (Christian Munck et al. 2014). Another recent study based on large scale laboratory evolution found that synergistic combinations can lead to population extinction while evolved collateral sensitivity between 2 drugs has the potential to reduce adaptation (Barbosa et al. 2018). In general, though, it seems

that drug interactions and collateral effects may be intertwined in a complex manner that gives rise to variable results.

One explanation for this variability could be that the effects are organism- and condition-specific. The work to date has focused on a limited number of species, including *E. coli, S. aureus,* and—very recently—*P. aeruginosa* (Hegreness et al. 2008; C Munck et al. 2014; S Kim, Lieberman, and Kishony 2014; Barbosa et al. 2018). Studies on a wider range of species—particularly other pathogenic species—are therefore needed. It may also be true that both collateral effects and drug interactions have the potential to dominate evolutionary trajectories, depending on specific situations or environments. The challenge, then, is to disentangle these effects to better understand which effect dominates and in what situations.

In this work, we use quantitative experiments on microbial populations to investigate the evolution of antibiotic resistance in an opportunistic pathogen—*E. faecalis*—during adaption to a number of clinically relevant drug combinations. To interpret our results, we extend previous arguments based on drug concentration rescaling (Chait, Craney, and Kishony 2007; Michel et al. 2008; Hegreness et al. 2008) to incorporate a range of collateral effects observed experimentally, including both cross resistance and collateral sensitivity (Figure 1.5). We show that these rescaling arguments accurately predict qualitative features of the observed experimental trajectories—including a number of unappreciated evolutionary features of common drug combinations. The power of this approach lies in making evolutionary predictions without detailed knowledge about molecular mechanisms of resistance or drug interactions, which can be particularly hard to elucidate for drug combinations.

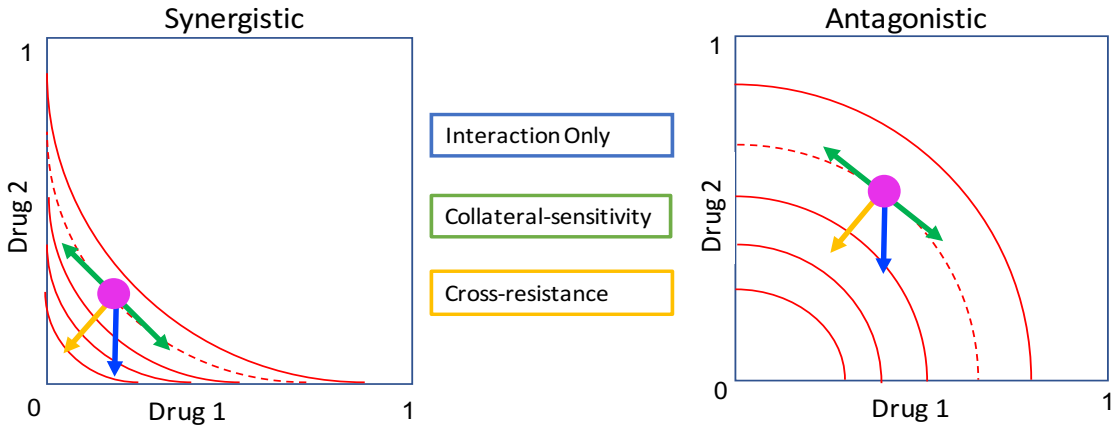

Figure 1.5: A Generalized Framework for Resistance Evolution Accounting for Both Drug Interaction and Collateral Effects Based on Rescaling of Effective Drug Concentration. Contours of constant growth in the space of two drug concentrations, indicating synergistic (left) and antagonistic (right) interactions. Dotted contour lines represent the same selection pressure in both synergistic and antagonistic interactions, and pink dots indicate the dosage combination used to evolve resistant mutants. Within this framework mutations are represented by effective changes in drug concentration (arrows). Different arrows represent resistance to drug 2 only (blue arrows), resistance to both drugs (collateral resistance, yellow arrow), or resistance to one drug and increased sensitivity to the other (green arrows). The effect of a given mutation on growth will depend on both the magnitude of the rescaling (in each direction) as well as the interaction between drugs (the shape of the isobole contours).

In what follows, we will briefly review the *Enterococcus* bacterial genus and provide an overview of our experimental approach for measuring evolutionary adaptation in drug combinations. We will conclude chapter 1 with an informational review of the specific drugs we used in this study. Each subsequent chapter will then discuss a lab evolution in a particular combination including: ceftriaxone and ampicillin (Chapter 2), ceftriaxone and ciprofloxacin (Chapter 3), ampicillin and streptomycin (Chapter 4), and lastly, ciprofloxacin and tigecycline (Chapter 5). Chapter 6 is a brief conclusion, outlining some limitations of the approach as well as future directions. Details of methodology and experimental protocols are covered in Chapter 7.

1.7 Enterococcus: An Opportunistic Pathogen Often Requiring Drug Combinations

The study of enterococcus began in the late 19th century with Thiercelin, MacCallum and Hastings, the latter two of whom provided the first detailed description of a lethal case of enterococcal endocarditis (Gilmore et al. 2014; Maccallum and Hastings 1899). From its earliest descriptions, enterococcus has been known as commensal opportunist. Since the application of multi-drug therapy over 50 years ago, multi-drug resistant enterococci have been a leading cause of nosocomial infection worldwide (Werner et al. 2008; Prabaker and Weinstein 2011). Enterococci are normally found in the gastro intestinal tract of humans and animals, where they make up less than 1% of the adult microflora (Mundt 1963; Sghir et al. 2000). The precise mechanism of how enterococci colonize the GI is not known, but in the hospital environment after patients have taken antibiotics, enterococci take advantage of the disrupted microbiota of the gut (Ubeda et al. 2010).

Among the enterococci *E. faecalis* is the species most abundantly found in humans and accounts for the most disease (Malani, Kauffman, and Zervos 2002). Furthermore, 90-95% of clinical isolates of enterococcus since the 1990s are *E. faecalis* (Huycke, Sahm, and Gilmore 1998). *E. faecalis* can cause life-threatening infections when found in hospital environments and is a leading source for urinary tract infection, bacteremia, wound infection and endocarditis (Malani, Kauffman, and Zervos 2002). Its ability to acquire resistance against most antibiotics and survive in deleterious conditions has made it a challenging pathogen to restrain (Kak and Chow 2002). Vancomycin resistant enterococcus (VRE) represent a particularly difficult challenge, and they have been found in many non-human reservoirs in Europe (Werner et al. 2008). In the US VRE is less likely to be found in non-human reservoirs due to banning of an antimicrobial used as a growth hormone (Avoparcin), but VRE is still found in US hospitals

(Hammerum 2012; Aarestrup, Butaye, and Witte 2002). Antibiotic resistant enterococci can also be found in food particular in meat, diary and even some probiotics (Giraffa 2002). Overall, antibiotic resistance in enterococcus is quite prevalent in hospital environments, animals and food, making humans more susceptible to acquiring resistant strains of the microbe.

Because of widespread multidrug resistance, drug combinations have been used for decades treat enterococci infections. Most commonly, beta lactams are combined with an aminoglycoside (e.g. streptomycin), yielding a strong synergistic combination (Miller, Munita, and Arias 2014). The success of early synergistic combinations drove the search for new cocktails, particularly those driven by drug synergy. Despite the identification of several potent drug pairs, relatively little is known about the evolutionary consequences of these combinations, particularly in regards to the rates of resistance. Thus, there is an urgent need to better understand how enterococci adapt in multidrug environments and whether that adaptation is dominated by drug interactions, collateral effects, or some combination of both.

1.8 Approach: Quantitative, High-Throughput Laboratory Evolution

To address these questions, we perform lab evolution on *E. faecalis* bacteria in the presence of clinically relevant drug combinations over multiple days. To identify a representative set of drug combinations, we began by measuring the per capita growth rate of vancomycin resistant *E. faecalis* (strain V583) in liquid cultures exposed to a wide range of drug pairs over many dosage combinations. After selecting drugs pairs spanning multiple interaction types (Figure 1.6; simulated data), we measured the longer-term growth response to multi-drug exposure in dozens of replicate populations using optical density time series acquired with an automated microplate reader and stacker (Enspire). Evolution is expected to depend heavily on the level of growth inhibition in the initial cultures, which sets the selection pressure favoring

resistant mutants. To control for selection pressure, we chose four dosage combinations for each drug pair—two corresponding to single drug treatments and two to drug combinations—that lie along a contour of constant growth (white line and four dots in Figure 1.6a). Because inhibition is constant across the four conditions, any differences between resistance adaptation should reflect drug concentration differences.

For each population, cells were inoculated into media and drug on day 1 and diluted daily into fresh media and drugs (Figure 1.6a, bottom panel). Growth was measured throughout the evolution experiment by taking the optical density (OD) using an automated plate reader and stacker. To quantify growth rate adaption, we estimated the per capita growth rate for each OD time series using nonlinear least squares fitting to an exponential function (Figure 1.6b) (see Methods for more details). To further quantify these trends, we estimated the rate of growth adaptation for each population over the number of days of evolution (Figure 1.6c).

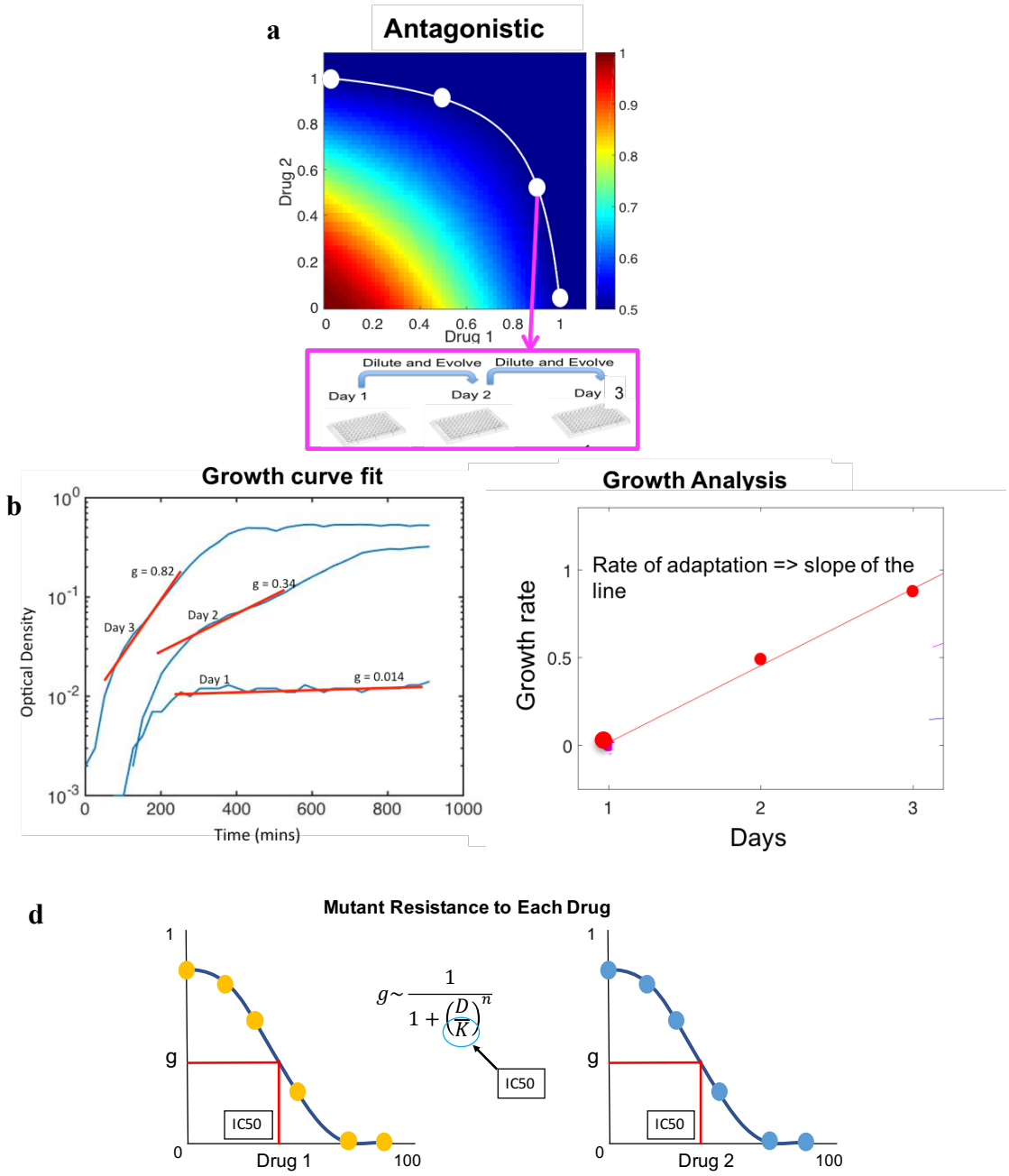

Figure 1.6: Measurement of Evolutionary Growth Rates and Resistance Characterization to Each Drug for a Single Mutant on a Drug Combination Surface. a. Cartoon depiction of antagonistic interaction with colors representing per capita growth rate as a function of two drug concentrations and white line highlighting a particular contour, here selected at 30% inhibition. Four white dots correspond to mutants selected along the white contour line with four different conditions, two single drug conditions (Drug 1 and Drug 2) and two combination drug conditions. Pink arrow indicates evolution of mutants in one of the four conditions over 3 days with N=24 mutants per condition, in 96 well plates. Mutants are diluted 1:100 per well (see methods for details). **b.** Growth rate (g) is estimated each day by fitting OD time series to a simple exponential function. **c.** Growth rate adaptation over multiple days is given by the slope

of the best-fit line through the growth evolution data. **d.** Dose response curves were measured in triplicate for each population to estimate each drug's IC_{50}, the half-maximal inhibitory concentration. The curve is fit to a hill function, where K is the concentration of drug at which 50% growth inhibition is obtained (IC_{50}).

The growth rate adaption observed in the presence of drugs is likely driven by a population's ability to survive higher concentrations of one or both drugs. To quantify this increased resistance, we selected 6 populations for each condition and directly measured the half-maximal inhibitory concentration (IC_{50}) of each drug (Figure 1.6d). Overall, this approach provides quantitative measures of both growth adaption and increased drug resistance for hundreds of microbial populations exposed to a wide range of drug combinations and drug doses, all at similar levels of inhibition

1.9 Antibiotics Used In This Work

Ampicillin

Ampicillin is from the beta-lactam family of antibiotics and its main mechanism of action is inhibition of the bacterial cell wall, which it accomplishes by serving as a suicide substrate and binding to penicillin-binding proteins (PBPs) resulting in the inhibition of the final transpeptidation step of peptidoglycan synthesis in bacterial cell wall. This results in continuous activity of cell wall autolytic enzymes while cell wall assembly is arrested, causing the bacteria to lyse (Kristich, Rice, and Arias 2014; Murray 2018). Enterococci are able to resist ampicillin through the saturating production of low-affinity class B penicillin-binding protein 5 (Pbp5), thereby blocking ampicillin activity (Arbeloa et al. 2004; Kristich, Rice, and Arias 2014). Ampicillin is still among the mostly commonly used treatments for enterococcus infections, particularly in *E. faecalis*.

Ceftriaxone

Ceftriaxone was discovered in the 1980s and is derived from the beta-lactam family of antibiotics, which targets the inhibition of the bacterial cell wall by binding to penicillin-binding proteins (PBPs) inhibiting transpeptidation and arresting cell wall assembly (Landau et al. 1999; Arbeloa et al. 2004). Unlike ampicillin resistance, which must be acquired, resistance to ceftriaxone is intrinsic in many enterococci. As consequence, ceftriaxone is often ineffective as a single-drug treatment (Arbeloa et al. 2004; Kristich, Rice, and Arias 2014). However, several works have shown ceftriaxone plus ampicillin to be an effective synergistic treatment strategy against *E. faecalis*, particularly in isolates with high-level aminoglycoside resistance (Gavaldà et al. 2003, 2007; Fernández-Hidalgo et al. 2013; Pericas et al. 2014).

Streptomycin

An aminoglycoside antibiotic, streptomycin binds the 16S rRNA of the 30S ribosomal subunit thereby interfering with protein synthesis (Kristich, Rice, and Arias 2014). In general enterococci demonstrate low level intrinsic aminoglycoside resistance which is attributed to weak uptake of the drug by cells (Aslangul et al. 2006). Due to poor penetration of aminoglycosides, traditional therapies of enterococci (e.g. endocarditis) combine aminoglycosides with a cell wall inhibiting antibiotic, which results in a synergistic effect (Kak et al. 2000; Murray 2018). However, enterococci are increasingly exhibiting high-level resistance to aminoglycosides, thus disabling the expected synergistic effect of the combination therapy (Kak et al. 2000; Kristich, Rice, and Arias 2014). This high-level resistance is mostly acquired due to the presence of aminoglycosides-modifying enzymes (Kak et al. 2000). In the case of *E.*

faecalis treatment when synergism is still possible between an aminoglycoside and a cell-wall inhibitor, streptomycin is most commonly used combination with ampicillin (Murray 2018). Even in the case of high-level aminoglycoside resistance, the streptomycin and ampicillin combination remains a potential therapeutic option (Fernández-Hidalgo et al. 2013).

Tigecycline

Tigecycline is a relatively new drug from the glycylcycline class of antibiotics, which targets the 30S subunit of the ribosome and in turn inhibits protein synthesis. Tigecycline has been shown through *in vitro* studies to have activity against both gram-negative and gram-positive bacterial species, including enterococci (Murray 2018; Miller, Munita, and Arias 2014). Thus, far there are no reports of Tigecycline resistance in *E. faecalis,* and its mechanism of resistance is unknown (Miller, Munita, and Arias 2014). Tigecycline has been used clinically for *E faecalis* infections such as in skin structure infections and intra-abdominal infections. Combination therapy with tigecycline and distamycin, a DNA synthesis inhibitor, against vancomycin resistant enterococci (VRE) has also proven to be an effective treatment strategy (Miller, Munita, and Arias 2014; Murray 2018).

Ciprofloxacin

A member of the quinolone class of antibiotics, ciprofloxacin is known to inhibit enzymes such as the DNA gyrase and topoisomerase IV which are responsible for relaxation of DNA supercoils necessary for transcription and replication before cell division (Miller, Munita, and Arias 2014). Resistance to quinolone in enterococci often occurs through mutations in genes that encode for DNA gyrase and topoisomerase IV, resulting in inefficient binding of the

antibiotic to the enzymes. (Miller, Munita, and Arias 2014; Arsène and Leclercq 2007). Another mechanism responsible for quinolone resistance is pumping of antibiotics out of the cell via multidrug-resistant efflux pumps (MDRs) (Miller, Munita, and Arias 2014). In particular, one study has found 34 MDRs in the V583 strain of *E. faecalis*, with two pumps specific to promoting quinolone resistance (Davis et al. 2001). Successful combination of ciprofloxacin and a beta-lactam (ampicillin) was demonstrated in the treatment of human endocarditis infection with high-level gentamicin resistance in *E. faecalis* (Tripodi et al. 1998).

A Brief Note on Terminology

Throughout this work, we (somewhat loosely) refer to populations undergoing laboratory evolution in the presence of antibiotics as "mutants", though it should be noted that the populations could contain heterogeneous mixtures of genotypes. We use the term "mutant" only to indicate that a particular population has been grown in the presence of the drugs. For example, we may refer to populations exposed to drugs for 2 days (one full day of growth followed by dilution into fresh media/drug and then a second day of growth) as "day 2 mutants", though we do not mean to imply that these are (necessarily) isogenic populations isolated from a single colony.

Chapter 2: Synergistic Interaction – Ceftriaxone plus Ampicillin

2.1 Introduction

Ampicillin (AMP) is commonly used in treatment of enterococcus infections, particularly in *E. faecalis* isolates, which remain frequently susceptible to beta lactams (Kristich, Rice, and Arias 2014; Murray 2018). On the other hand, enterococci frequently exhibit increased resistance to ceftriaxone (CRO), a newer beta lactam, making it ineffective in treatment therapies (Arbeloa et al. 2004; Kristich, Rice, and Arias 2014). Despite the limited utility of ceftriaxone alone, it can be combined with ampicillin to yield an effective synergistic treatment strategy against *E. faecalis*. This combination remains a particularly viable option for *E. faecalis* harboring high-level aminoglycoside resistance, which thwarts first line combination therapies (Gavaldà et al. 2003, 2007; Fernández-Hidalgo et al. 2013; Pericas et al. 2014). Ceftriaxone and ampicillin have been particularly effective in treatment of endocarditis infections in the clinical setting (Fernández-Hidalgo et al. 2013). The strong synergy of the combination make it attractive as a treatment option, and the molecular mechanisms of resistance to each drug are increasingly understood. Unfortunately, little is known about how *E. faecalis* evolve resistance when the drugs are combined. In this chapter, we measure evolutionary adaptation to ceftriaxone and ampicillin alone and in combination using laboratory evolution experiments spanning several days. Our results reveal strong correlations between phenotypic resistance to ampicillin and ceftriaxone across multiple conditions. More importantly, we find accelerated growth adaption when the drugs are combined, highlighting an unappreciated drawback to combined ampicillin-ceftriaxone therapy for *E faecalis*.

2.2 Ceftriaxone and Ampicillin Combination Gives Rise to Synergistic Interaction in *E. faecalis*

To investigate evolution in ceftriaxone-ampicillin combinations, we first measured the per capita growth rate of *E. faecalis* strain V583 in liquid cultures exposed to a large range of drug doses. Note that strain V83 exhibits high level aminoglycoside resistance, typical of isolates that may benefit from ceftriaxone-ampicillin combination therapy (Gavaldà et al. 2003, 2007; Fernández-Hidalgo et al. 2013; Pericas et al. 2014). As expected, we observed a strongly synergistic interaction between the two drugs, as indicated by the convex contours of the growth isoboles (Figure 2.1a; raw data; 2.1b smoothed data).

To understand why the combination is considered synergistic, consider the growth in the presence of 5ug/mL of ceftriaxone and 0.2ug/mL of ampicillin in Figure 2.1a. At those concentrations, the drugs alone have little to no inhibitory effect. On the other hand, the combination entirely eliminates growth. This drastic shift in growth demonstrates a clearly strong synergism in this combination. While the mechanism of drug synergy is not completely understood, both drugs are cell wall inhibitors and may mutually benefit each other by targeting the same mechanism (Fernández-Hidalgo et al. 2013; Gavaldà et al. 2007, 2003).

Next, we set out to measure the longer-term growth response to this drug pair. Evolution is expected to depend heavily on the level of growth inhibition in the initial cultures, which sets the selection pressure favoring resistant mutants. To control for initial inhibition, we chose four dosage combinations—two corresponding to single drug treatments and two to drug combinations—that lie along a contour where growth is approximately 30% of the native (drug free) growth (Figure 2.1). Thus, each condition was selected based on a particular drug

concentration corresponding to 70% growth inhibition. Because inhibition is constant across the four conditions, any differences between resistance adaptation should reflect drug concentration differences.

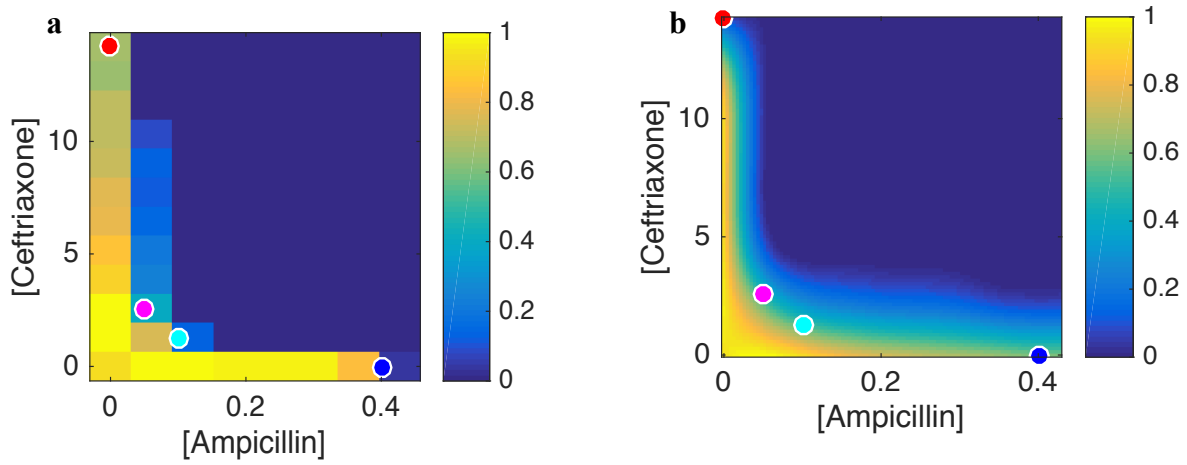

Figure 2.1: Ceftriaxone and Ampicillin Combination Gives Rise to Synergistic Interaction in *E. faecalis*. a. Interaction with colors representing per capita growth rate as a function of two drug concentrations space. Four dots correspond to mutants selected with the same selective pressure at ~30% inhibition of growth with four different drug conditions. The first condition (in red) corresponds to [CRO] = 48.51ug/mL and [AMP]=0, the second condition (in magenta) corresponds to [CRO] = 2.59ug/mL, and [AMP]=0.051ug/m, the third condition (in cyan) corresponds to [CRO] = 1.29ug/mL, and [AMP]=0.102ug/mL, and the fourth condition (in blue) correspond to [CRO] = 0, and [AMP]=0.431ug/mL. Each condition is evolved over 4 days with N=24 mutants per condition, in 96 well plates. **b.** Smoothed version of interaction. See methods for smoothing details. Note that in both plots, the red point actually lies far above the axis, at the point where ceftriaxone inhibition first reaches approximately 70%. For visualization purposes, however, we have zoomed in on the primary region of interest but keep the red point as a reminder of the CRO-only point. Colors from blue to yellow represent growth rates.

2.3 Mutants Evolve in the Presence of Ceftriaxone and Ampicillin Combination

To perform the evolution, we evolved twenty-four (24) replicate populations of *E. faecalis* at each of the four conditions for a total of 4 days. Approximately 10^7 cells were inoculated into 200 uL of BHI each drug condition on day 1, and each day the populations were diluted by 100X into fresh media and drugs. Growth was measured throughout the evolution experiment by taking optical density (OD) (A_{600}) readings every 25 mins using an automated plate reader and stacker. The first day (blue) and last day OD (red) growth curves are shown in Figure 2.2. It is clear that, for the majority of the populations, growth had significantly increased by the last day of evolution, consistent with evolved resistance to one or more drugs.

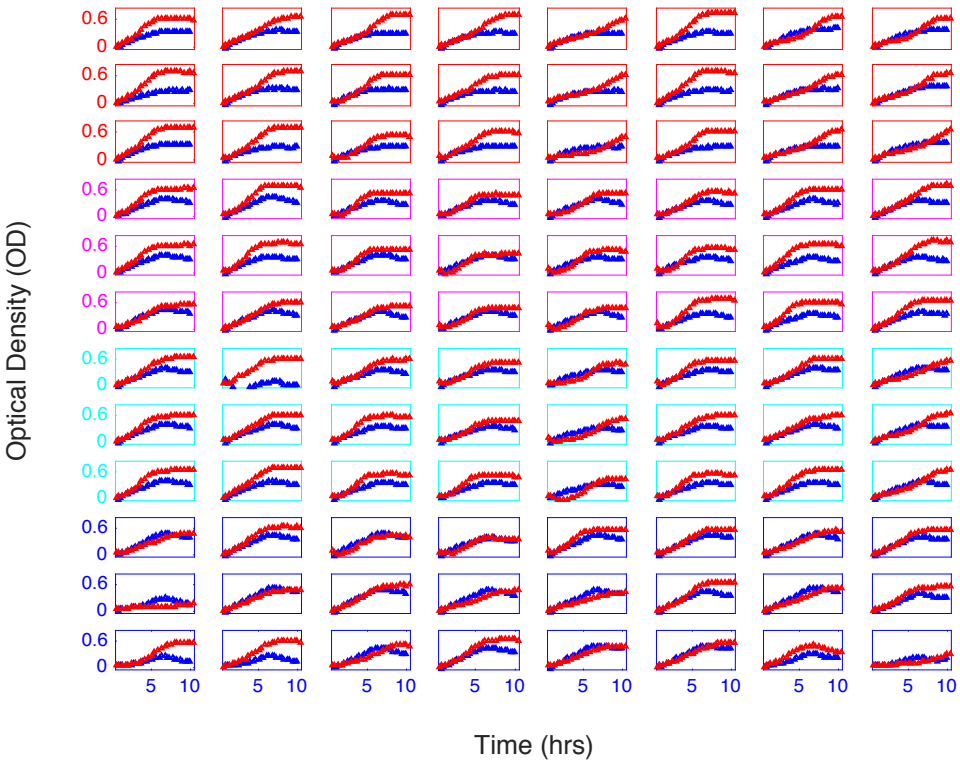

Figure 2.2: Growth Curves of Day 1 and Day 4 for All Mutants Indicate Resistance at a Glance. Optical density time series measured in liquid cultures of *E. faecalis* on the first (blue) and last (red) day of laboratory evolution. Plots are arranged in 4 groups of 24 (three rows) corresponding to the four different conditions in Figure 2.1. Rows 1-3: ([CRO],[AMP])=(48.51, 0) (red axes); Rows 4-6: ([CRO],[AMP])=(2.59, 0.051) (magenta axes); Rows 7-9: ([CRO],[AMP])=(1.29, 0.102) (cyan axes); Rows 9-12: ([CRO],[AMP])=(0, 0.43) (blue axes). All concentrations are given in micrograms per mL.

2.4 Ceftriaxone and Ampicillin Combinations Accelerate Growth Adaptation

To quantify adaption, we estimated the per capita growth rate for each OD times series using nonlinear least squares fitting to an exponential function (Methods). As expected, we can see in Figure 2.3 that the growth of each population is similarly inhibited on day one—consistent with the choice of dosage conditions providing constant inhibition levels. On the other hand, the growth rate varies considerably after Day 1, with mutants in each condition responding differently. Some populations exhibit a very fast adaption and approach wild-type drug-free levels within one day, while others increase slowly or not at all.

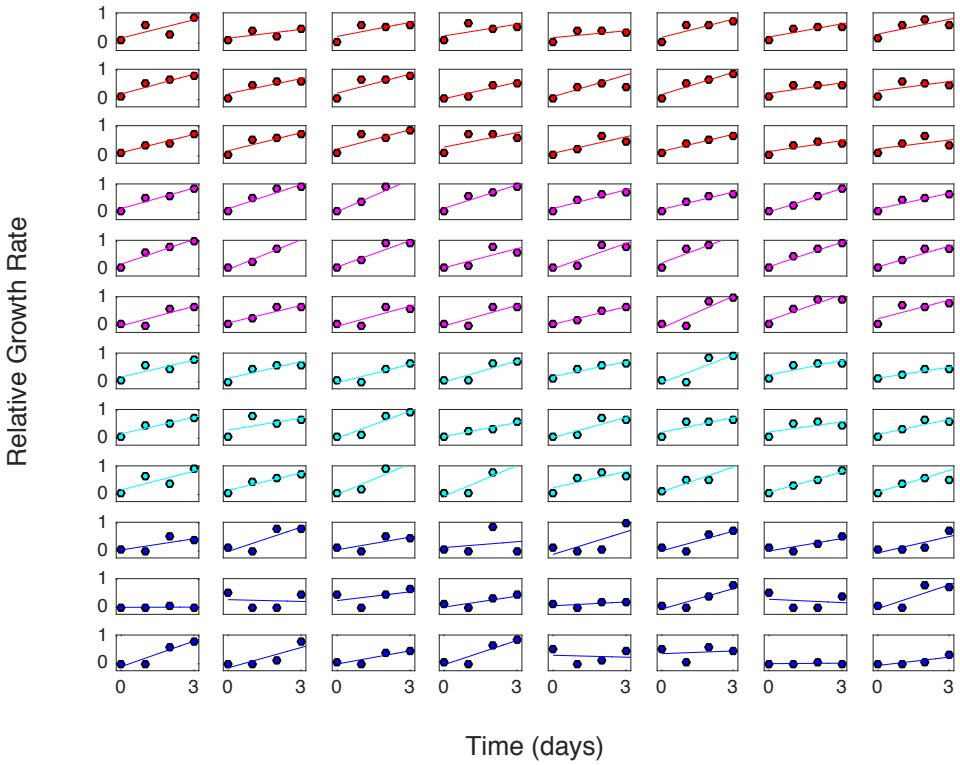

Figure 2.3: Growth Rate Adaptation Over 4 days of Evolution for All Mutants. Per capita growth rate of *E. faecalis* cultures over 4 consecutive days of laboratory evolution. Rows 1-3: ([CRO],[AMP])=(48.51, 0) (red axes); Rows 4-6: ([CRO],[AMP])=(2.59, 0.051) (magenta axes); Rows 7-9: ([CRO],[AMP])=(1.29, 0.102) (cyan axes); Rows 9-12: ([CRO],[AMP])=(0, 0.43) (blue axes). All concentrations are given in micrograms per mL. Adaptation rate for each mutant is given by the slope of the best-fit (least-squares) trend line through the relative growth rate time series.

To visualize these trends, we separated the populations by condition and plotted the growth rate over time for each population (Figure 2.4, top panel; small points) as well as the mean growth rate across all mutants in a given condition (Figure 2.4, top panel; small points). First, consider the cases where the drugs are used alone. Adaptation to CRO only (left panel, red) is initially rapid followed by gradual increase on days 3 and 4, while adaption to AMP (right panel, blue) rises more slowly, with almost no adaption by day 2. Interestingly, however, adaption in both conditions containing two drugs (middle panels, magenta and cyan) rises rapidly and steadily all four days and, on average, reaches a higher final growth rate that populations exposed to single drug conditions.

To further quantify these trends, we estimated the rate of growth adaptation r—defined as the slope of the best-fit trend line through the relative growth rate time series—for each population (Figure 2.4, bottom panel). On average, growth rate adaptation is significantly faster for the drug combinations (magenta and cyan) than for the individual drugs (red and blue) (student t-test, $p<0.001$ for all pair combinations between 2-drug and 1-drug conditions). The fact that growth adaption is accelerated in the presence of two drugs is provocative because it highlights an otherwise unappreciated drawback of CRO-AMP combination therapy: despite short-term efficacy at low drug doses, the combination facilitates rapid adaptation after only a few days.

a

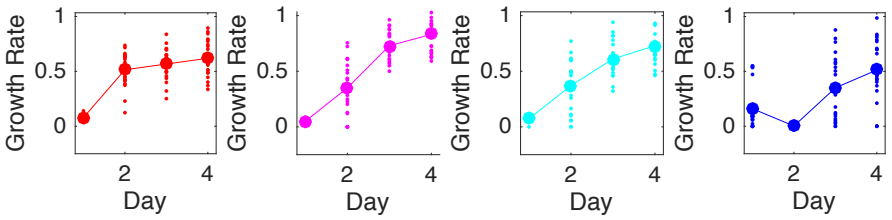

b

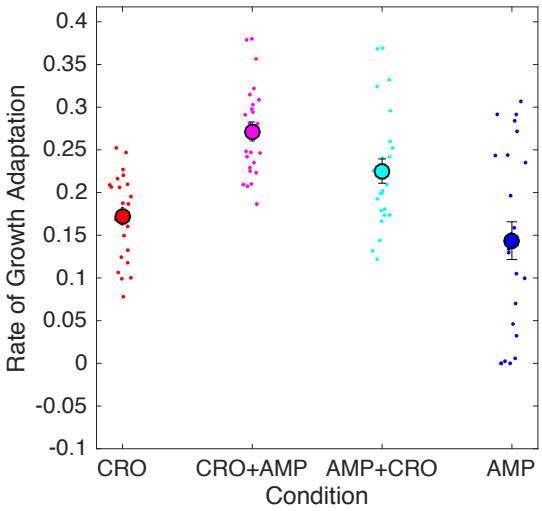

Figure 2.4: Synergistic Combinations of Ceftriaxone and Ampicillin Leads to Faster Evolution of Resistance in *E. faecalis*. a. Adaptation time series (per capita growth rate) over 4 days of evolution, in each of the 4 conditions: condition 1 [CRO] = 48.51ug/mL, and [AMP]=0 (red point in Figure 2.1), condition 2 [CRO] = 1.29ug/mL, and [AMP]=0.102ug/mL (cyan point in Figure 2.1), condition 3 [CRO] = 2.59ug/mL, and [AMP]=0.051ug/mL (magenta point in Figure 2.1), and condition 4 [CRO] = 0, and [AMP]=0.431ug/mL (blue point in Figure 2.1). Small points represent individual mutants. Large circles are means taken across all mutants in a given condition (N=24 mutants). **b.** Growth adaptation rate for each condition; the units of adaptation are *growth rate/day*, where *growth rate* is measured in units such that the ancestral strains grow at a rate of 1 in the absence of drug. As an example, an adaptation rate of 0.25 means it takes, on average, 4 days of adaption for the strains to fully adapt to the drug (i.e. to reach the drug-free growth rate of ancestral cells). Small points correspond to individual mutants; large points represent the mean of all mutants in a given condition.

2.5 Cross-resistance Found in Both Drugs, with Stronger Ceftriaxone Resistance and Weaker Ampicillin Resistance

Growth rate adaption indicates the population's ability to survive higher concentrations of one or both drugs. To better understand these dynamics, as discussed in the introduction, we selected 6 populations for each condition and directly measured the half-maximal inhibitory concentration (IC_{50}) of each drug. Specifically, we diluted a sample of each population (in technical replicates of 8) into fresh media containing a range of AMP (or CRO) concentrations. After 12 hours, we measured the optical density (OD) and generated a dose response curve for each drug and each population. For each dose response curve, we estimated the half maximal inhibitory concentration (IC_{50}) using nonlinear least squares fitting to a logistic binding function (see Methods for representative IC50 curve). We then quantify the resistance level to each drug using $R_{drug} = \log_2(IC_{50,drug}/IC_{50,WT})$, where $IC_{50,drug}$ is the population's IC_{50} to the drug and $IC_{50,WT}$ is the IC_{50} of the wild type (ancestral) strain to the same drug. Positive values of R_{drug} indicate increased resistance, while negative values indicate increased sensitivity (relative to ancestral strain).

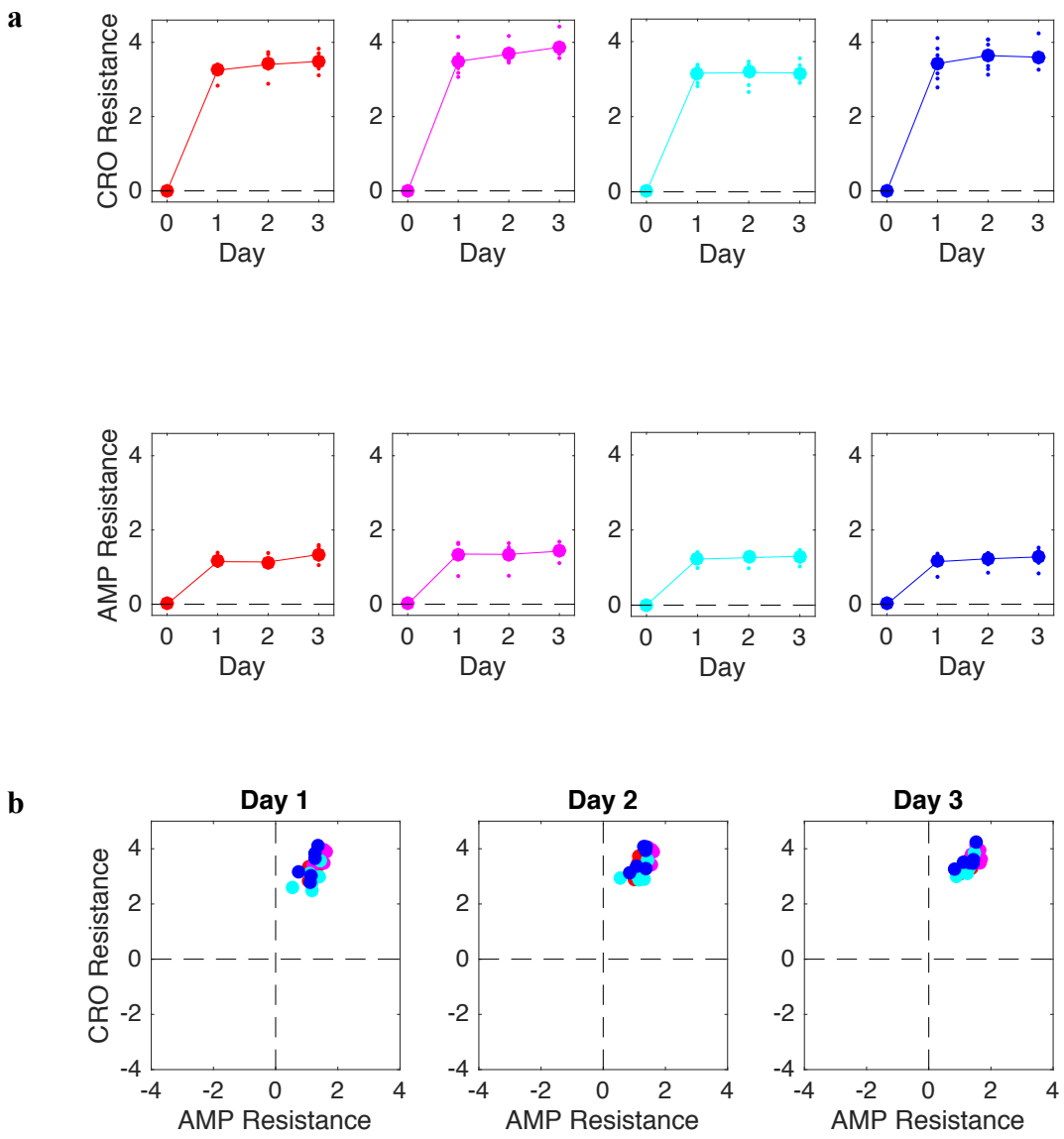

Figure 2.5: Mutants Across All Conditions Exhibit Strong Ceftriaxone Resistance and Moderate Ampicillin Resistance. a. Resistance to ceftriaxone (CRO, top panels) and ampicillin (AMP, bottom panels) over time for populations evolved under 4 conditions: condition 1 [CRO] = 48.51ug/mL, and [AMP]=0 (red point in Figure 2.1), condition 2 [CRO] = 1.29ug/mL, and [AMP]=0.102ug/mL (cyan point in Figure 2.1), condition 3 [CRO] = 2.59ug/mL, and [AMP]=0.051ug/mL (magenta point in Figure 2.1), and condition 4 [CRO] = 0, and [AMP]=0.431ug/mL (blue point in Figure 2.1). Resistance to each drug is defined as the log2 scaled ratio of IC50 values between mutant and wild-type (ancestral) cells, with positive values indicating increased resistance and negative values increased sensitivity. Small points correspond to individual mutants, while large points are the population mean across mutants (N=6 mutants). **b.** Two-dimensional representation of joint drug resistance at each day of the laboratory evolution. Each point corresponds to a single mutant, with time moving from left (Day 1) to right (Day 4).

Interestingly, we find that the populations quickly find high-level resistance to ceftriaxone (Figure 2.5a, top panel) and slightly lower-level resistance to ampicillin (Figure 2.5a, bottom panel), regardless of the condition. Indeed, all populations show increased resistance to both drugs, a fact that is perhaps not surprising given the drugs' similar mechanisms of action. However, what is surprising is that the level of resistance in all four conditions is the same even though different conditions correspond to considerably different concentrations and exhibit different rates of growth adaptation. One might naively expect the cells to evolve to higher resistance levels with higher concentrations of drug.

To reconcile these apparently contradictory results, we assume that the effect of a mutation is to rescale the effective drug concentration, so that the mutant "experiences" a different concentration than the wild-type (see Section 1.4). With this assumption, we can use the drug interaction surface measured in drug sensitive cells (Figure 2.1) to estimate how a particular mutation--which corresponds to a specific rescaling-- would impact growth at each condition. In Figure 2.6, we use the exact same rescaling at all conditions and try to understand why the effects (growth) are different.

Our IC50 results indicated that on average, AMP increases resistance by 2.5X and CRO by 11.9X in day 4 mutants. Hence, we rescale the concentration of AMP by 2.5 and the concentration of CRP by 11.9 for each condition (Figure 2.6, arrows). Despite the fact that the same rescaling is used for each condition, Figure 2.6 indicates that the final growth rate is expected to differ in a condition-dependent manner. Most notably, the rescaling results in higher growth for conditions containing both drugs (magenta and cyan) than for single drug conditions, consistent with the trends observed experimentally (Figure 2.4b).

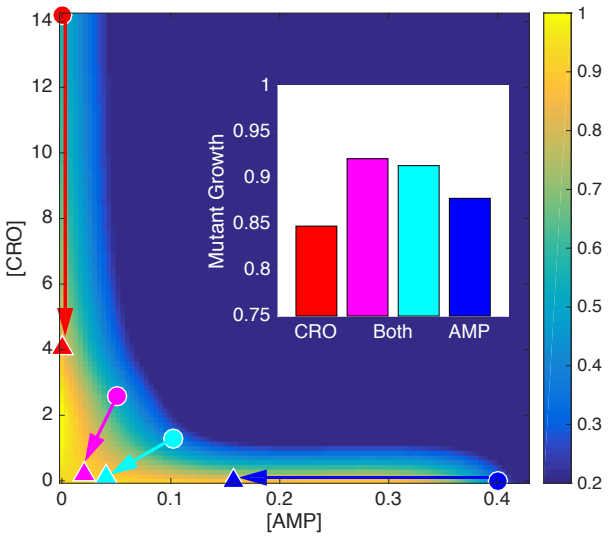

Figure 2.6: Rescaling of Drug Concentrations Point to Cross-Resistance and Accelerated Resistance Adaptation of Ceftriaxone-Ampicillin Combination. Smoothed drug interaction plot of ceftriaxone-ampicillin combination with arrows indicating rescaling of drug concentrations of each condition after 4 days of evolution. Adjusted growth of mutants from each condition shown in inset. Original concentration of four conditions: Condition 1: ([CRO],[AMP])=(48.51, 0) (red); Condition 2: ([CRO],[AMP])=(2.59, 0.051) (magenta); Condition 3: ([CRO],[AMP])=(1.29, 0.102) (cyan); Condition 4: ([CRO],[AMP])=(0, 0.43) (blue). Colors from blue to yellow represent growth rates.

2.6 Conclusion

Combination therapy with ampicillin and ceftriaxone is a potentially powerful clinical option for treating *E. faecalis* infections, in part because strong synergy between the drugs allows for potent inhibitory action at relatively low doses. Using large-scale laboratory evolution experiments, we quantified in vitro adaptation to different dosage combinations spanning several days. Our results reveal accelerated growth adaption when the drugs are combined, underscoring an underappreciated limitation to treatments based on this combination. Despite significant

differences in the adaptation rates between populations exposed to single drugs and drug combinations, we found strong correlations between phenotypic resistance to ampicillin and ceftriaxone, regardless of the selecting condition. These results suggest that a common genetic mechanism may underlie adaptation in all conditions. Our results are intriguing because they illustrate how growth rate adaption may depend dramatically on drug dosage, even when levels of phenotypic resistance (IC_{50}'s)—and perhaps, genetic mechanisms of resistance—show remarkably similar dynamics. In the long term, our results may lay the groundwork for improved combination therapies based on trade-offs between inhibitory potential and evolutionary adaptation.

Chapter 3: Antagonistic Interaction – Ampicillin plus Streptomycin

3.1 Introduction

Streptomycin is rarely used in a single-drug therapy for enterococcus due to poor intracellular penetration of aminoglycosides. However, despite this limitation, therapies combining an aminoglycoside with a cell wall inhibiting antibiotic can be strongly synergistic and are commonly used for treating drug resistant strains (Kak et al. 2000; Murray 2018). In particular, the ampicillin and streptomycin combination has been a first line of treatment for infections (endocarditis) in *E. faecalis* (Murray 2018; Kristich, Rice, and Arias 2014). However, enterococci isolates are increasingly exhibiting high-level resistance to aminoglycosides, which has been shown to reduce the synergistic effect of the combination therapy (Kak et al. 2000; Kristich, Rice, and Arias 2014; Fernández-Hidalgo et al. 2013). In general, aminoglycoside resistance is a growing problem, but little is known about how high-level aminoglycoside resistant *E. faecalis* cells adapt to combination therapies.

In this chapter, we evolve dozens of replicate populations to ampicillin and streptomycin alone and in combination over several days. Our results indicate that the streptomycin-ampicillin combination is antagonistic in strains (V583) exhibiting high-level aminoglycoside resistance. More importantly, using the drugs in combination results in significantly slowed growth adaptation, indicating that aminoglycoside + beta lactam combinations may remain feasible even for strains with high-level aminoglycoside resistance. Furthermore, IC50 measurements demonstrate drugs alone lead to evolutionary "solutions" that result in competition between cross-resistance and collateral sensitivity. Thus, competing solutions result in lower adaptation

rates for the combination. While synergy is typically considered the underlying reason for short-term efficacy in aminoglycoside-sensitive cells, our results suggest that the antagonism observed in aminoglycoside-resistant cells may render the therapies stable against adaptation on longer timescales.

3.2 Ampicillin and Streptomycin Combination Gives Rise to Antagonistic Interaction

To better understand evolution in ampicillin-streptomycin combinations, we first measured the per capita growth rate (as in chapter 2) of *E. faecalis* strain V583 in liquid cultures exposed to a large range of drug doses. Note that strain V583 exhibits high level aminoglycoside resistance (Gavaldà et al. 2003, 2007; Fernández-Hidalgo et al. 2013; Pericas et al. 2014). We expected a synergistic interaction however to our surprise, we observed an antagonistic interaction between the two drugs, as indicated by the concave (down) contours of the growth isoboles (Figure 3.1a; raw data; 3.1b smoothed data).

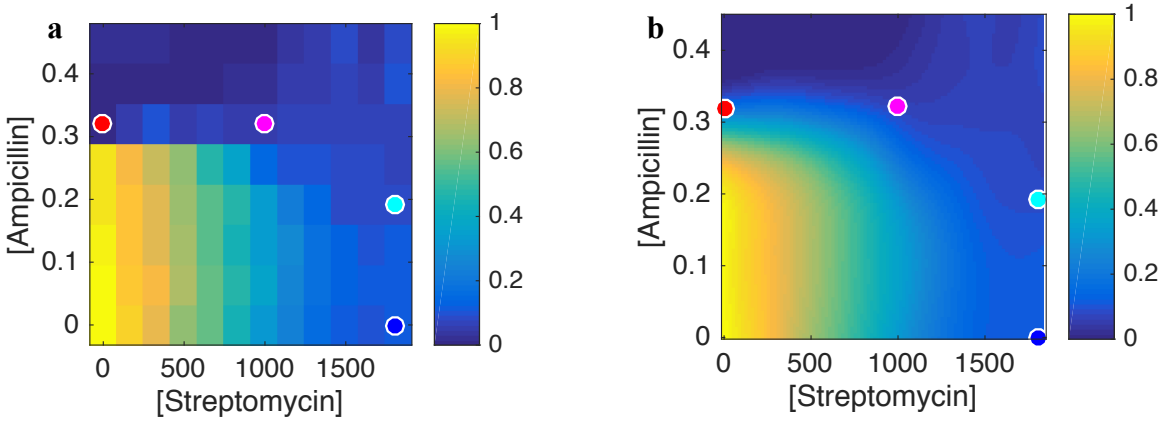

Figure 3.1: Ampicillin and Streptomycin Combination Gives Rise to Antagonistic Interaction in *E. faecalis*. **a.** Interaction with colors representing per capita growth rate as a function of two drug concentrations space. Four dots correspond to mutants selected with the same selective pressure at ~30% inhibition of growth with four different drug conditions. The first condition (in red) corresponds to [AMP] = 0.32ug/mL and [STR]=0, the second condition (in magenta) corresponds to [AMP] = 0.321ug/mL, and [STR]=1000ug/m, the third condition (in cyan) corresponds to [AMP] = 0.192ug/mL, and [STR]=1800ug/mL, and the fourth condition (in blue) correspond to [AMP] = 0, and [STR]=1800ug/mL. Each condition is evolved over 4 days with N=24 mutants per condition, in 96 well plates. **b.** Smoothed version of interaction. Colors from blue to yellow represent growth rates. See methods for smoothing details.

Given that the contour lines of this interaction are bowed out similar to the cartoon example of an antagonistic interaction in Figure 1.2 of Chapter 1, we can conclude an antagonistic interaction. While the mechanism of antagonistic interactions is not completely understood, the high-level resistance of the V583 strain to streptomycin may contribute to the shift from the normal synergistic interaction of the combination (Aslangul et al. 2006; Gavaldà et al. 2003).

After identifying the combination's inhibitory effects over a wide range of doses, we set out to measure the evolutionary adaptation to this drug pair over a longer period. As in previous chapters, we controlled for potential differences in selection pressure by choosing four dosage combinations (two corresponding to single drug treatments and two to drug combinations) that lie along a contour of constant inhibition (Figure 3.1).

3.3 Mutants Evolve in the presence of Ampicillin and Streptomycin Combination

We performed lab evolution, as described in Chapter 2, by evolving twenty-four (24) replicate populations of *E. faecalis* at each of the four conditions for a total of 3 days. The first day (blue) and last day OD (red) growth curves are shown in Figure 3.2. It is evident from these plots that growth of single drugs (red and blue axes) conditions were significantly increased by the last day of evolution, consistent with evolved resistance to one or more drugs, while growth in combination (magenta and cyan axes) seem to be much slower.

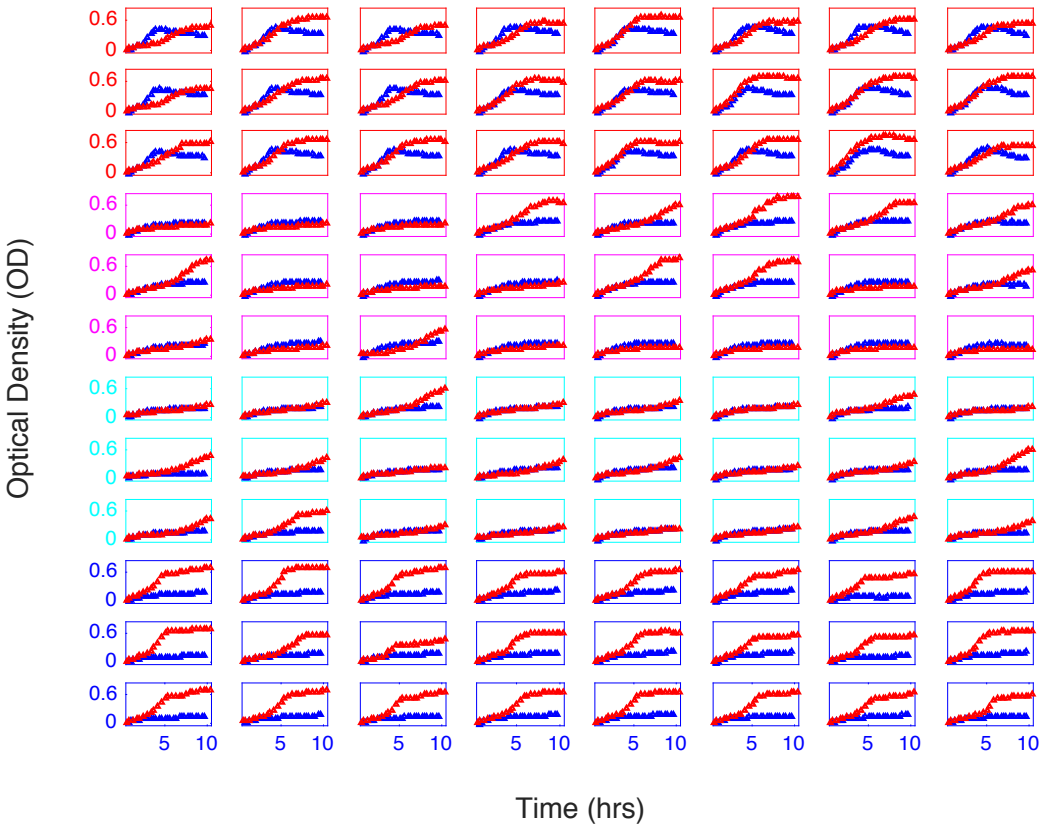

Figure 3.2: Growth Curves of Day 1 and Day 3 for All Mutants Indicate Resistance at a Glance. Optical density time series measured in liquid cultures of *E. faecalis* on the first (blue) and last (red) day of laboratory evolution. Plots are arranged in 4 groups of 24 (three rows) corresponding to the four different conditions in Figure 3.1. Rows 1-3: (AMP],[STR])=(0.320, 0) (red axes); Rows 4-6: ([AMP],[STR])=(0.321, 1000) (magenta axes); Rows 7-9: ([AMP],[STR])=(0.192, 1800) (cyan axes); Rows 9-12: ([AMP],[STR])=(0, 1800) (blue axes). All concentrations are given in micrograms per mL.

3.4 Combinations of Ampicillin and Streptomycin Leads to Slower Evolution of Resistance

To measure growth rate adaption over all 3 days, we estimated the per capita growth rate for each OD times series using nonlinear least squares fitting to an exponential function (see Methods). We can see in Figure 3.3 that the growth of each population is similarly inhibited on day one, as expected—consistent with our choice of dosage conditions providing constant inhibition levels. Meanwhile, the growth rate varies considerably after Day 1, with mutants in each condition responding differently. Similar to previous growth rate plots (Figures 2.3), some

populations exhibit fast adaption and approach wild-type drug-free levels within one day, while others increase slowly or not at all.

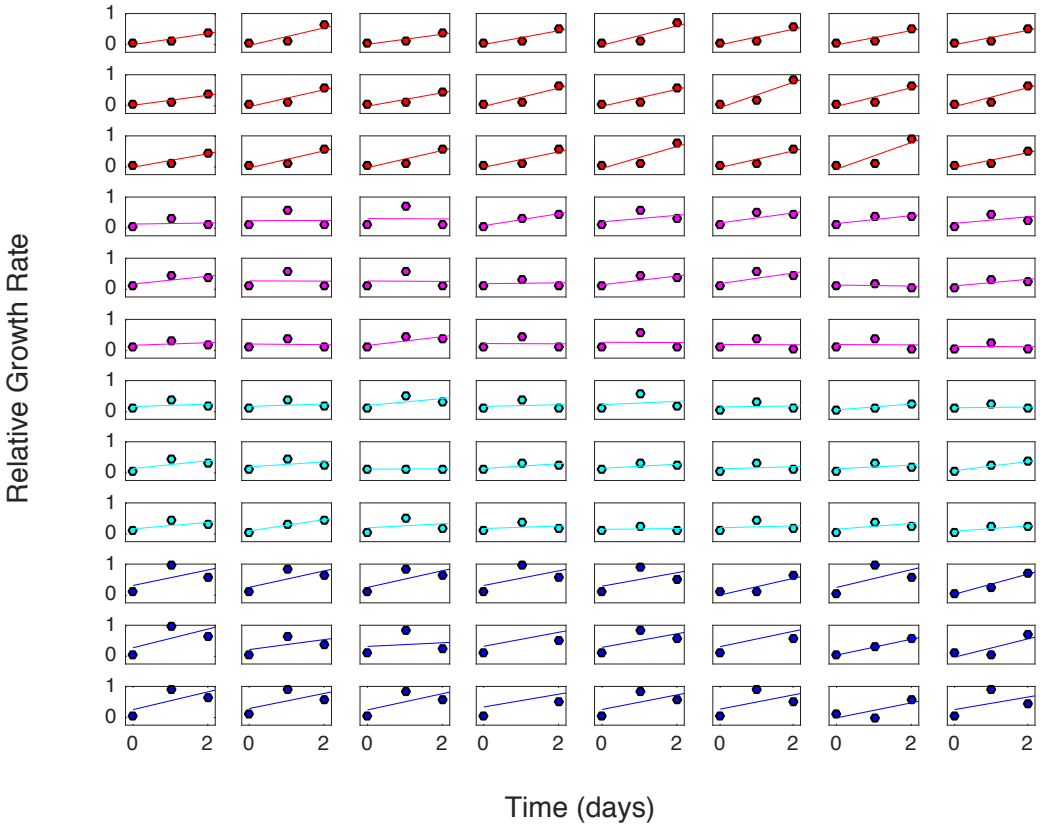

Figure 3.3: Growth Rate Adaptation Over 3 days of Evolution for All Mutants. Per capita growth rate of *E. faecalis* cultures over 3 consecutive days of laboratory evolution. Rows 1-3: (AMP],[STR])=(0.320, 0) (red axes); Rows 4-6: ([AMP],[STR])=(0.321, 1000) (magenta axes); Rows 7-9: ([AMP],[STR])=(0.192, 1800) (cyan axes); Rows 9-12: ([AMP],[STR])=(0, 1800) (blue axes). Adaptation rate for each mutant is given by the slope of the best-fit (least-squares) trend line through the relative growth rate time series. All concentrations are given in micrograms per mL.

We can better interpret these trends by separating the populations by condition and plotting the growth rate over time for each population (Figure 3.4a; small points) as well as the mean growth rate across all mutants in a given condition (Figure 3.4a; large points). Adaptation to AMP only (left panel, red) is gradual, with biggest step increase by day 3, while adaption to

STR alone (right panel, blue) increases rapidly by day 2 but plateaus, or even slightly decreases (on average), at day 3. Interestingly, however, adaption in both conditions containing two drugs (middle panels, magenta and cyan) is much slower, with both exhibiting low level growth on day 2 and slightly decreased growth on day 3. To better understand these trends, we estimated the rate of growth adaptation for each population (Figure 3.4b). On average, growth rate adaptation is significantly slower for the drug combinations (magenta and cyan) than for the individual drugs (red and blue) (student t-test, $p<0.001$ for all pair combinations between 2-drug and 1-drug conditions).

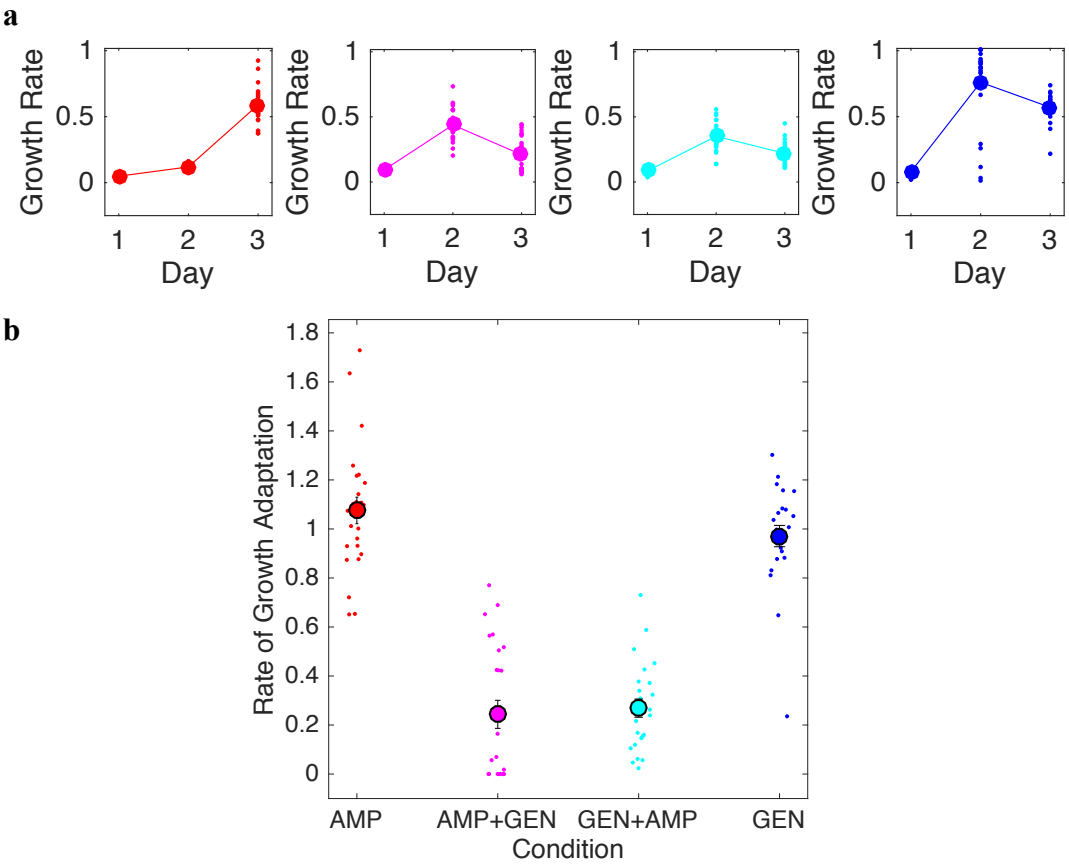

Figure 3.4: Combinations of Ampicillin and Streptomycin Leads to Slower Evolution of Resistance in *E. faecalis*. a. Adaptation time series (per capita growth rate) over 3 days of evolution, in each of the 4 conditions: condition 1 [AMP] = 0.321ug/mL, and [STR]=0 (red point in Figure 3.1), condition 2 [AMP] = 0.321ug/mL, and [STR]=1000ug/mL (cyan point in Figure 3.1), condition 3 [AMP] = 0.192ug/mL, and [STR]=1800ug/mL (magenta point in Figure 3.1), and condition 4 [AMP] = 0, and [STR]=1800ug/mL (blue point in Figure 3.1). Small points represent individual mutants. Large circles are means taken across all mutants in a given condition (N=24 mutants). **b.** Growth adaptation rate for each condition; the units of adaptation are growth rate/day, where growth rate is measured in units such that the ancestral strains grow at a rate of 1 in the absence of drug. As an example, an adaptation rate of 0.25 means it takes, on average, 3 days of adaption for the strains to fully adapt to the drug (i.e. to reach the drug-free growth rate of ancestral cells). Small points correspond to individual mutants; large points represent the mean of all mutants in a given condition.

3.5 Characterizing Resistance Levels of Selected Mutants to Individual Drugs

To further dissect the growth rate adaption observed and understand the population's slower growth adaptation in higher concentrations of both drugs, we measured resistance (IC_{50}) to each drug across all conditions. Similar to previous experiments we selected 6 populations for each condition and directly measured the half-maximal inhibitory concentration (IC_{50}) of each drug. Our results indicate that mutants evolved to drugs alone exhibited resistance to the selecting drug but, at day 3, show little to no collateral effects to the second drug (Figure 3.5a, red and blue plot). When the drugs are used in combination, cross-resistance is observed in both conditions, albeit at different levels (Figure 3.5a, magenta and cyan plot). In particular, resistance is lower to the drug used at the lower concentration in each mixture, indicating that resistance is driven by the more dominant drug in each of the two combinations. For example, in condition 2 (Figure 3.5a, magenta plot) we observe increased resistance to AMP and slightly lower resistance to STR. Similarly, condition 3 (Figure 3.5a, cyan plot) leads to increased resistance to STR and much lower resistance to AMP. Because collateral effects are relatively weak in this example, the decrease in adaptation rate when the drugs are used in combination must arise primarily from the drug interaction. As an example, compare the day 3 results between conditions 1 (red) and 2 (magenta). While the resistance levels to both drugs are virtually identical on day 3 (see top row, leftmost two panels of Figure 3.5a), the growth is significantly higher in ampicillin only (Figure 3.4a, leftmost two panels). The selecting concentration of ampicillin is approximately equal in the two conditions—because of the antagonism between drugs, the addition of STR in condition 2 yields no additional inhibition. But despite the lack of inhibitory effect, the addition of STR dramatically slows adaptation of growth, revealing an evolutionary advantage of the antagonistic interaction.

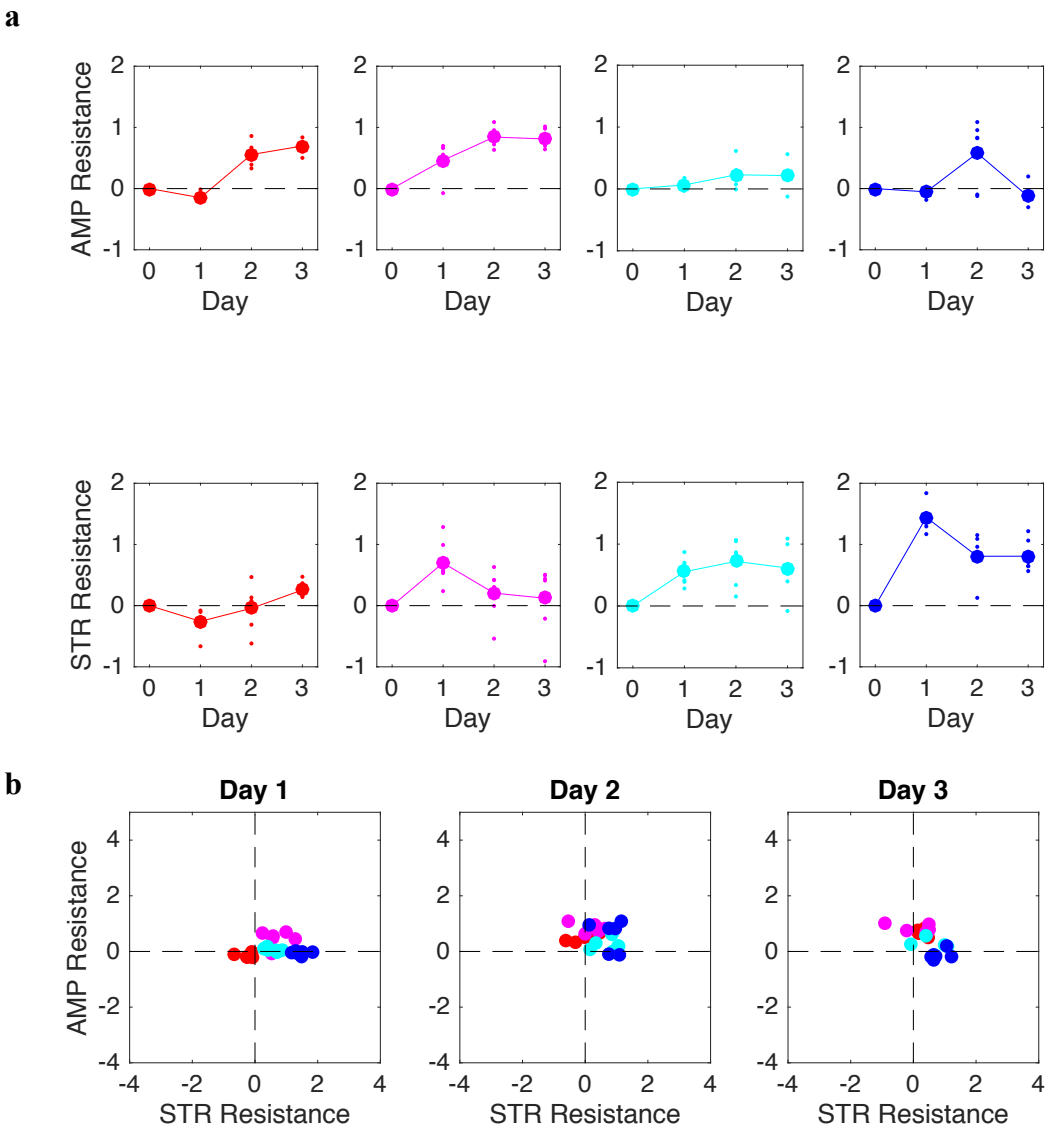

Figure 3.5: Resistance of Mutants to Ampicillin Decreases with Streptomycin Dominant Combination. a. Resistance to ampicillin (AMP) over time for populations evolved under 4 conditions: condition 1 [AMP] = 0.321ug/mL, and [STR]=0 (red point in Figure 3.1), condition 2 [AMP] = 0.321ug/mL, and [STR]=1000ug/mL (cyan point in Figure 3.1), condition 3 [AMP] = 0.192ug/mL, and [STR]=1800ug/mL (magenta point in Figure 3.1), and condition 4 [AMP] = 0, and [STR]=1800ug/mL (blue point in Figure 3.1). Small points represent individual mutants. Large circles are means taken across all mutants in a given condition (N=24 mutants). **b.** Two-dimensional representation of joint drug resistance at each day of the laboratory evolution. Each point corresponds to a single mutant, with time moving from left (Day 1) to right (Day 3).

3.6 Conclusion

Combination therapy with ampicillin and streptomycin is a potentially powerful clinical option for treating *E. faecalis* infections, in part because strong synergy between the drugs allows for potent inhibitory action at relatively low doses. However, this synergistic effect is often thwarted in the presence in *E. faecalis* cells with high-level aminoglycoside resistance, making this combination less likely to be utilized in clinical settings. Using large-scale laboratory evolution experiments, we quantified in vitro adaptation to different dosage combinations spanning several days. Our results reveal slower growth adaption when the drugs are combined, underscoring an underappreciated evolutionary advantage to this combination when the synergy has been eliminated. Slowed adaptation appears to be driven by the antagonistic interaction between the drugs, as IC50 results indicate weak levels of cross-resistance and collateral sensitivity. Overall, these results suggest that aminoglycoside + beta lactam combinations may be viable options even for strains with high-level aminoglycoside resistance, where the resulting antagonism has the unexpected benefit of stabilizing the combination against adaptation.

Chapter 4: Antagonistic Interaction 2 – Ceftriaxone plus Ciprofloxacin

4.1 Introduction

Ciprofloxacin is a member of the quinolone class of antibiotics, and resistance to quinolone in enterococci often occurs through target modifying mutations or multidrug efflux. (Miller, Munita, and Arias 2014; Arsène and Leclercq 2007;.Miller, Munita, and Arias 2014). While not used alone in the treatment of enterococci, ciprofloxacin combined with a beta-lactam has been successful in the treatment of human endocarditis infection with high-level aminoglycoside resistance in *E. faecalis* (Tripodi et al. 1998). In this chapter, we investigate evolution of *E. faecalis* exposed to combinations of ciprofloxacin and ceftriaxone, a beta lactam that—like ciprofloxacin—is not typically used in single-drug therapies (Arbeloa et al. 2004; Kristich, Rice, and Arias 2014). We show the combination to be antagonistic, making it an unlikely a priori choice for clinical treatment. However, our results indicate dramatically slowed growth adaption when the drugs are combined, highlighting an unappreciated advantage in antagonistic interactions in clinical therapy for *E faecalis*. Furthermore, we show that resistance to single drug treatments results in collateral sensitivity to the other drug, an effect that—along with the antagonistic interaction—leads to slowed evolutionary adaptation to the combination.

4.2 Ceftriaxone and Ciprofloxacin Combination Gives Rise to Antagonistic Interaction in *E. faecalis*

Evolution in ceftriaxone-ciprofloxacin combinations was measured using *E. faecalis* strain V583 in liquid cultures was exposed to a large range of drug doses. We observed an

antagonistic interaction between the two drugs, as indicated by the concave contours of the growth isoboles (Figure 4.1a, raw data; 4.1b smoothed data). To understand why the combination is considered antagonistic, consider the growth in the presence of 25ug/mL of ceftriaxone and 0.15ug/mL of ciprofloxacin in Figure 4.1a. At such concentration, the drugs alone have a ~50-70% inhibition effect. However, when the drugs are combined, the result is an approximately 70% inhibition effect—that is, the combination does not inhibit growth much more than one of the drugs alone.

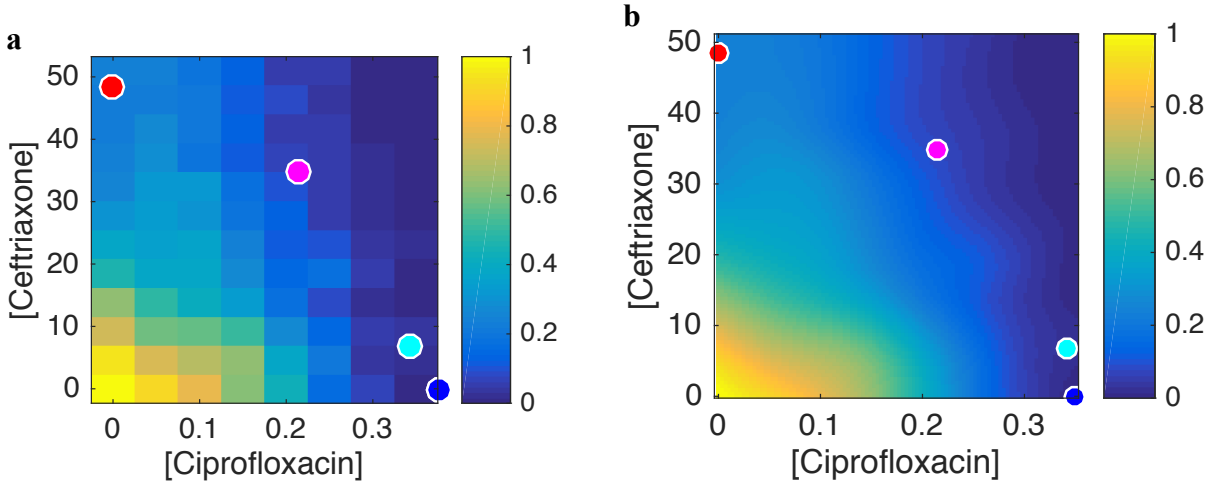

Figure 4.1: Ceftriaxone and Ciprofloxacin Combination Gives Rise to Antagonistic Interaction in *E. faecalis*. **a.** Interaction with colors representing per capita growth rate as a function of two drug concentrations space. Four dots correspond to mutants selected with the same selective pressure at ~30% inhibition of growth with four different drug conditions. The first condition (in red) correspond to [CRO] = 48.51ug/mL, and [CIP]=0, the second condition (in cyan) correspond to [CRO] = 6.93ug/mL, and [CIP]=0.342ug/mL, the third condition (in magenta) correspond to [CRO] = 34.65ug/mL, and [CIP]=0.214ug/mL, and the fourth condition (in blue) correspond to [CRO] = 0, and [CIP]=0.4633ug/mL. Each condition is evolved over 4 days with N=24 mutants per condition, in 96 well plates. **b.** Smoothed version of interaction. Colors from blue to yellow represent growth rates. See methods for smoothing details.

After measuring the drug interaction, we selected four dosage combinations for longer-term evolution. We chose four dosage combinations—two corresponding to single drug treatments and two to drug combinations—to lie along a contour where growth is approximately 30% of the native (drug free) growth (Figure 4.1). Keeping initial inhibition levels constant across all four conditions allowed us to interpret any differences in resistance adaptation as a reflection of drug concentration differences.

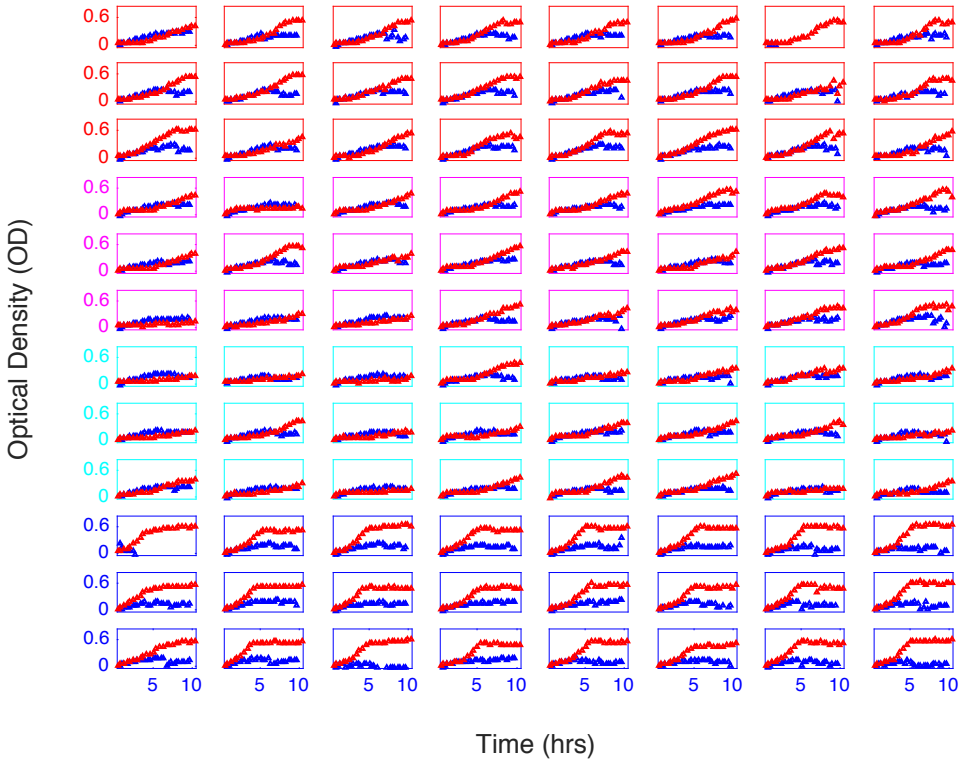

Figure 4.2: Growth Curves of Day 1 and Day 4 for All Mutants Indicate Resistance at a Glance. Optical density time series measured in liquid cultures of *E. faecalis* on the first (blue) and last (red) day of laboratory evolution. Plots are arranged in 4 groups of 24 (three rows) corresponding to the four different conditions in Figure 4.1. Rows 1-3: ([CRO],[CIP])=(48.51, 0) (red axes); Rows 4-6: ([CRO],[CIP])=(6.93, 0.342) (magenta axes); Rows 7-9: ([CRO],[CIP])=(34.65, 0.214) (cyan axes); Rows 9-12: ([CRO],[CIP])=(0, 0.4633) (blue axes). All concentrations are given in micrograms per mL.

4.3 Mutants Evolve in the Presence of Ceftriaxone and Ciprofloxacin Combination

We evolved twenty-four (24) replicate populations of *E. faecalis* at each of the four conditions for a total of 4 days. The first day (blue) and last day OD (red) growth curves are shown in Figure 4.2. We observe that the population of cells in one of the single drug conditions (blue) has a faster overall growth by day 4 followed by a higher growth towards the end of the day by the second single drug condition (red), while both combination conditions (magenta and cyan) were slowest. In general, most of the population in this drug pair demonstrated growth adaptation, albeit at different levels depending on condition.

4.4 Combinations of Ceftriaxone and Ciprofloxacin Leads to Slower Rate of Growth Adaptation

To further quantify growth rate adaption, we fit each OD time series to an exponential function (see Methods) to estimate the per capita growth rate at each curve. In Figure 4.3 we can see that the growth of each population is similarly inhibited on day one—consistent with the choice of dosage conditions providing constant inhibition levels. By contrast, the growth rate varies after Day 1, with mutants in each condition responding differently. Some populations indicate a very rapid adaption and approach wild-type drug-free levels within one day, while others increase slowly or not at all.

To further understand these dynamic, we separated the populations by condition and plotted the growth rate over time for each population (Figure 4.4a; small points) as well as the mean growth rate across all mutants in a given condition (Figure 4.4b; large points). First, consider the cases where the drugs are used alone. Adaptation to CRO only (left panel, red) is initially fast followed by gradual increase on days 3 and 4, while adaption to CIP only (right

panel, blue) rapidly increases after day 1 and plateaus by day 3 and 4. By contrast, the adaption in both conditions containing the drugs together (middle panels, magenta and cyan) is much slower, with both exhibiting substantial growth only at day 4 of the evolution.

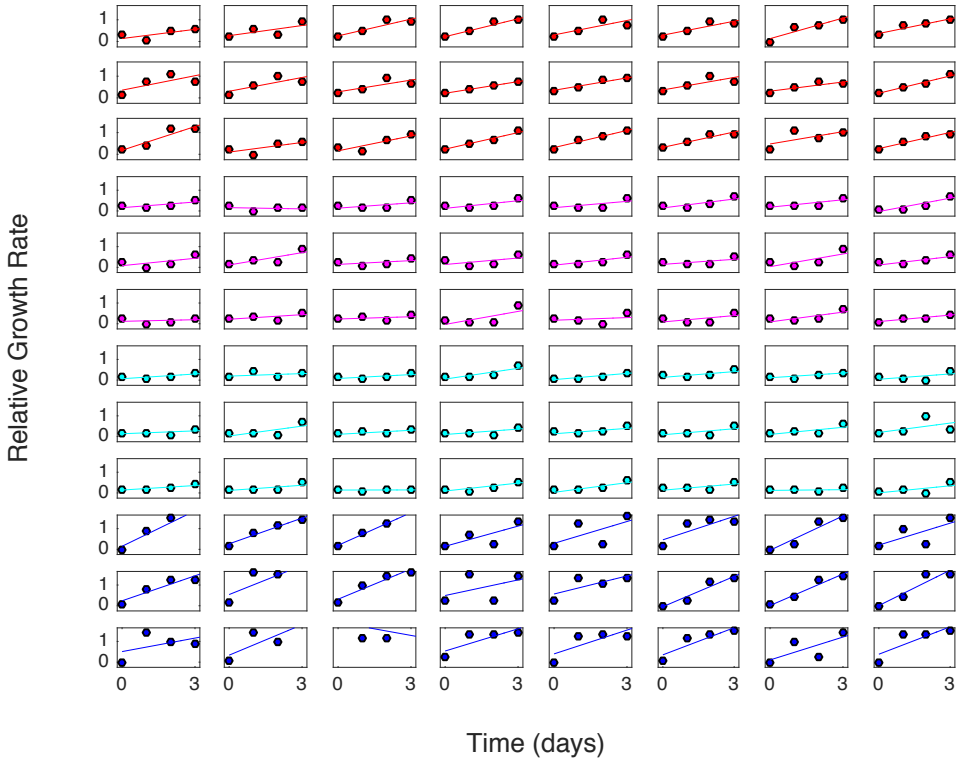

Figure 4.3: Growth Rate Adaptation Over 4 days of Evolution for All Mutants. Per capita growth rate of *E. faecalis* cultures over 4 consecutive days of laboratory evolution. Rows 1-3: ([CRO],[CIP])=(48.51, 0) (red axes); Rows 4-6: ([CRO],[CIP])=(6.93, 0.342) (magenta axes); Rows 7-9: ([CRO],[CIP])=(34.65, 0.214) (cyan axes); Rows 9-12: ([CRO],[CIP])=(0, 0.4633) (blue axes). Adaptation rate for each mutant is given by the slope of the best-fit (least-squares) trend line through the relative growth rate time series. All concentrations are given in micrograms per mL.

To quantify these trends, as described in Chapter 2, we estimated the rate of growth adaptation r— defined as the slope of the best-fit trend line through the relative growth rate time series—for each population (Figure 4.4b). Growth rate adaptation, is significantly slower, on average, for the drug combinations (magenta and cyan) than for the individual drugs (red and

blue) (student t-test, $p<0.001$ for all pair combinations between 2-drug and 1-drug conditions). A slower growth adaption in the presence of two drugs is interesting because it highlights a highly unappreciated advantage of CRO-CIP combination therapy: even at higher dosage of drugs, the combination facilitates slower adaptation after four days of evolution.

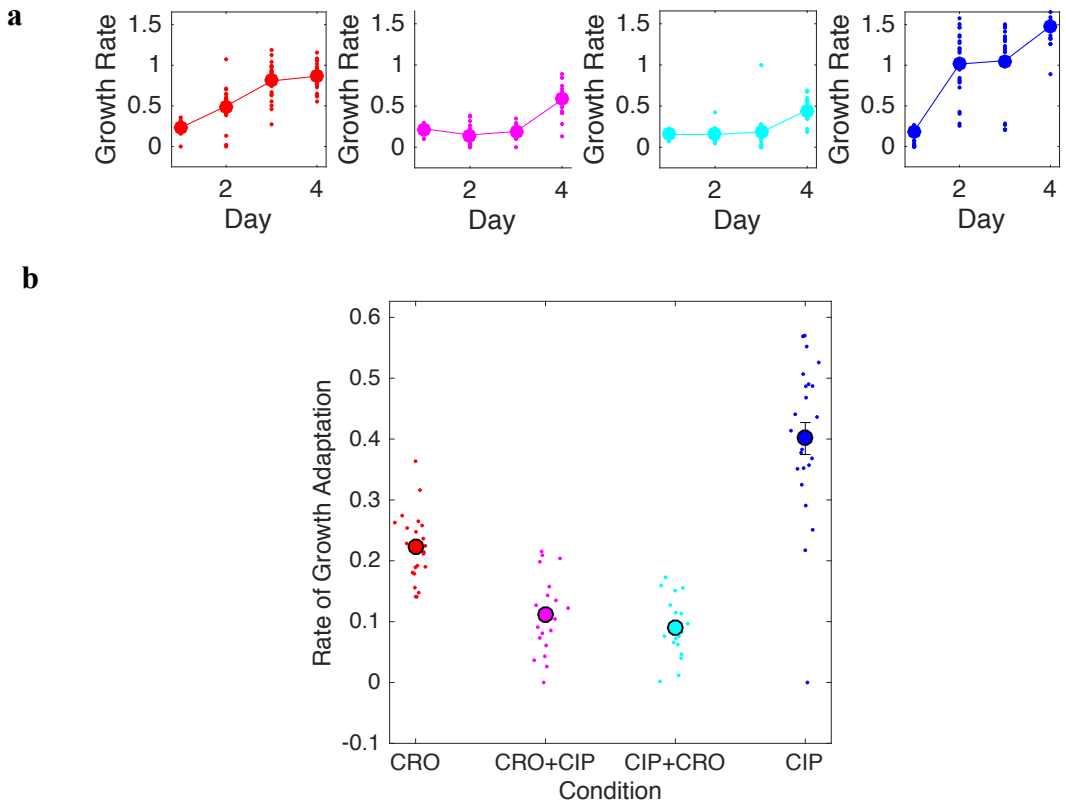

Figure 4.4: Antagonistic Combinations of Ceftriaxone and Ciprofloxacin Leads to Slower Evolution of Resistance in *E. faecalis*. a. Adaptation time series (per capita growth rate) over 4 days of evolution, in each of the 4 conditions: condition 1 [CRO] = 48.51ug/mL, and [CIP]=0 (red point in Figure 4.1), condition 2 [CRO] = 6.93ug/mL, and [CIP]=0.342ug/mL (cyan point in Figure 4.1), condition 3 [CRO] = 34.65ug/mL, and [CIP]=0.214ug/mL (magenta point in Figure 4.1), and condition 4 [CRO] = 0, and [CIP]=0.4633ug/mL (blue point in Figure 4.1). Small points represent individual mutants. Large circles are means taken across all mutants in a given condition (N=24 mutants). **b.** Growth adaptation rate for each condition; the units of adaptation are *growth rate/day*, where *growth rate* is measured in units such that the ancestral strains grow at a rate of 1 in the absence of drug. As an example, an adaptation rate of 0.25 means it takes, on average, 4 days of adaption for the strains to fully adapt to the drug (i.e. to reach the drug-free growth rate of ancestral cells). Small points correspond to individual mutants; large points represent the mean of all mutants in a given condition.

4.5 Individual Drugs Tend toward Collateral Sensitivity and Combinations Tend Toward Cross-Resistance

The slower growth rate adaptation observed for conditions with both drugs may be due to the populations' weakened ability to survive in the presence of both drugs. To investigate these dynamics, we select 6 populations for each condition and directly measured the half-maximal inhibitory concentration (IC_{50}) of each drug. These results demonstrate that mutants evolved to a single drug alone quickly become resistant to that drug, as expected. Surprisingly, however, they exhibit increased sensitivity to the second drug (Figure 4.5a, red and blue plot).

Resistance in the drug combination is quite different. When evolved in either of the conditions involving both drugs, the populations exhibit collateral resistance, with a higher relative resistance to CRO than CIP in both combinations, (Figure 4.5a, magenta and cyan plot). Although resistance to CIP in the case of the third condition (cyan) is quite variable across biological replicates, the general trend is in the direction of higher resistance. We also notice that mutants from the combination condition converge in the first quadrant of a drug-drug resistance plot by day 3, signifying cross resistance, while individual drags converge close to quadrant 2 and 4, where there is more collateral sensitivity to ciprofloxacin and ceftriaxone (Figure 4.5b). Interestingly, these results suggest that the populations are, on average, finding different evolutionary solutions to each dosage combination, with high-level resistance to each drug associated with a collateral sensitivity that makes it an untenable solution in the presence of both drugs.

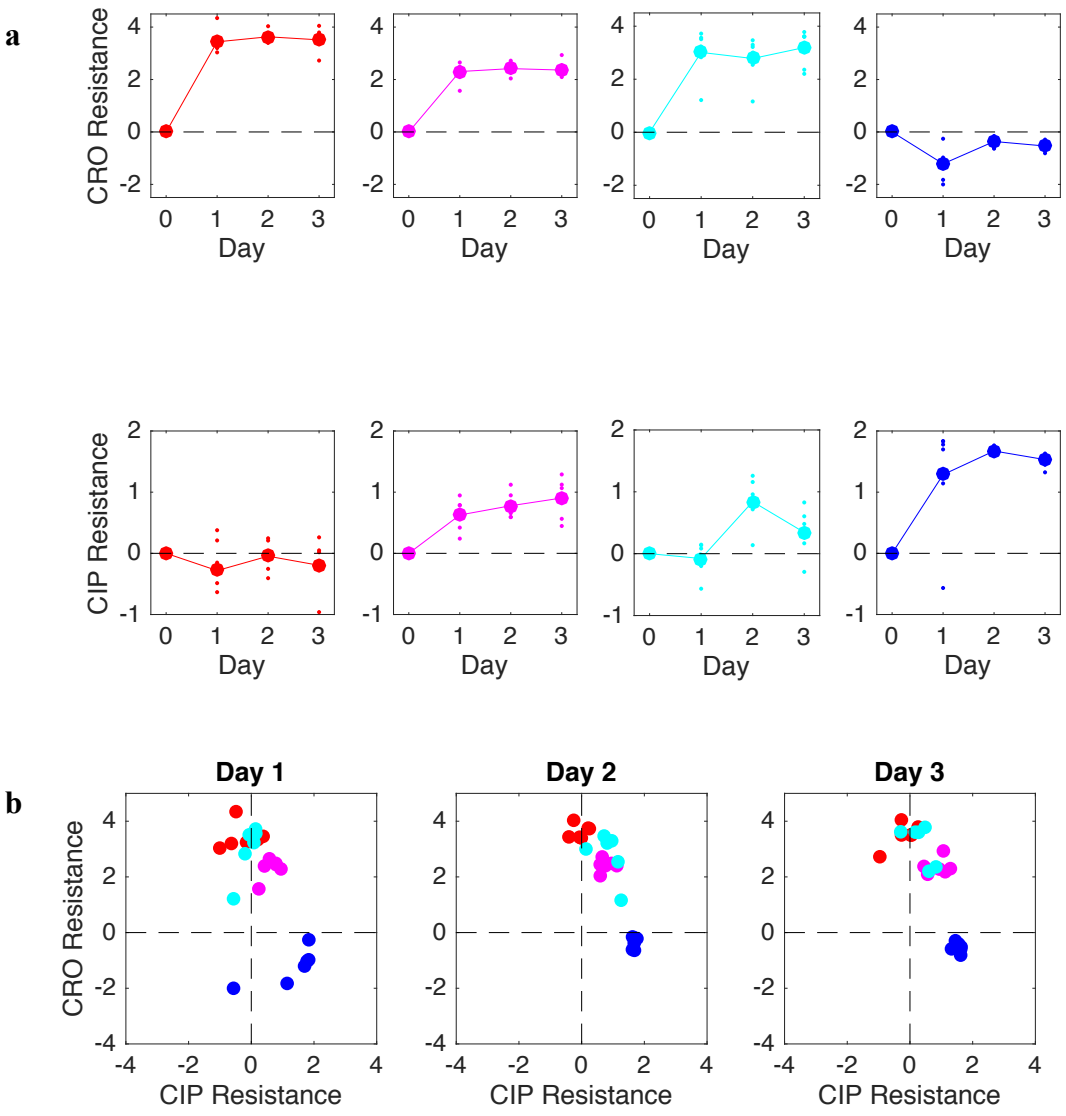

Figure 4.5: Single Drug Conditions Tend Toward Collateral Sensitivity and Combinations Tend Toward Cross-Resistance a. Resistance to ceftriaxone (CRO, top panels) and ciprofloxacin (CIP, bottom panels) over time for populations evolved under 4 conditions: condition 1 [CRO] = 48.51ug/mL, and [CIP]=0 (red point in Figure 4.1), condition 2 [CRO] = 6.93ug/mL, and [CIP]=0.342ug/mL (cyan point in Figure 4.1), condition 3 [CRO] = 34.65ug/mL, and [CIP]=0.214ug/mL (magenta point in Figure 4.1), and condition 4 [CRO] = 0, and [CIP]=0.4633ug/mL (blue point in Figure 4.1). Resistance to each drug is defined as the log2 scaled ratio of IC50 values between mutant and wild-type (ancestral) cells, with positive values indicating increased resistance and negative values increased sensitivity. Small points correspond to individual mutants, while large points are the population mean across mutants (N=6 mutants). **b.** Two-dimensional representation of joint drug resistance at each day of the laboratory evolution. Each point corresponds to a single mutant, with time moving from left (Day 1) to right (Day 3).

To understand these trade-offs, we again assume that the effect of a mutation is to rescale the effective concentration of each drug (see Section 1.4 for more details). For each condition involving both drugs (magenta and cyan, Figure 4.6), we compared the rescaling of drug concentrations observed in that condition to the rescaling observed in each of the drugs alone (blue and red). In each case, the rescaling observed in mutants exposed to CRO alone (blue) or CIP alone (red) would produce suboptimal growth when compared to the rescaling observed at that particular condition (magenta or cyan arrows). The sub-optimality of the single-drug "solutions"—each of which shows high-level resistance to one drug—arises from a combination of an antagonistic interaction and the collateral sensitivity to the other drug.

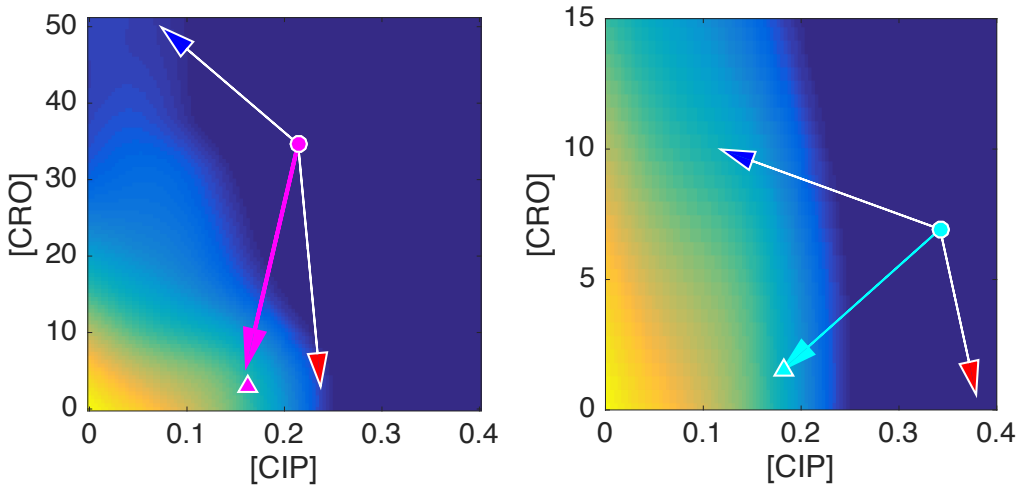

Figure 4.6: Combination Drugs Evolve to Find Most Optimal Rescaling Compared to Single Drug. The red and blue arrows represent the rescaling seen (on average) in mutants selected from the blue (CIP: 2.9X; CRO: 0.7X) and red conditions (CIP: 0.9X; CRO: 11.8X), respectively. The magenta (or cyan, depending on the panel) arrow is the average rescaling of the mutants selected from the magenta (CIP: 1.3X; CRO: 11.8X) or cyan condition (CIP: 1.9X; CRO: 4.5X). Colors from blue to yellow represent growth rates.

4.6 Conclusion

Treating enterococcus infections with high-level aminoglycoside resistance is an ongoing and serious clinical challenge. One potential option involves combining ciprofloxacin with a beta

lactam, a multi-drug therapy with demonstrated efficacy against *E. faecalis* endocarditis (Tripodi et al. 1998). While past studies have used ampicillin, rather than ceftriaxone, as the beat lactam in the combination, the results of this chapter motivate continued investigation of ceftriaxone in combination therapies—specifically with fluoroquinolones—despite its ineffectiveness as a solo agent. Such combinations would potentially require high doses of one or both drugs, yet our results point to several potential evolutionary advantages of the combination. First, high level resistance to each drug can be associated with collateral sensitivity to the other drug, potentially slowing the evolutionary adaptation in combination treatments. In addition, the drugs interact antagonistically, reducing their inhibitory effects (at a given concentration) upon initial treatment but potentially slowing adaption due to the convexity of the 2-drug growth surface. Our results are intriguing because they illustrate how both growth rate adaption and phenotypic resistance (IC_{50}'s) may depend dramatically on drug dosage, even when inhibition level is unchanged. In the long run, we hope these results encourage further investigation of antagonistic combinations, in general, and combinations of beta lactams and fluoroquinolones, more specifically, to optimize trade-offs between inhibitory potential and evolutionary adaptation in therapies targeting enterococci.

Chapter 5: Additive Interaction – Ceftriaxone plus Ciprofloxacin

5.1 Introduction

To better understand the affects of evolution at longer time scales, we performed laboratory evolution starting from an *E. faecalis* strain that had previously been selected by increasing concentrations of ceftriaxone over approximately 30 generations. This strain, which we refer to as a high-level ceftriaxone resistant (HLCER) mutant, was then evolved in combinations of ceftriaxone and ciprofloxacin that all provide the same initial level of inhibition. Although high-level resistance to ampicillin, a beta-lactam like ceftriaxone, has been reported in literature, little is known regarding HLCER (Fontana et al. 1994). By combining ceftriaxone with ciprofloxacin we can directly compare our analysis with previous results of this combination (Chapter 4) of ancestral (drug-free wild-type) *E. faecalis* cells. Firstly, we show an additive drug interaction with this combination, a slight shift from the previously observed (weak) antagonistic interaction. Secondly, after three days of evolution, we observed slow and fast adaptation rates to ceftriaxone and ciprofloxacin alone, respectively, while the combination indicated adaptation rates in between the two extremes. Finally, our IC50 results shed light on the variable adaptation rates by indicating strong effects of collateral sensitivity and cross resistance. These results suggest that collateral effects may perhaps have a larger role to play in deriving resistance evolution at longer evolutionary timescales.

5.2 Ceftriaxone and Ciprofloxacin Combination Gives Rise to Additive Interaction in *E. faecalis*

Growth of *E. faecalis* strain V583 in liquid cultures was measured with a large range of doses of ceftriaxone-ciprofloxacin combinations. We observed an additive interaction between the two drugs, as indicated by the flat contour of the growth isoboles (Figure 5.1a, raw data; 5.1b smoothed data). To understand why the combination is considered additive, consider the growth in the presence of 800ug/mL of ceftriaxone and 0.2ug/mL of ciprofloxacin in Figure 5.1a. This point is at approximately 50% of minimum inhibitory concentration of the drugs alone. Meanwhile the drugs in combination indicate an ~50% inhibition effect, thus clearly indicating an additive interaction, where the combined effect is neither stronger nor weaker.

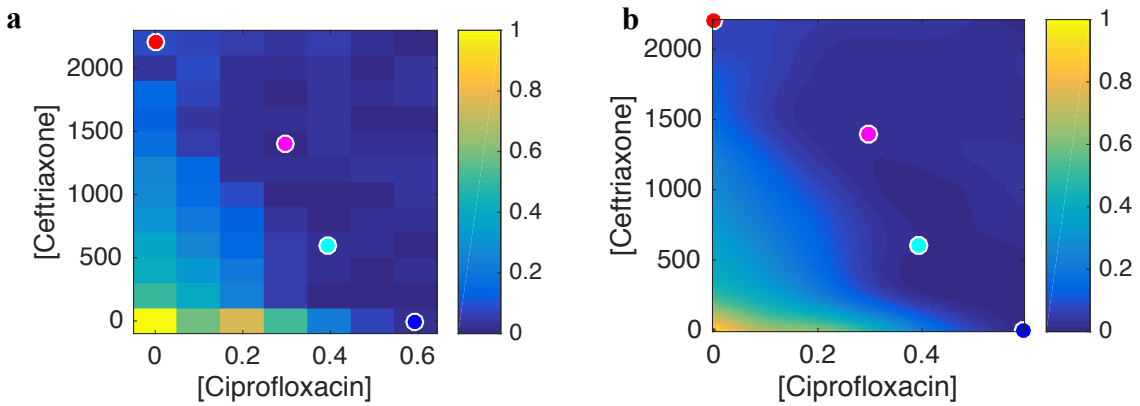

Figure 5.1: Ceftriaxone and Ciprofloxacin Combination Gives Rise to Additive Interaction in *E. faecalis*. a. Interaction with colors representing per capita growth rate as a function of two drug concentrations space. Four dots correspond to mutants selected with the same selective pressure at ~30% inhibition of growth with four different drug conditions. The first condition (in red) correspond to [CRO] = 2200ug/mL, and [CIP]=0, the second condition (in cyan) correspond to [CRO] = 1400ug/mL, and [CIP]=0.296ug/mL, the third condition (in magenta) correspond to [CRO] = 600ug/mL, and [CIP]=0.395ug/mL, and the fourth condition (in blue) correspond to [CRO] = 0, and [CIP]=0.593ug/mL. Each condition is evolved over 3 days with N=24 mutants per condition, in 96 well plates. **b.** Smoothed version of interaction. See methods for smoothing details. Note that in both plots, the red point actually lies far above the axis, at the point where ceftriaxone inhibition first reaches approximately 70%. For visualization purposes, however, we have zoomed in on the primary region of interest but keep the red point as a reminder of the CRO-only point. Colors from blue to yellow represent growth rates.

With the drug interaction measured, we then selected four dosage combinations just as in chapter 4 that provide equal levels of initial inhibition. The four dosage combinations—two corresponding to single drug treatments and two to drug combinations—lie along a contour where growth is approximately 30% of the native (drug free) growth (Figure 5.1). Keeping initial inhibition levels constant across all four conditions allowed us to interpret any differences in resistance adaptation as a reflection of drug concentration differences.

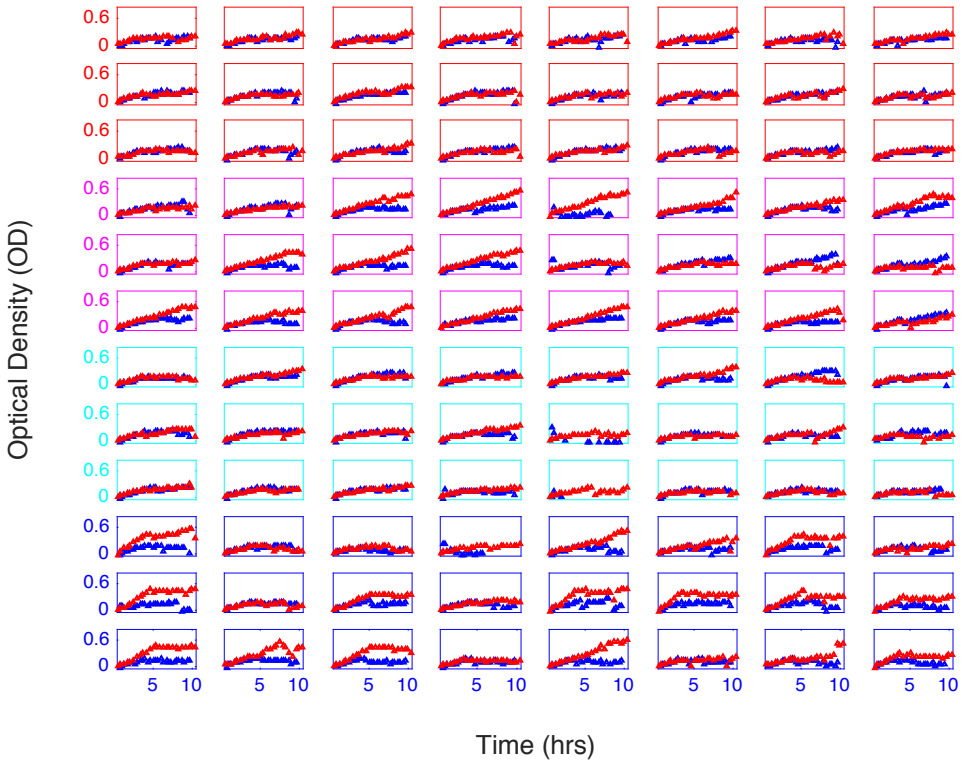

Figure 5.2: Growth Curves of Day 1 and Day 3, Most Mutants Indicate Resistance at a Glance. Optical density time series measured in liquid cultures of *E. faecalis* on the first (blue) and last (red) day of laboratory evolution. Plots are arranged in 4 groups of 24 (three rows) corresponding to the four different conditions in Figure 5.1. Rows 1-3: ([CRO],[CIP])=(2200, 0) (red axes); Rows 4-6: ([CRO],[CIP])=(1400, 0.296) (magenta axes); Rows 7-9: ([CRO],[CIP])=(600, 0.395) (cyan axes); Rows 9-12: ([CRO],[CIP])=(0, 0.593) (blue axes). All concentrations are given in micrograms per mL.

5.3 Mutants Evolve in the Presence of Ceftriaxone and Ciprofloxacin Combination

Twenty-four (24) replicate populations of *E. faecalis* at each of the four conditions was evolved for a total of 3 days. The first day (blue) and last day OD (red) growth curves are shown in Figure 5.2. We observe that the population of cells in one of the single drug and combination condition (blue and magenta, respectively) have a faster overall growth by day 3, while the second single drug and combination condition (red and cyan) were slowest. In general, most of the population in this drug pair demonstrated growth adaptation, albeit at different levels depending on condition.

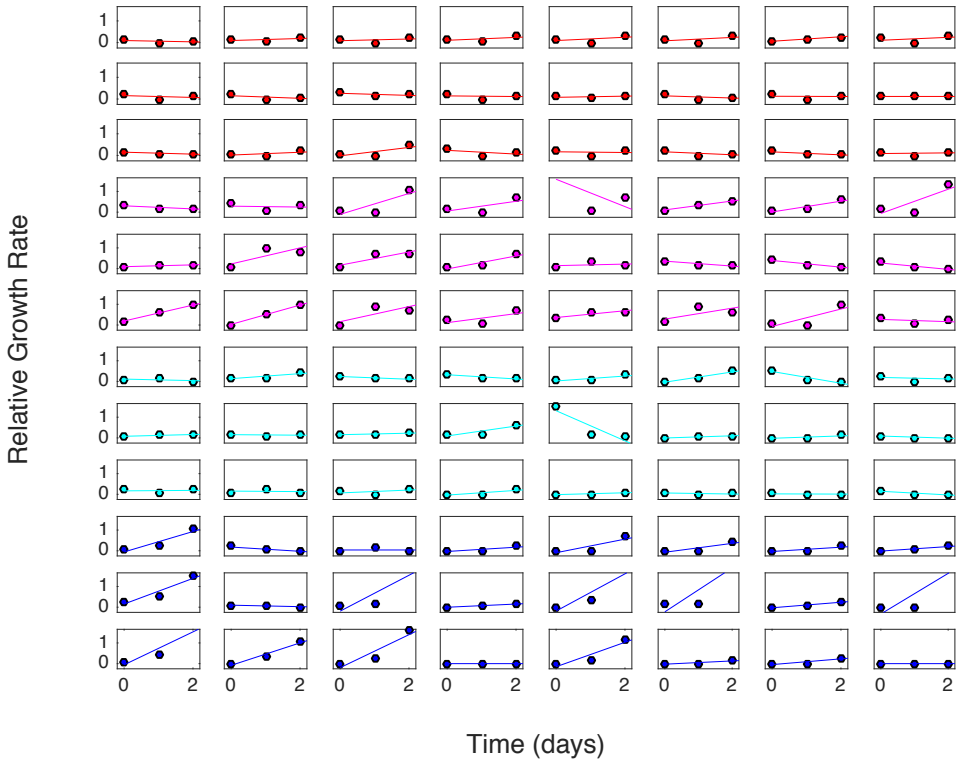

Figure 5.3: Growth Rate Adaptation Over 3 days of Evolution for All Mutants. Per capita growth rate of *E. faecalis* cultures over 3 consecutive days of laboratory evolution. Rows 1-3: ([CRO],[CIP])=(2200, 0) (red axes); Rows 4-6: ([CRO],[CIP])=(1400, 0.296) (magenta axes); Rows 7-9: ([CRO],[CIP])=(600, 0.395) (cyan axes); Rows 9-12: ([CRO],[CIP])=(0, 0.593) (blue axes). Adaptation rate for each mutant is given by the slope of the best-fit (least-squares) trend line through the relative growth rate time series. All concentrations are given in micrograms per mL.

5.4 Combinations of Ceftriaxone and Ciprofloxacin Leads to Variable Evolution of Resistance in E. faecalis.

Growth rate adaptation was quantified by fitting each OD time series to an exponential function (see Methods) to estimate the per capita growth rate at each curve. Similar to chapter 4 the growth of each population is inhibited on day one—consistent with constant inhibition levels provided by dosage condition selections. The growth rate after Day 1 varies, with mutants in each condition responding differently. Some of the populations exhibit fast adaptation and approach wild-type drug-free levels within two days, while others increase slowly or not at all.

As in previous chapters, we separated the populations by condition and plotted the growth rate over time for each population (Figure 5.4a; small points) as well as the mean growth rate across all mutants in a given condition (Figure 5.4b; large points). First, consider the cases where the drugs are used alone. Adaptation to CRO only (Figure 5.4a, left panel, red) is very slow with little to no adaptation, while adaption to CIP only (Figure 5.4a, right panel, blue) rapidly increases after day 2. The adaptation in condition 2 containing the drugs together (Figure 5.4a, middle-left panel, magenta) is faster then condition 3 (Figure 5.4a, middle-right panel, cyan), which shows no adaptation.

To further quantify these trends, as described in Chapter 2-4, we estimated the rate of growth adaptation by finding the slope of the line—for each population over the three days of adaptation (Figure 5.4b). Growth rate adaptation is significantly slower, on average, for CRO and CIP+CRO conditions (red and cyan) than for CIP and CRO+CIP conditions (blue and magenta) (student t-test, $p<0.001$ for all pair combinations between 2-drug and 1-drug conditions). These opposing trends indicate interplay due to resistance in the two drugs, which can only be further characterized by understanding collateral effects.

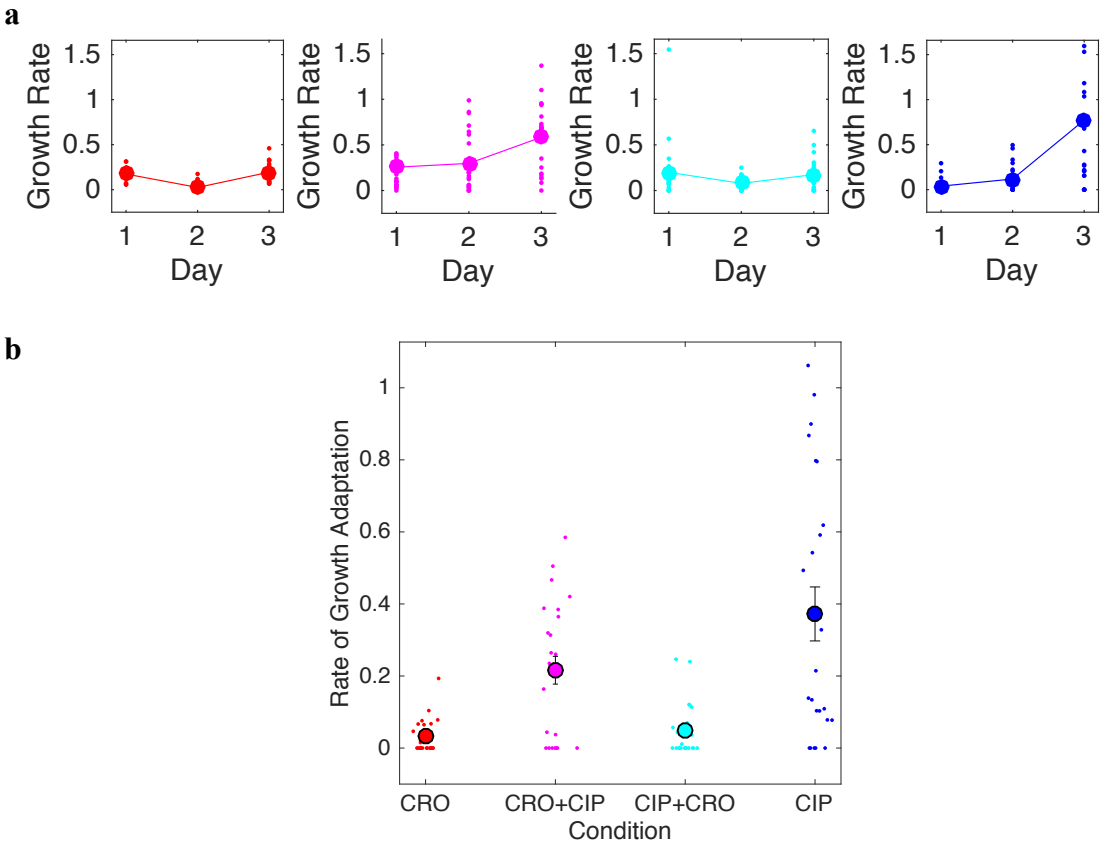

Figure 5.4: Additive Combinations of Ceftriaxone and Ciprofloxacin Leads to Variable Evolution of Resistance in *E. faecalis*. a. Adaptation time series (per capita growth rate) over 4 days of evolution, in each of the 4 conditions: condition 1 [CRO] = 2200ug/mL, and [CIP]=0 (red point in Figure 5.1), condition 2 [CRO] = 1400ug/mL, and [CIP]=0.296ug/mL (cyan point in Figure 5.1), condition 3 [CRO] = 600ug/mL, and [CIP]=0.395ug/mL (magenta point in Figure 5.1), and condition 4 [CRO] = 0, and [CIP]=0.593ug/mL (blue point in Figure 5.1). Small points represent individual mutants. Large circles are means taken across all mutants in a given condition (N=24 mutants). **b.** Growth adaptation rate for each condition; the units of adaptation are *growth rate/day*, where *growth rate* is measured in units such that the ancestral strains grow at a rate of 1 in the absence of drug. As an example, an adaptation rate of 0.25 means it takes, on average, 3 days of adaption for the strains to fully adapt to the drug (i.e. to reach the drug-free growth rate of ancestral cells). Small points correspond to individual mutants; large points represent the mean of all mutants in a given condition.

5.5 Single and Combination Drugs Exhibit Both Collateral Sensitivity and Cross-Resistance Effects

The trends observed in the growth rate adaptations across the four conditions indicate trade-offs between resistance levels to the two drugs that result in variable outcomes in combination. To investigate these dynamics, as in chapter 2-4 we selected 6 populations for each condition and directly measured the half-maximal inhibitory concentration (IC_{50}) of each drug. These results demonstrate that mutants evolved to CRO alone show low level resistance to both drugs (Figure 5.5a). Meanwhile, mutants evolved to CIP alone quickly become resistant to that drug (Figure 5.5a, bottom panel), but exhibit increased sensitivity to the second drug (Figure 5.5a, top panel).

Furthermore, evolution in condition 2 leads to little resistance to CRO (Figure 5.5a, top panel) but increased resistance to CIP (Figure 5.5a, bottom panel). On the other hand, evolution in condition 3 leads to sensitivity to CRO (Figure 5.5a, top panel), but resistance to CIP (Figure 5.5a, CIP panel). These results make the significant role of cross-resistance and collateral sensitivity evident and clarify our evolution where adaptation is faster in condition 2 and much slower in condition 3 (Figure 5.4b, magenta and cyan). In particular, due to weak cross-resistance shown by CRO, the strong collateral sensitivity exhibited by CIP to CRO is responsible for driving adaptation in the combination to be much slower.

There is also a clear spread of mutants across the different conditions that are between quadrant 2 and 3 signifying cross resistance and collateral sensitivity to ciprofloxacin and ceftriaxone (Figure 5.5b). Intriguingly, these results suggest that while populations adapted to ceftriaxone might have run out of solutions, in the presence of ciprofloxacin the adaptation to those mutants can be slowed to a halt.

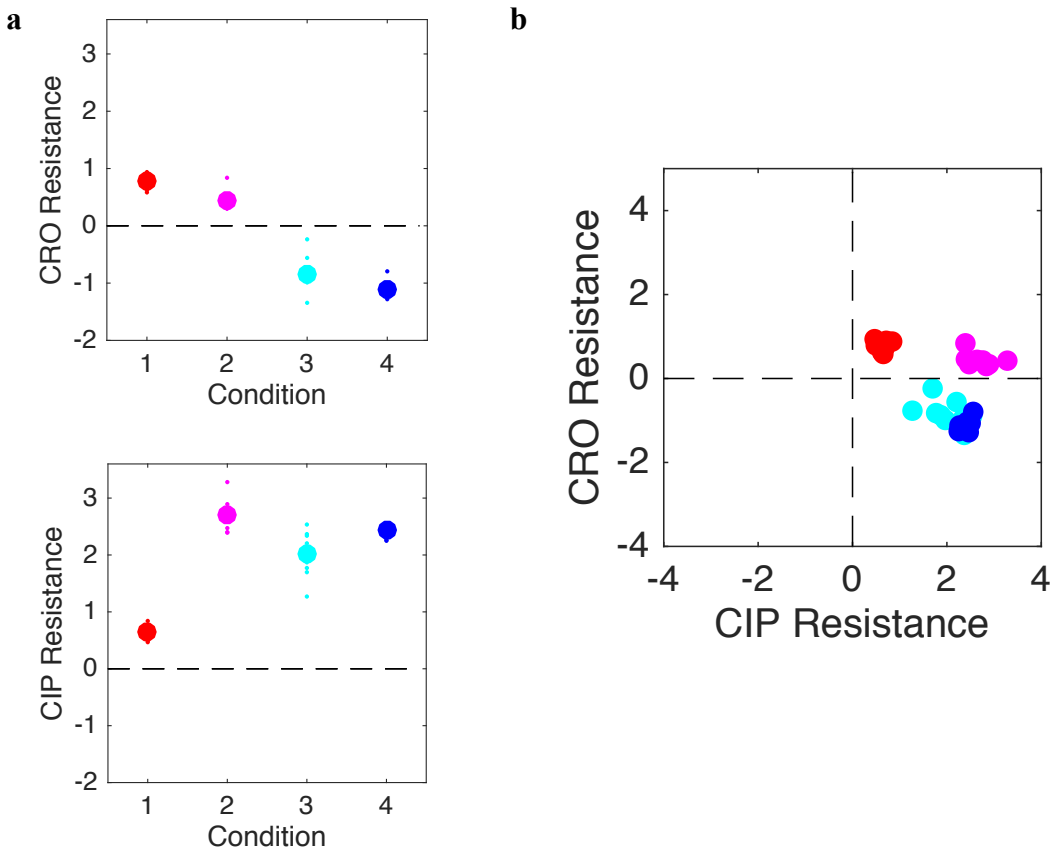

Figure 5.5: Single and Combination Drugs Exhibit Both Collateral Sensitivity and Cross-Resistance Effects a. Resistance to ceftriaxone (CRO, top panels) and ciprofloxacin (CIP, bottom panels) over time for populations evolved under 4 conditions: condition 1 [CRO] = 2200ug/mL, and [CIP]=0 (red point in Figure 5.1), condition 2 [CRO] = 1400ug/mL, and [CIP]=0.296ug/mL (cyan point in Figure 5.1), condition 3 [CRO] = 600ug/mL, and [CIP]=0.395ug/mL (magenta point in Figure 5.1), and condition 4 [CRO] = 0, and [CIP]=0.593ug/mL (blue point in Figure 5.1). Small points represent individual mutants. Resistance to each drug is defined as the log2 scaled ratio of IC50 values between mutant and wild-type (Ceft Mutant) cells, with positive values indicating increased resistance and negative values increased sensitivity. Small points correspond to individual mutants, while large points are the population mean across mutants (N=6 mutants). **b.** Two-dimensional representation of joint drug resistance after three days of the laboratory evolution. Each point corresponds to a single mutant.

5.6 Conclusion

To better understand the dynamics of drug combinations against mutants evolved at longer-timescales we chose to apply our experimental methods to a mutant with high-level ceftriaxone resistance (HLCER) after four days. Although the presences of these specific mutants in enterococci have not been identified in the clinic, they serve as an example for testing the power of combination therapy and understanding the phenotypic outcomes to be expected. An additive drug interaction was determined for HLER mutants grown in the combination of ceftriaxone and ciprofloxacin, which is a shift from ancestral interaction results being antagonistic. These results are consistent with previous studies that show drug interactions can change following the acquisition of resistance (Wood et al. 2014; C Munck et al. 2014) and they represent a notable limitation to the current approach. Specifically, the change in the drug interaction on longer timescales (in this case, roughly 30 generations) indicates that the growth response surface measured in ancestral cells can only be used for interpreting evolution on shorter timescales. Furthermore, because the interaction is essentially additive in the initial ceft-resistant strain, variation in adaptation rate is primarily attributable to collateral effects between the two drugs. Overall, these findings represent one example where drug interaction changes as evolution progresses, leading to evolutionary dynamics dominated by collateral effects.

Chapter 6: Suppressive Interaction – Ciprofloxacin plus Tigecycline

6.1 Introduction

Tigecycline is a new antibiotic and there are no reports of its resistance in *E. faecalis* (Miller, Munita, and Arias 2014). It has been used in clinic at low minimum inhibitory concentrations (MIC) against infections, which include *E. faecalis,* such as in skin structure infections and intra-abdominal infections. Combination therapy with tigecycline and daptomycin a DNA synthesis inhibitor, against vancomycin resistant enterococci (VRE) has proven to be an effective treatment strategy (Miller, Munita, and Arias 2014; Murray 2018). Thus, in this combination of ciprofloxacin, a DNA synthesis inhibitor, and tigecycline we are testing two classes of antibiotics with clinical relevance for treatment of *E. faecalis.* While the ciprofloxacin-tigecycline combination has not itself been applied in clinic, combinations between these drug classes have been used (O'Driscoll and Crank 2015).

In this chapter, we measure evolutionary adaptation to the ciprofloxacin-tigecycline alone and in combination using laboratory evolution experiments spanning several days. Our results reveal that resistance to ciprofloxacin inclines towards low-level collateral sensitivity passed a critical concentration of tigecycline with no collateral effects in tigecycline. More importantly, we find drastically slower growth adaption passed the same critical concentration of tigecycline with ciprofloxacin, highlighting a significant feature of suppressive interactions.

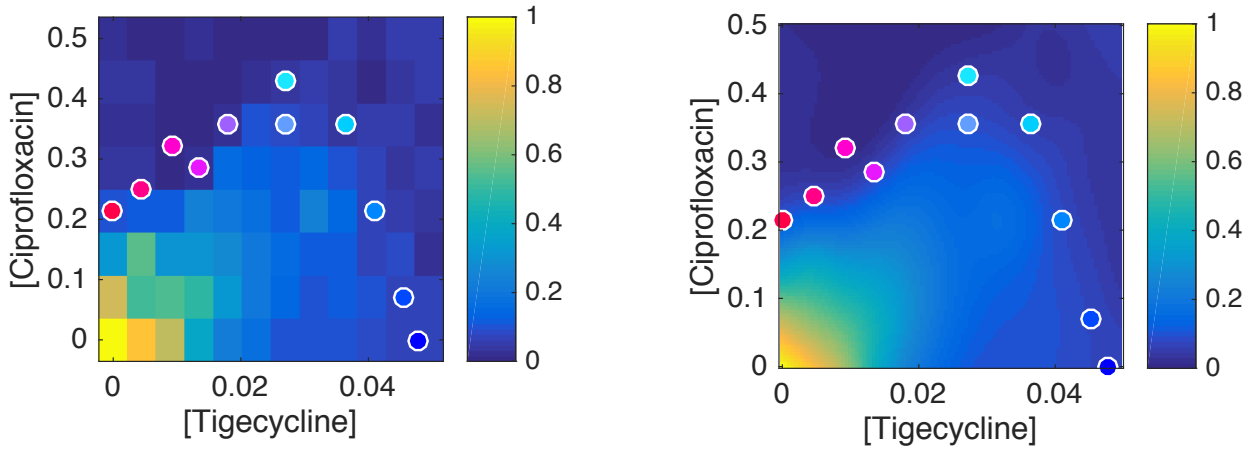

Figure 6.1: Ciprofloxacin and Tigecycline Combination Gives Rise to Suppressive Interaction in *E. faecalis*. a. Interaction with colors representing per capita growth rate as a function of two drug concentrations space. Eleven dots correspond to mutants selected with the same selective pressure at ~30% inhibition of growth with eleven different drug conditions. The first condition (in red) correspond to [CIP] = 0.214ug/mL, and [TIG]=0, the second condition (in light red) correspond to [CIP] = 0.071ug/mL, and [TIG]=0.045ug/mL, the third condition (rose) correspond to [CIP] = 0.321ug/mL, and [TIG]=0.009ug/mL, the fourth condition (in warm rose) correspond to [CIP] = 0.285ug/mL, and [TIG]=0.013ug/mL, fifth condition (purple) corresponds to [CIP]=0.357ug/mL and [TIG]=0.018ug/mL, sixth condition (in navy) corresponds to [CIP]=0.357ug/mL and [TIG]=0.027ug/mL, seventh condition (sky blue) corresponds to [CIP]=0.428ug/mL and [TIG]=0.027ug/mL, eight condition (light blue) corresponds to [CIP]=0.357ug/mL and [TIG]=0.036ug/mL, ninth condition (warm sky blue) corresponds to [CIP]=0.214ug/mL and [TIG]=0.041ug/mL, tenth condition (warm blue) corresponds to [CIP]=0.071ug/mL and [TIG]=0.045ug/mL, eleventh condition (blue) corresponds to [CIP]=0ug/mL and [TIG]=0.047ug/mL condition is evolved over 3 days with N=24 mutants per condition, in 96 well plates. Refer to table 6.1 for color references **b.** Smoothed version of interaction. Colors from blue to yellow represent growth rates. See methods for smoothing details.

6.2 Ciprofloxacin and Tigecycline Combination Gives Rise to Suppressive Interaction in *E. faecalis*.

To investigate evolution in ciprofloxacin-tigecycline combinations, we first measured the per capita growth rate of *E. faecalis* strain V583 in liquid cultures exposed to a large range of drug doses. We observed a strongly antagonistic (suppressive) interaction between the two drugs,

as indicated by the concave contours of the growth isoboles (Figure 6.1a; raw data; 6.1b smoothed data).

Condition	Cipro	Tige	
1	0.214	0	
2	0.25	0.0045	
3	0.321	0.009	
4	0.285	0.013	
5	0.357	0.018	
6	0.357	0.027	
7	0.428	0.027	
8	0.357	0.036	
9	0.214	0.041	
10	0.071	0.045	
11	0	0.047	

Table 6.1: Eleven conditions corresponding to particular concentrations of ciprofloxacin and tigecycline and their associated colors in Figure 6.1.

To understand why the combination is suppressive, consider what happens when TIG is added to cells initially exposed to 0.2 ug/mL of CIP (Figure 6.1a). In this regime, adding low concentrations of TIG—up to approximately 0.02ug/mL—will actually *increase* the population growth, despite the fact that CIP inhibits growth when administered on its own. This type of drug interaction, indicates that the joint effect of the combination is significantly lower than one would anticipate based on single drug effects. Stated simply, the addition of an otherwise inhibitory drug TIG can actually promote growth in the presence of high concentrations of CIP.

Next, we set out to measure the longer-term growth response to this drug pair. Evolution is expected to depend heavily on the level of growth inhibition in the initial cultures, which sets the selection pressure favoring resistant mutants. To control for initial inhibition, we chose eleven dosage combinations—two corresponding to single drug treatments and nine to drug

combinations—that lie along a contour where growth is approximately 30% of the native (drug free) growth (Figure 6.1). Because inhibition is constant across the four conditions, any differences between resistance adaptation should reflect drug concentration differences.

6.3 Mutants Evolve in the Presence of Ciprofloxacin and Tigecycline Combination

To perform the evolution, we evolved eight (8) replicate populations of *E. faecalis* at each of the eleven conditions for a total of 3 days. Similar to Chapter 2 we inoculated cells into media with each drug condition on Day 1, and each day following the populations were diluted into fresh media and drugs. After each inoculation, we measured the growth over time. In Figure 6.2 we illustrate growth curves for the first day (blue) and last day OD (red). Evidently, the growth of single drugs (red and blue) conditions were significantly increased by the last day of evolution, while growth in combinations seem to vary across the range of conditions.

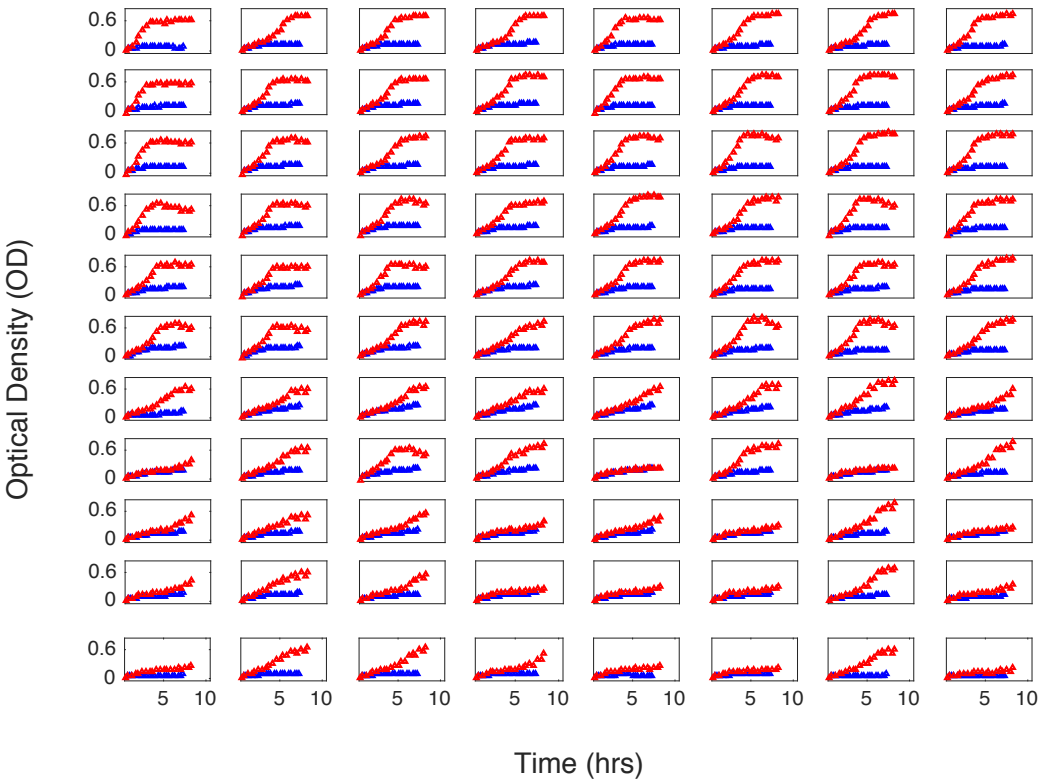

Figure 6.2: Growth Curves of Day 1 and Day 3 for All Mutants Indicate Resistance at a Glance. Optical density time series measured in liquid cultures of *E. faecalis* on the first (blue) and last (red) day of laboratory evolution. Plots are arranged in 11 groups of 8 corresponding to the 11 different conditions in Figure 6.1: row 1: [CIP] = 0.214ug/mL, and [TIG]=0, row 2: [CIP] = 0.071ug/mL, and [TIG]=0.045ug/mL, row 3: [CIP] = 0.321ug/mL, and [TIG]=0.009ug/mL, row 4: [CIP] = 0.285ug/mL, and [TIG]=0.013ug/mL, row 5: [CIP]=0.357ug/mL and [TIG]=0.018ug/mL, row 6: [CIP]=0.357ug/mL and [TIG]=0.027ug/mL, row 7: [CIP]=0.428ug/mL and [TIG]=0.027ug/mL, row 8: [CIP]=0.357ug/mL and [TIG]=0.036ug/mL, row 9: [CIP]=0.214ug/mL and [TIG]=0.041ug/mL, row 10: [CIP]=0.071ug/mL and [TIG]=0.045ug/mL, row 11: [CIP]=0ug/mL and [TIG]=0.047ug/mL condition is evolved over 3 days with N=8 mutants per condition, in 96 well plates. Refer to table 6.1 for color references.

6.4 Combination of Ciprofloxacin and Tigecycline Leads to Drastically Slower Rate of Growth Adaptation

Growth rate adaption was quantified just as in Chapter 2, by estimating the per capita growth rate for each OD times series using nonlinear least squares fitting to an exponential

function (see Methods). As predicted, in Figure 6.3 we can see that the growth of each population is inhibited the same on Day 1, this is in line with our choices of dosage conditions providing constant inhibition levels. Meanwhile, the growth rates are highly variable after Day 1, just as in previous growth rate curves (Chapters 2-5).

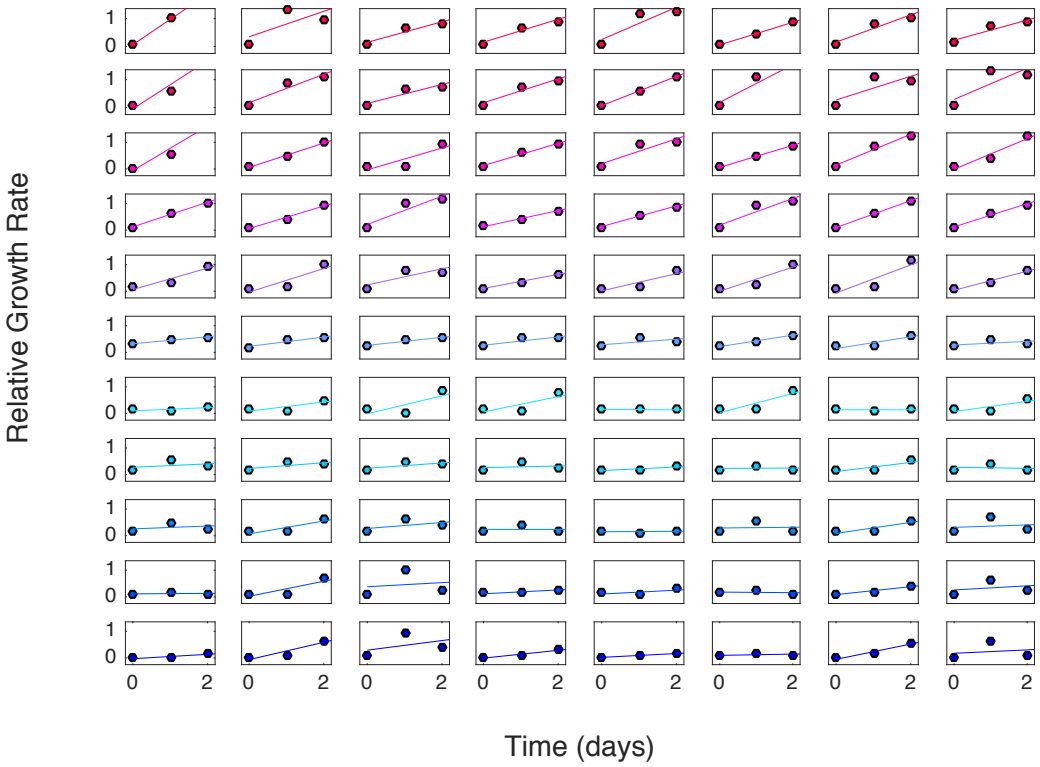

Figure 6.3: Growth Rate Adaptation Over 3 days of Evolution for All Mutants. Per capita growth rate of *E. faecalis* cultures over 4 consecutive days of laboratory evolution. row 1: [CIP] = 0.214ug/mL, and [TIG]=0, row 2: [CIP] = 0.071ug/mL, and [TIG]=0.045ug/mL, row 3: [CIP] = 0.321ug/mL, and [TIG]=0.009ug/mL, row 4: [CIP] = 0.285ug/mL, and [TIG]=0.013ug/mL, row 5: [CIP]=0.357ug/mL and [TIG]=0.018ug/mL, row 6: [CIP]=0.357ug/mL and [TIG]=0.027ug/mL, row 7: [CIP]=0.428ug/mL and [TIG]=0.027ug/mL, row 8: [CIP]=0.357ug/mL and [TIG]=0.036ug/mL, row 9: [CIP]=0.214ug/mL and [TIG]=0.041ug/mL, row 10: [CIP]=0.071ug/mL and [TIG]=0.045ug/mL, row 11: [CIP]=0ug/mL and [TIG]=0.047ug/mL condition is evolved over 3 days with N=8 mutants per condition, in 96 well plates. Adaptation rate for each mutant is given by the slope of the best-fit (least-squares) trend line through the relative growth rate time series. Refer to table 6.1 for color references.

The dynamics of the population were further analyzed by plotting the growth rate over time for each population (Figure 6.4a; small points) as well as the mean growth rate across all mutants in a given condition (Figure 6.4a; large points). First, consider the cases where the drugs are used alone. Adaptation to CIP only (to left panel, red) is initially rapid followed by gradual increase on days 2 and 3, while adaption to TIG (bottom right panel, blue) shows only minimal change in growth.

Interestingly, however, adaption to conditions containing two drugs slowly decreases to minimal growth, with day 2 decreasing first and then day 3 after, going through the spectrum of conditions from the first condition (CIP only, red) to the eleventh condition (TIG only, blue). To further quantify these trends, we estimated the rate of growth adaptation for each population (Figure 6.4b), as in previous chapters. On average, we notice a marked and sudden decrease in growth adaptation as a function of tigecycline concentration, with adaption being minimal after a critical concentration (0.02ug/mL-0.04ug/mL) of tigecycline (red and blue).

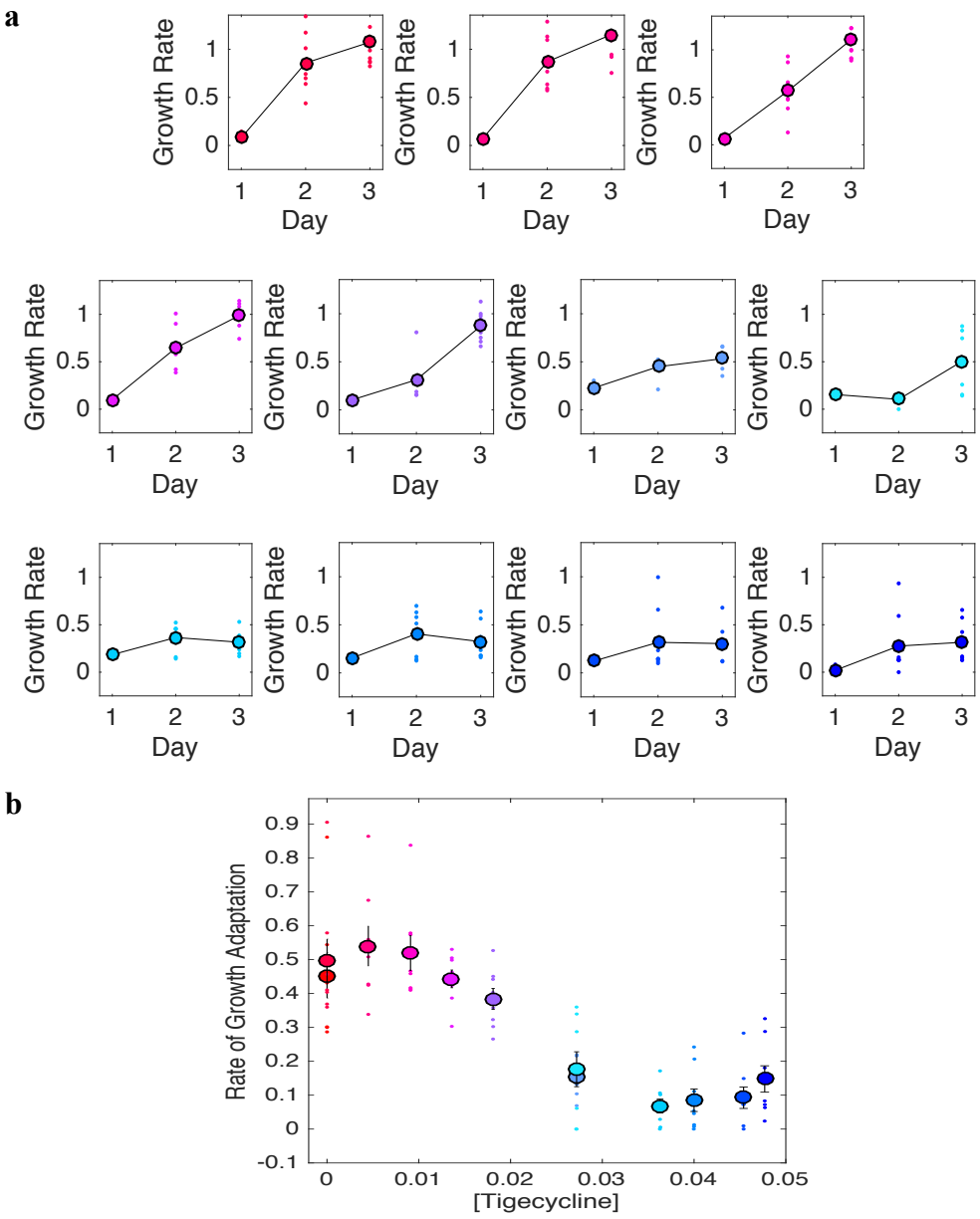

Figure 6.4: Combination of Ciprofloxacin and Tigecycline Leads to Drastically Slower Evolution of Resistance in *E. faecalis*. a. Adaptation time series (per capita growth rate) over 3 days of evolution, in each of the 11 conditions: condition 1: [CIP] = 0.214ug/mL, and [TIG]=0, condition 2: [CIP] = 0.071ug/mL, and [TIG]=0.045ug/mL, condition 3: [CIP] = 0.321ug/mL, and [TIG]=0.009ug/mL, condition 4: [CIP] = 0.285ug/mL, and [TIG]=0.013ug/mL, condition 5: [CIP]=0.357ug/mL and [TIG]=0.018ug/mL, condition 6: [CIP]=0.357ug/mL and [TIG]=0.027ug/mL, condition 7: [CIP]=0.428ug/mL and [TIG]=0.027ug/mL, condition 8: [CIP]=0.357ug/mL and [TIG]=0.036ug/mL, condition 9: [CIP]=0.214ug/mL and [TIG]=0.041ug/mL, condition 10: [CIP]=0.071ug/mL and [TIG]=0.045ug/mL, condition 11: [CIP]=0ug/mL and [TIG]=0.047ug/mL. Refer to table 6.1 for color references. **b.** Growth

adaptation rate for each condition; the units of adaptation are growth rate/day, where growth rate is measured in units such that the ancestral strains grow at a rate of 1 in the absence of drug. As an example, an adaptation rate of 0.25 means it takes, on average, 3 days of adaption for the strains to fully adapt to the drug (i.e. to reach the drug-free growth rate of ancestral cells). Small points correspond to individual mutants; large points represent the mean of all mutants in a given condition.

6.5 Resistance to Ciprofloxacin Tends Towards Low-Level Collateral Sensitivity at High Concentrations of Tigecycline With No Collateral Effects in Tigecycline

To understand these dynamics, we selected 6 populations for each condition and measured the half-maximal inhibitory concentration (IC_{50}) of each drug. Interestingly, these results indicate that as we step through the combination conditions, from low to high tigecycline, we notice a drastic shift down in ciprofloxacin resistance at a critical concentration (0.02ug/mL-0.04ug/mL) of tigecycline (Figure 6.5, left panel), while tigecycline resistance is essentially unchanged (Figure 6.5, right panel). In particular, it seems that resistance is mostly driven by drug interaction at lower concentrations of tigecycline but a shift at a critical concentration of tigecycline leads to low-level sensitivity. Thus, what occurs before and after the critical concentration (0.02ug/mL-0.04ug/mL) suggests a phenotypic change that completely alters ciprofloxacin resistance.

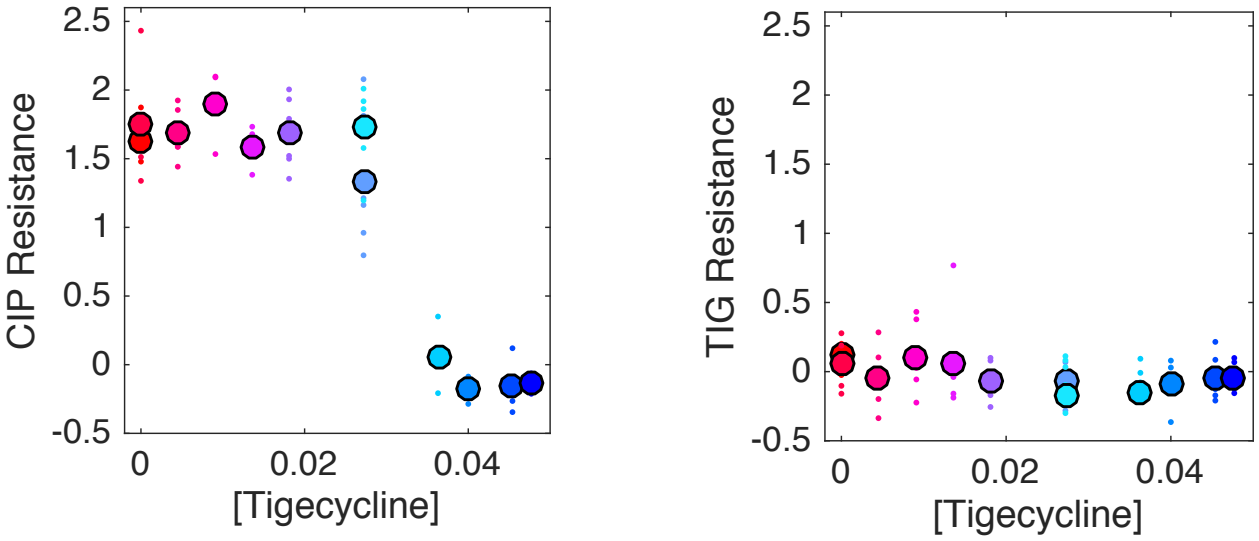

Figure 6.5: Resistance to Ciprofloxacin Tends Towards Low-Level Collateral Sensitivity at High Concentrations of Tigecycline With No Collateral Effects in Tigecycline. Resistance to ceftriaxone (CIP, left panel) and tigecycline (TIG, right panel) as a function of tigecycline concentration for populations evolved under 11 conditions: condition 1: [CIP] = 0.214ug/mL, and [TIG]=0, condition 2: [CIP] = 0.071ug/mL, and [TIG]=0.045ug/mL, condition 3: [CIP] = 0.321ug/mL, and [TIG]=0.009ug/mL, condition 4: [CIP] = 0.285ug/mL, and [TIG]=0.013ug/mL, condition 5: [CIP]=0.357ug/mL and [TIG]=0.018ug/mL, condition 6: [CIP]=0.357ug/mL and [TIG]=0.027ug/mL, condition 7: [CIP]=0.428ug/mL and [TIG]=0.027ug/mL, condition 8: [CIP]=0.357ug/mL and [TIG]=0.036ug/mL, condition 9: [CIP]=0.214ug/mL and [TIG]=0.041ug/mL, condition 10: [CIP]=0.071ug/mL and [TIG]=0.045ug/mL, condition 11: [CIP]=0ug/mL and [TIG]=0.047ug/mL. Refer to table 6.1 for color references.

The adaptation behavior can be understood by again considering the effects of rescaled drug concentrations on the two-drug growth surface. Figure 6.6 illustrates the expected growth effect at each condition due to a 3X reduction in CIP, similar to what is observed in populations selected by CIP only. The results indicate that growth drastically decreases as TIG concentration increases, becoming zero at the critical TIG concentration. Consistent with our experiments, this analysis shows that the growth benefit of CIP rescaling is eliminated at higher TIG concentrations, as the growth rate isoboles become almost vertical, minimizing any effect of CIP

rescaling. As a result, adding TIG to a CIP therapy can potentially stall resistance evolution, even when the concentration of CIP has not changed.

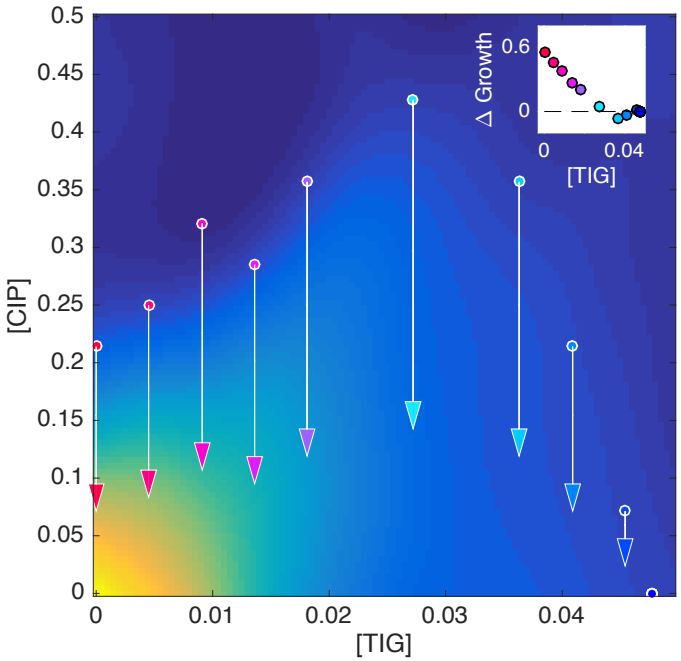

Figure 6.6: Rescaling CIP Results in Drastic Decline of Growth at Higher TIG. Isobole plot of TIG-CIP combination with arrows from red to blue which corresponding to the 3X rescaling of CIP concentration of each condition (colored dot) after evolution. Inset on the top right corner illustrates growth after rescaling of CIP as a function of increasing TIG concentration.

6.6 Conclusion

Although combination therapy with ciprofloxacin and tigecycline has not been shown directly in clinic, combinations with drugs from similar classes have been shown as a clinical option for treating *E. faecalis* infections. We find that TIG-CIP combinations are strongly suppressive, which conventional wisdom says would be sub-optimal to clinical use. However, our results reveal that growth adaption and ciprofloxacin resistance can be entirely eliminated by adding a sufficiently high concentration of tigecycline. This result is unexpected because it

suggests that suppressive interactions—which would typically be ignored in clinical therapies—can have a strong evolutionary advantage, similar to results in *E. coli* (R Chait, Craney, and Kishony 2007). In addition, our findings suggest that tigecycline may be an important component of combination therapies, not merely because resistance to tigecycline is rare, but also because its suppressive effects can potentially stall resistance to DNA synthesis inhibitors.

Chapter 7: Conclusion

In this work, we investigated the impact of drug interaction and collateral effects on evolutionary adaptation in multidrug resistant *E. faecalis*. *E. faecalis* is an opportunistic pathogen that contributes to multiple human infections, including endocarditis, bacteremia, urinary tract infections, and medical device infections. Numerous synergistic drug combinations for *E. faecalis* have been identified—and several are commonly used in clinical practice as the first-line of care. However, the evolution of resistance arising in these combinations is not well-understood, as the combined effects of drug interactions and collateral sensitivity can be difficult to disentangle. We therefore had two main goals: 1) to investigate clinically relevant drug combinations through high-throughput laboratory evolution, and 2) to provide a new case study that addresses an outstanding question in the field: whether collateral effects or drug interactions drive the rate of resistance adaptation. Our results indicate that both effects can play important roles, depending on the drug pair and the exact dosages. Furthermore, our work extends previous arguments based on geometric rescaling of drug concentrations to provide a simple template for predicting adaptation when both drug interactions and collateral effects are present.

Drug Combo	Drug Interaction	Adaptation Response	Collateral Response
CRO+AMP	Synergistic	2 drug adaptation > 1 drug	Cross-Resistance
AMP+STR	Antagonistic 1	2 drug adaptation < 1 drug	Drug alone: collateral sensitivity Drugs Together: weak cross-resistance
CRO+CIP	Antagonistic 2	2 drug adaptation < 1 drug	Drug alone: collateral sensitivity Drugs Together: cross-resistance
CRO+CIP	Additive	2 drug adaptation ~ 1 drug	Drug alone and together show cross-resistance and collateral sensitivity.
CIP+TIG	Suppressive	2 drug adaptation << 1 drug	Collateral effect from one adapted drug and no effect from second

Table 7.1: Summary of adaptation and collateral responses from all drug interactions examined in this study.

Our experiments quantified the rate of growth adaptation and drug resistance of *E. faecalis* exposed to clinically relevant drug combinations exhibiting four different classes of interactions, which included synergistic, additive, antagonistic and suppressive (Table 7.1). By keeping selective pressure constant at the onset of evolution among all of the tested drug interactions we were able to clearly identify the impact of drug concentrations on the evolution of resistance. We identified a wide range of evolutionary behavior, including both increased and decreased rates of adaptation, depending on the specific interplay between drug interaction and collateral drug sensitivity (Table 7.1).

To further understand the dynamics leading to these effects we generalized previous quantitative models based on drug concentration rescaling to account for collateral sensitivity between drugs. Our results stress trade-offs between drug interactions and collateral effects

during the evolution of multi-drug resistance and, more specifically, emphasize unrecognized evolutionary benefits of particular drug pairs in targeting aminoglycoside-resistant enterococcus. Most notably, our results demonstrate slowed growth adaptation in antagonistic combinations, with the strongest antagonistic (suppressive) combination leading to completely halted adaptation. Although higher concentrations of drugs may carry more risk in terms of potential exposure to drugs alone, faster adaptation to synergistic combinations as seen in these *in vitro* laboratory experiments are potentially as risky.

While we hope these studies will motivate continued work, both in vitro and in clinic, we would like to point out several limitations to our study. First, our goal was not to investigate the specific molecular mechanisms involved in drug adaption, but instead to provide a quantitative picture of resistance evolution that does not require extensive molecular-level knowledge, which many times is not available. However, the richness of the observed phenotypes points to complex and potentially interesting genetic changes that can be partially resolved with modern sequencing technologies. For example, cross-resistance observed between ceftriaxone and ampicillin could arise due to mutations leading to saturating production of penicillin-binding protein 5 (Pbp5), which is a common binding protein for both drugs and a known mechanism of resistance to ampicillin in enterococci, thus indicating a single mutation capable of resisting both drugs and leading to cross-resistance (Arbeloa et al. 2004; Kristich, Rice, and Arias 2014). We can also speculate that the collateral sensitivity seen between ceftriaxone and ciprofloxacin could be due to mutations which up regulate the production of multi-drug efflux pumps (MDRs), a known mechanism of resistance found in Enterococci against ciprofloxacin (Miller, Munita, and Arias 2014; Davis et al. 2001) , which could conceivably alter ceftriaxone resistance in counterintuitive ways. Perhaps most importantly, our results are based on in vitro laboratory experiments, which

provide a well-controlled but potentially artificial environment for evolutionary selection. While in vitro studies form the basis for many pharmacological regimens, the ultimate success or failure of new therapies must be evaluated using *in vivo* model systems and, ultimately, controlled clinical trials.

Our future work will hope to build on these results in several important ways. Firstly, computer automated bioreactors allow for the application of more complex—and perhaps clinically relevant—drug dosing schedules, which may more accurately capture evolutionary pressures driving drug resistance (Karslake et al. 2016; Toprak et al. 2013). By applying more evolutionarily informed strategies of drug combinations based on methods developed in this work, it might be possible to mimic realistic drug dosing schedules and determine optimal dosing of drug combinations. Secondly, it is well known that in physiological conditions, multiple bacterial species may coexist in a given habitat; it would be interesting to extend the current approach to include increasingly complex, multispecies bacterial communities. Thirdly, microbial growth often occurs not in planktonic populations, but instead in surface-associated biofilms, where spatial heterogeneity and complex community dynamics can dramatically alter the response to antibiotics. In *E. faecalis*, for example, sub-inhibitory doses of cell wall inhibitors may actually promote biofilm growth (Yu, Hallinen, and Wood 2018). Adaptation to combination therapies may also differ between biofilm and planktonic communities, and approaches similar to those used in this thesis may help unravel evolutionary impacts of drug interactions and collateral effects in this unique context (Stewart and William Costerton 2001). Finally, our results reveal that simple rescaling arguments—similar to those originally introduced in (Remy Chait, Craney, and Kishony 2007)—can be used to understand many features of evolution in two-drug environments. Extending and formalizing these qualitative findings using

mathematical models—where evolutionary dynamics on faster timescales correspond to drug rescaling in pairwise interaction landscapes, while the landscape itself changes on slower timescales—is an exciting avenue for future work that is likely to provide both general insight as well as specific, experimentally testable predictions for how resistance evolves in multi-drug environments.

Antibiotic resistance is a growing threat to public health, as modern medicine relies heavily on effective drugs for combatting bacterial infections. With more multi-drug resistance pathogens being discovered every day and the slow pace of discovery of new drugs to counter act pathogens, we are in the midst of a growing medical crisis, the impact of which was only recently recognized by the international community. Drug combinations are one potential approach to combat antibiotic resistance, but as this study demonstrates, evolution in multidrug environments is a complex process that will require continued investigation. Overall, our results represent a quantitative case study in the evolution of multidrug resistance in an opportunistic human pathogen, highlight both potential limitations and unappreciated evolutionary benefits of commonly used drug combinations, and provide a general framework for evaluating and predicting resistance evolution in multi-stress environments.

Chapter 8: Materials and Methods

8.1 Bacterial strains and media

In these studies, I used the *Enterococcus faecalis* V583 and OG1RF bacterial species. The V583 strain of *E. faecalis* was isolated from blood culture of patients from Barnes Hospital, St. Louis in 1987 whilst undergoing antimicrobial susceptibility profiling (Sahm et al. 1989). The OG1RF strain is a rifampicin and fusidic acid resistant derivative of OG1, which is human oral isolate (Gold, Jordan, and van Houte 1975; Oliver, Brown, and Clewell 1977; Dunny, Brown, and Clewell 1978). The V583 strain was used for all interaction and subsequent evolution experiments and the OG1RF strain was used initially for interaction experiments.

The *E. faecalis* bacteria was inoculated from a single colony grown in brain heart infusion (BHI) medium containing 1.5% (w/v) bacteriological agar. BHI media was prepared using Millipore water and sterilized with autoclaving at 121^0 C for 15 minutes. *E. faecalis* bacterial strains were grown overnight in the presence of BHI medium in a 37^0 C incubator with no shaking. Bacterial stocks were prepared for long term storage by mixing overnight cultures with sterilized 30% glycerol solution.

Antibiotics utilized in these studies (Table 8.1) were prepared using sterilized Millipore water, diluted and aliquoted into single use micro-centrifuge tubes and stored in either -20^0 C or -80^0 C for 3-6 months. All drugs and media were purchased from Dot Scientific, Sigma-Aldrich or Fisher Scientific unless indicated otherwise.

Antibiotic	Inhibition Mechanism	Abbreviation
Ampicillin	Cell wall synthesis	AMP
Ceftriaxone	Cell wall synthesis	CRO
Ciprofloxacin	DNA synthesis	CIP
Tigecycline	Ribosomal 30S subunit	TIG
Streptomycin	Ribosomal 30S subunit	STR

Table 8.1: List of antibiotics used in this thesis.

8.2 Measuring growth curves of *Enterococcus faecalis*

Overnight cultures of *E. faecalis* V583 bacteria were initially diluted 1:4 in fresh BHI medium and further diluted 1:100 in 96-well plates making a final 400x dilution. Dosage response curves were determined by introducing bacteria to 8 or 12-point increasing drug concentration gradient. Measurement of growth was accomplished by utilizing an EnSpire Multimode Plate Reader set to measure optical density (OD) at 600 nm wavelength (A_{600}) every 25 minutes for 12-14 hours at 30^0 C. Controls included measurement of drug-free wild-type cells and BHI medium as a blank.

From the time series of A_{600}, we determined growth rates by fitting the early exponential phase portion of curves ($0.01 < A_{600} < 0.1$) to an exponential function (MATLAB 7.6.0 curve fitting toolbox, Mathworks). We normalized growth rates in the presence of single drugs (gi) or multiple drugs (gij) by the growth rate of cells in the absence of drugs. An example growth curve is shown in Figure 8.1. Standard Error of the fitted growth parameter is used to estimate uncertainty in growth rates.

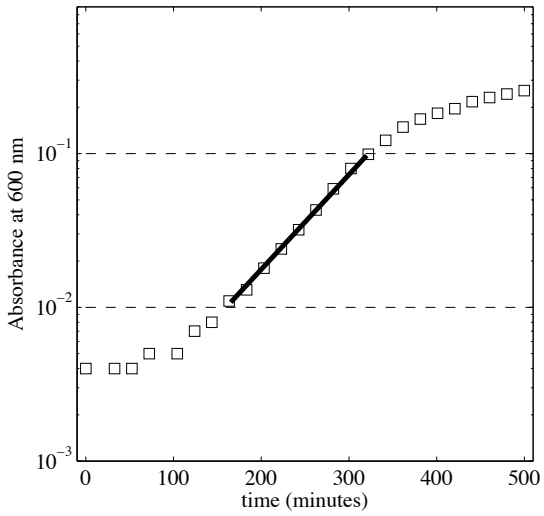

Figure 8.1: Growth Rate Measurement. Time series of OD (A_{600}) vs. time. Solid line is fitting to exponential function. Dashed lines show region of exponential growth. Growth rate is given by the slope of the line.

8.3 Selecting drug pairs to obtain complete interaction contour curvature

Drug interaction in *E. faecalis* has not been adequately studied before, thus we were required to obtain drug pairs in this model system that could serve to mimic the different drug interaction types (synergistic, antagonistic, additive and suppressive). Several combinations of drug pairs and corresponding drug ranges for each pair was tested in V583 and OG1RF strains to achieve complete interaction contour curvature. We began with a wide dynamic range of drug concentrations for each pair and decreased and further tuned the concentration levels to achieve complete curvature. Synergistic and suppressive combinations proved most difficult as the contour curvatures were either hidden in lower drug concentrations as in the case synergistic interactions or farther beyond the inhibition ranges of drug concentration as in the case of suppressive interactions. Drug interactions plots were smoothed using the cubic smoothing spline

function built into MATLab. In the end, we were able to obtain all of the different interaction types in the V583 strain with the following pairs:

	Drug Pair	Interaction Type
1	Ampicillin and Ceftriaxone	Synergistic
2	Ceftriaxone and Ciprofloxacin	Additive/Antagonistic
3	Ampicillin and Streptomycin	Antagonistic
4	Ciprofloxacin and Tigecycline	Suppressive

Table 8.2: List of drug pairs and corresponding interactions found in *E. faecalis* V583 cells.

8.4 *Enterococcus faecalis* evolution assay

To perform evolution with a constant selection pressure 96-well plates were prepared with drug concentrations pre-determined based on drug interaction results. Accordingly, single and combination drugs were added to BHI media in 96-well plates. Based on the number of days of evolution with 1 plate per day, 3-4 plates were prepared and frozen in -20^0 C. The overnight culture of *E. faecalis* V583 was diluted 1:4 initially. After thawing 96-well evolution plates, 2μL of culture was inoculated into 200μL of solution (Drug and BHI) in each well, resulting in 400x diluted culture in the presence of drug. Plate tops were sealed with BIO-RAD Microseal 'A' film to minimize evaporation and prevent cross contamination. The plates were then taken to the EnSpire Multimode Plate Reader to measure growth over 18-24 hours at 30^0 C as discussed above. At the end of Day 1, the day's plate was diluted 1:100 into the next day (Day 2) and grown again in the same way.

Day 1 plates were stored by add 30% sterilized glycerol and freezing in -20^0 C/-80^0 C. This process was repeated for the rest of the 3-4 days of evolution until all growth measurements were completed. Growth data was transferred out of the EnSpire module for further analysis. Growth rate is determined by fitting growth data into a simple exponential function and calculating its slope. Growth adaptation rate for each condition over 3-4 days of evolution is

determined by finding the slope of the best-fit trend line through the relative growth rate time series. All experiments were performed inside a ThermoFisher 1300 Series A2 safety cabinet to achieve ample sterile conditions.

8.5 Measuring IC_{50} of *Enterococcus faecalis* mutants

In order to determine resistance and sensitivity of mutants to each drug, experiments were performed to estimate the IC_{50} of each drug by inoculating mutants into a drug gradient of 8-points of increasing drug concentration (Figure 8.2). Initially, 96-well plates were prepared with set drug concentrations diluted with BHI medium consisting of a total volume of 200 µL per well. Selected mutants were grown from a frozen stock by swabbing and inserting into 1mL BHI medium and grown overnight at 37^0 C. After inoculation mutants were grown in 37^0 C for 20 hours and taken to the EnSpire Multimodal Plate Reader for final optical density (OD) measurement at 600nm.

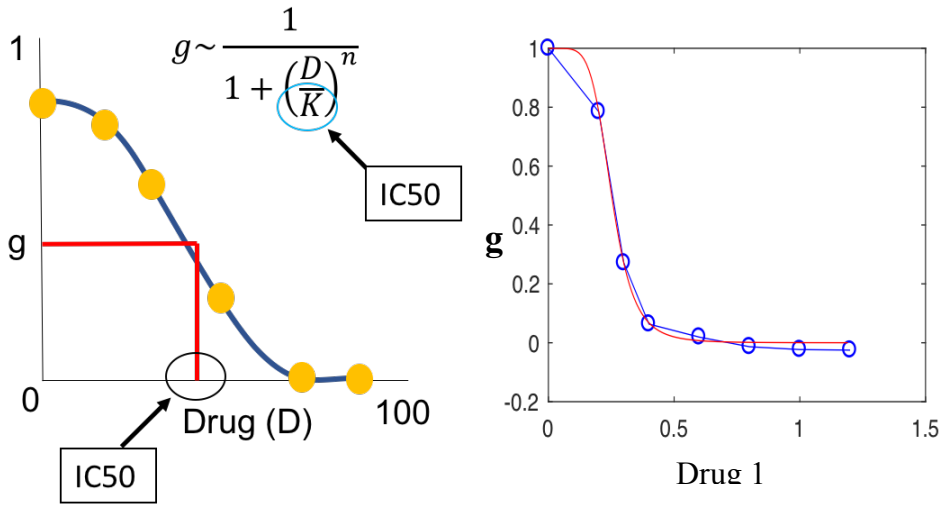

Figure 8.2: IC_{50} Measurement. Cartoon depiction of a normal dosage response curve obtained to characterize mutant resistance to each drug. The curve is fit to a hill function, where K is the concentration of drug at which 50% growth inhibition is obtained (IC50). The average IC50 of three replicates for each mutant provided its resistance to each drug (left panel). Example fitted growth curve from actual data of WT cells (right panel).

OD measurements of *E. faecalis* mutants in the presence of drug were normalized to wild-type drug-free *E. faecalis* V583 cells. The dosage response curve of each mutant to each drug was fit to a Hill function $f(x) = (1/1 + (x/K)^h)$ using nonlinear least squares fitting, where *K* is the half-maximal inhibitory concentration (IC_{50}) and *h* is a Hill-coefficient defining the steepness of the dose-response. To determine resistance and sensitivity we define ε as log_2 of mutant IC_{50} normalized by the IC_{50} of wild-type drug free cells, wherein ε greater than zero indicated increased resistance and ε less than zero indicated increased sensitivity to one drug.

$$\varepsilon = log_2\left(\frac{IC_{50}(Mut)}{IC_{50}(WT)}\right)$$

Bibliography

Aarestrup, F M, P Butaye, and W Witte. 2002. “Nonhuman Reservoirs of Enterococci.” *Enterococci: Pathogenesis, Molecular Biology, and Antibiotic Resistance*, 55–99.

Abraham, E. P., E. Chain, C. M. Fletcher, A. D. Gardner, N. G. Heatley, M. A. Jennings, and H. W. Florey. 1941. “FURTHER OBSERVATIONS ON PENICILLIN.” *The Lancet*. https://doi.org/10.1016/S0140-6736(00)72122-2.

Arbeloa, Ana, Heidi Segal, Jean-Emmanuel Hugonnet, Nathalie Josseaume, Lionnel Dubost, Jean-Paul Brouard, Laurent Gutmann, Dominique Mengin-Lecreulx, and Michel Arthur. 2004. “Role of Class A Penicillin-Binding Proteins in PBP5-Mediated Beta-Lactam Resistance in Enterococcus Faecalis.” *Journal of Bacteriology*. https://doi.org/10.1128/JB.186.5.1221.

Arsène, Stéphanie, and Roland Leclercq. 2007. “Role of a Qnr-like, Gene in the Intrinsic Resistance of Enterococcus Faecalis to Fluoroquinolones.” *Antimicrobial Agents and Chemotherapy*. https://doi.org/10.1128/AAC.00274-07.

Aslangul, Elisabeth, Laurent Massias, Alain Meulemans, Françoise Chau, Antoine Andremont, Patrice Courvalin, Bruno Fantin, and Raymond Ruimy. 2006. “Acquired Gentamicin Resistance by Permeability Impairment in Enterococcus Faecalis.” *Antimicrobial Agents and Chemotherapy*. https://doi.org/10.1128/AAC.00390-06.

Barbosa, Camilo, Robert Beardmore, Hinrich Schulenburg, and Gunther Jansen. 2018. “Antibiotic Combination Efficacy (ACE) Networks for a Pseudomonas Aeruginosa Model.” *PLoS Biology*. https://doi.org/10.1371/journal.pbio.2004356.

Barbosa, Camilo, Vincent Trebosc, Christian Kemmer, Philip Rosenstiel, Robert Beardmore, Hinrich Schulenburg, and Gunther Jansen. 2017. “Alternative Evolutionary Paths to Bacterial Antibiotic Resistance Cause Distinct Collateral Effects.” *Molecular Biology and Evolution*. https://doi.org/10.1093/molbev/msx158.

Baym, M, L K Stone, and R Kishony. 2016. “Multidrug Evolutionary Strategies to Reverse Antibiotic Resistance.” *Science* 351 (6268): aad3292. https://doi.org/10.1126/science.aad3292aad3292 [pii]351/6268/aad3292 [pii].

Baym, Michael, Laura K. Stone, and Roy Kishony. 2016. “Multidrug Evolutionary Strategies to Reverse Antibiotic Resistance.” *Science*. https://doi.org/10.1126/science.aad3292.

Becker's Clinical Leadership & Infection Control. 2016. "CDC's 7 Public Health Threats in Focus for 2017." 2016. https://www.beckershospitalreview.com/quality/cdc-s-7-public-health-threats-in-focus-for-2017.html.

Berlanga, M, and M Viñas. 2000. "Salicylate Induction of Phenotypic Resistance to Quinolones in Serratia Marcescens." *The Journal of Antimicrobial Chemotherapy*.

Blair, Jessica M.A., Mark A. Webber, Alison J. Baylay, David O. Ogbolu, and Laura J.V. Piddock. 2011. "Molecular Mechanisms of Antibiotic Resistance." *Nature Reviews Microbiology*. https://doi.org/10.1039/c0cc05111j.

Boucher, H. W., G. H. Talbot, D. K. Benjamin, J. Bradley, R. J. Guidos, R. N. Jones, B. E. Murray, R. A. Bonomo, and D. Gilbert. 2013. "10 x '20 Progress--Development of New Drugs Active Against Gram-Negative Bacilli: An Update From the Infectious Diseases Society of America." *Clinical Infectious Diseases*. https://doi.org/10.1093/cid/cit152.

Bozic, Ivana, Johannes G. Reiter, Benjamin Allen, Tibor Antal, Krishnendu Chatterjee, Preya Shah, Yo Sup Moon, et al. 2013. "Evolutionary Dynamics of Cancer in Response to Targeted Combination Therapy." *ELife*. https://doi.org/10.7554/eLife.00747.

Bush, Karen, Patrice Courvalin, Gautam Dantas, Julian Davies, Barry Eisenstein, Pentti Huovinen, George A. Jacoby, et al. 2011. "Tackling Antibiotic Resistance." *Nature Reviews Microbiology*. https://doi.org/10.1038/nrmicro2693.

CDC. 2013. "Antibiotic Resistance Threats in the United States, 2013." *Current*. https://doi.org/CS239559-B.

Chait, R, A Craney, and R Kishony. 2007. "Antibiotic Interactions That Select against Resistance." *Nature* 446 (7136): 668–71. https://doi.org/10.1038/nature05685.

Chait, Remy, Allison Craney, and Roy Kishony. 2007. "Antibiotic Interactions That Select against Resistance." *Nature*. https://doi.org/10.1038/nature05685.

Chernish, Robert N., and Shawn D. Aaron. 2003. "Approach to Resistant Gram-Negative Bacterial Pulmonary Infections in Patients with Cystic Fibrosis." *Current Opinion in Pulmonary Medicine*. https://doi.org/10.1097/00063198-200311000-00011.

Cohen, S. P., S. B. Levy, J. Foulds, and J. L. Rosner. 1993. "Salicylate Induction of Antibiotic Resistance in Escherichia Coli: Activation of the Mar Operon and a Mar-Independent Pathway." *Journal of Bacteriology*. https://doi.org/10.1128/jb.175.24.7856-7862.1993.

Cooper, Matthew A., and David Shlaes. 2011. "Fix the Antibiotics Pipeline." *Nature*. https://doi.org/10.1038/472032a.

Davies, Julian, and Dorothy Davies. 2010. "Origins and Evolution of Antibiotic Resistance." *Microbiology and Molecular Biology Reviews* 74 (3): 417–33. https://doi.org/10.1128/MMBR.00016-10.

Davis, D R, J B McAlpine, C J Pazoles, M K Talbot, E a Alder, C White, B M Jonas, B E Murray, G M Weinstock, and B L Rogers. 2001. "Enterococcus Faecalis Multi-Drug Resistance Transporters: Application for Antibiotic Discovery." *Journal of Molecular Microbiology and Biotechnology*.

Demain, Arnold L, and Sergio Sanchez. 2009. "Microbial Drug Discovery: 80 Years of Progress." *The Journal of Antibiotics*. https://doi.org/10.1038/ja.2008.16.

Dhawan, Andrew, Daniel Nichol, Fumi Kinose, Mohamed E. Abazeed, Andriy Marusyk, Eric B. Haura, and Jacob G. Scott. 2017. "Collateral Sensitivity Networks Reveal Evolutionary Instability and Novel Treatment Strategies in ALK Mutated Non-Small Cell Lung Cancer." *Scientific Reports*. https://doi.org/10.1038/s41598-017-00791-8.

Donadio, Stefano, Sonia Maffioli, Paolo Monciardini, Margherita Sosio, and Daniela Jabes. 2010. "Antibiotic Discovery in the Twenty-First Century: Current Trends and Future Perspectives." *The Journal of Antibiotics*. https://doi.org/10.1038/ja.2010.62.

Dragosits, Martin, Vadim Mozhayskiy, Semarhy Quinones-Soto, Jiyeon Park, and Ilias Tagkopoulos. 2013. "Evolutionary Potential, Cross-Stress Behavior and the Genetic Basis of Acquired Stress Resistance in Escherichia Coli." *Molecular Systems Biology*. https://doi.org/10.1038/msb.2012.76.

Dunny, G M, B L Brown, and D B Clewell. 1978. "Induced Cell Aggregation and Mating in Streptococcus Faecalis: Evidence for a Bacterial Sex Pheromone." *Proceedings of the National Academy of Sciences of the United States of America*. https://doi.org/10.1073/pnas.75.7.3479.

Fernández-Hidalgo, Nuria, Benito Almirante, Joan Gavaldà, Mercè Gurgui, Carmen Peña, Arístides De Alarcón, Josefa Ruiz, et al. 2013. "Ampicillin plus Ceftriaxone Is as Effective as Ampicillin plus Gentamicin for Treating Enterococcus Faecalis Infective Endocarditis." *Clinical Infectious Diseases*. https://doi.org/10.1093/cid/cit052.

Fontana, R., M. Aldegheri, M. Ligozzi, H. Lopez, A. Sucari, and G. Satta. 1994. "Overproduction of a Low-Affinity Penicillin-Binding Protein and High-Level Ampicillin Resistance in Enterococcus Faecium." *Antimicrobial Agents and Chemotherapy*. https://doi.org/10.1128/AAC.38.9.1980.

Gavaldà, Joan, Oscar Len, José M. Miró, Patricia Muñoz, Miguel Montejo, Aristides Alarcón, Julián De La Torre-Cisneros, et al. 2007. "Brief Communication: Treatment of Enterococcus Faecalis Endocarditis with Ampicillin plus Ceftriaxone." *Annals of Internal Medicine*. https://doi.org/10.7326/0003-4819-146-8-200704170-00008.

Gavaldà, Joan, Pedro López Onrubia, María Teresa Martín Gómez, Xavier Gomis, José Luis Ramírez, Oscar Len, Dolors Rodríguez, Manuel Crespo, Isabel Ruíz, and Albert Pahissa. 2003. "Efficacy of Ampicillin Combined with Ceftriaxone and Gentamicin in the Treatment of Experimental Endocarditis Due to Enterococcus Faecalis with No High-Level Resistance to Aminoglycosides." *Journal of Antimicrobial Chemotherapy*. https://doi.org/10.1093/jac/dkg360.

Gilmore, Michael S, Don B Clewell, Yasuyoshi Ike, and Nathan Shankar. 2014. "Enterococci: From Commensals to Leading Causes of Drug Resistant Infection." *Enterococci: From Commensals to Leading Causes of Drug Resistant Infection*.

Giraffa, Giorgio. 2002. "Enterococci from Foods." *FEMS Microbiology Reviews*. https://doi.org/10.1016/S0168-6445(02)00094-3.

Golan, David E., Armen H. Tashjan, Ehrin J. Armstrong, and April W. Armstrong. 2012. "Principles of Pharmacology. The Pathophysiologic Basis of Drug Therapy." *Pediatric Clinics of North America*. https://doi.org/10.1016/j.pcl.2010.10.005.

Gold, Olga G., H. V. Jordan, and J. van Houte. 1975. "The Prevalence of Enterococci in the Human Mouth and Their Pathogenicity in Animal Models." *Archives of Oral Biology*. https://doi.org/10.1016/0003-9969(75)90236-8.

Greco, W R, G Bravo, and J C Parsons. 1995. "The Search for Synergy: A Critical Review from a Response Surface Perspective." *Pharmacological Reviews*.

Gupta, Ravindra K, Michael R Jordan, Binta J Sultan, Andrew Hill, Daniel H J Davis, John Gregson, Anthony W Sawyer, et al. 2012. "Global Trends in Antiretroviral Resistance in Treatment-Naive Individuals with HIV after Rollout of Antiretroviral Treatment in Resource-Limited Settings: A Global Collaborative Study and Meta-Regression Analysis." *Lancet*. https://doi.org/10.1016/S0140-6736(12)61038-1.

Hammerum, A. M. 2012. "Enterococci of Animal Origin and Their Significance for Public Health." *Clinical Microbiology and Infection*. https://doi.org/10.1111/j.1469-0691.2012.03829.x.

Hede, Karyn. 2014. "Antibiotic Resistance: An Infectious Arms Race." *Nature*. https://doi.org/10.1038/509S2a.

Hegreness, M, N Shoresh, D Damian, D Hartl, and R Kishony. 2008. "Accelerated Evolution of Resistance in Multidrug Environments." *Proceedings of the National Academy of Sciences of the United States of America* 105 (37): 13977–81. https://doi.org/10.1073/pnas.0805965105.

Holohan, Caitriona, Sandra Van Schaeybroeck, Daniel B. Longley, and Patrick G. Johnston. 2013. "Cancer Drug Resistance: An Evolving Paradigm." *Nature Reviews Cancer*. https://doi.org/10.1038/nrc3599.

Huycke, Mark M., Daniel F. Sahm, and Michael S. Gilmore. 1998. "Multiple-Drug Resistant Enterococci: The Nature of the Problem and an Agenda for the Future." *Emerging Infectious Diseases*. https://doi.org/10.3201/eid0402.980211.

Imamovic, Lejla, Mostafa Mostafa Hashim Ellabaan, Ana Manuel Dantas Machado, Linda Citterio, Tune Wulff, Soren Molin, Helle Krogh Johansen, and Morten Otto Alexander Sommer. 2018. "Drug-Driven Phenotypic Convergence Supports Rational Treatment Strategies of Chronic Infections." *Cell*. https://doi.org/10.1016/j.cell.2017.12.012.

Imamovic, Lejla, and Morten O.A. Sommer. 2013. “Use of Collateral Sensitivity Networks to Design Drug Cycling Protocols That Avoid Resistance Development.” *Science Translational Medicine*. https://doi.org/10.1126/scitranslmed.3006609.

Kak, V., S. M. Donabedian, M. J. Zervos, R. Kariyama, H. Kumon, and J. W. Chow. 2000. “Efficacy of Ampicillin plus Arbekacin in Experimental Rabbit Endocarditis Caused by an Enterococcus Faecalis Strain with High-Level Gentamicin Resistance.” *Antimicrobial Agents and Chemotherapy*. https://doi.org/10.1128/AAC.44.9.2545-2546.2000.

Kak, V, and J W Chow. 2002. “Acquired Antibiotic Resistances in Enterococci.” *Enterococci: Pathogenesis, Molecular Biology, and Antibiotic Resistance*, 355–83.

Karslake, Jason, Jeff Maltas, Peter Brumm, and Kevin B. Wood. 2016. “Population Density Modulates Drug Inhibition and Gives Rise to Potential Bistability of Treatment Outcomes for Bacterial Infections.” *PLoS Computational Biology*. https://doi.org/10.1371/journal.pcbi.1005098.

Keith, Curtis T., Alexis A. Borisy, and Brent R. Stockwell. 2005. “Multicomponent Therapeutics for Networked Systems.” *Nature Reviews Drug Discovery*. https://doi.org/10.1038/nrd1609.

Kim, S, T D Lieberman, and R Kishony. 2014. “Alternating Antibiotic Treatments Constrain Evolutionary Paths to Multidrug Resistance.” *Proc Natl Acad Sci U S A* 111 (40): 14494–99. https://doi.org/10.1073/pnas.14098001111409800111 [pii].

Kim, Seungsoo, Tami D. Lieberman, and Roy Kishony. 2014. “Alternating Antibiotic Treatments Constrain Evolutionary Paths to Multidrug Resistance.” *Proceedings of the National Academy of Sciences*. https://doi.org/10.1073/pnas.1409800111.

Kristich, Christopher J., Loius B. Rice, and Cesar A. Arias. 2014. “Enterococcal Infection—Treatment and Antibiotic Resistance.” *Enterococci: From Commensals to Leading Causes of Drug Resistant Infection*.

Landau, Ralph, Basil Achilladelis, Alexandre Scriabine, and Eds. 1999. *Pharmaceutical Innovation: Revolutionizing Human Health.* Philadelphia, Pa, USA: Chemical Heritage Press.

Laxminarayan, Ramanan. 2014. “Antibiotic Effectiveness: Balancing Conservation against Innovation.” *Science*. https://doi.org/10.1126/science.1254163.

Lázár, Viktória, István Nagy, Réka Spohn, Bálint Csörgo ’, Ádám Györkei, Ákos Nyerges, Balázs Horváth, et al. 2014. “Genome-Wide Analysis Captures the Determinants of the Antibiotic Cross-Resistance Interaction Network.” *Nature Communications*. https://doi.org/10.1038/ncomms5352.

Lázár, Viktória, Gajinder Pal Singh, Réka Spohn, István Nagy, Balázs Horváth, Mónika Hrtyan, Róbert Busa-Fekete, et al. 2013. “Bacterial Evolution of Antibiotic Hypersensitivity.” *Molecular Systems Biology*. https://doi.org/10.1038/msb.2013.57.

Lewis, Kim. 2013. “Platforms for Antibiotic Discovery.” *Nature Reviews Drug Discovery*. https://doi.org/10.1038/nrd3975.

LOEWE, S. 1953. “The Problem of Synergism and Antagonism of Combined Drugs.” *Arzneimittel-Forschung*. https://doi.org/10.1016/j.bbcan.2009.11.002.

Maccallum, W G, and T W Hastings. 1899. “A CASE OF ACUTE ENDOCARDITIS CAUSED BY MICROCOCCUS ZYMOGENES (NOV. SPEC.), WITH A DESCRIPTION OF THE MICROORGANISM.” *The Journal of Experimental Medicine*. https://doi.org/10.1084/jem.4.5-6.521.

Malani, P N, C A Kauffman, and M J Zervos. 2002. “Enterococcal Disease, Epidemiology, and Treatment.” *Enterococci: Pathogenesis, Molecular Biology, and Antibiotic Resistance*, 385–408.

McClure, Nathan S, and Troy Day. 2014. “A Theoretical Examination of the Relative Importance of Evolution Management and Drug Development for Managing Resistance.” *Proceedings. Biological Sciences / The Royal Society*. https://doi.org/10.1098/rspb.2014.1861.

Michel, J.-B., P. J. Yeh, R. Chait, R. C. Moellering, and R. Kishony. 2008. “Drug Interactions Modulate the Potential for Evolution of Resistance.” *Proceedings of the National Academy of Sciences*. https://doi.org/10.1073/pnas.0800944105.

Miller, William R., Jose M. Munita, and Cesar A. Arias. 2014. “Mechanisms of Antibiotic Resistance in Enterococci.” *Expert Review of Anti-Infective Therapy*. https://doi.org/10.1586/14787210.2014.956092.

Moreno-Gamez, Stefany, Alison L. Hill, Daniel I. S. Rosenbloom, Dmitri A. Petrov, Martin A. Nowak, and Pleuni S. Pennings. 2015. “Imperfect Drug Penetration Leads to Spatial Monotherapy and Rapid Evolution of Multidrug Resistance.” *Proceedings of the National Academy of Sciences*. https://doi.org/10.1073/pnas.1424184112.

Munck, C, H K Gumpert, A I Wallin, H H Wang, and M O Sommer. 2014. “Prediction of Resistance Development against Drug Combinations by Collateral Responses to Component Drugs.” *Sci Transl Med* 6 (262): 262ra156. https://doi.org/10.1126/scitranslmed.30099406/262/262ra156 [pii].

Munck, Christian, Heidi K. Gumpert, Annika I.Nilsson Wallin, Harris H. Wang, and Morten O.A. Sommer. 2014. “Prediction of Resistance Development against Drug Combinations by Collateral Responses to Component Drugs.” *Science Translational Medicine*. https://doi.org/10.1126/scitranslmed.3009940.

Mundt, J O. 1963. “Occurrence of Enterococci on Plants in a Wild Environment.” *Applied Microbiology*.

Murray, Barbara E. 2018. “Treatment of Enterococcal Infections.” UpToDate Inc. 2018. https://www.uptodate.com/contents/treatment-of-enterococcal-infections.

Neu, Harold C. 1992. “The Crisis in Antibiotic Resistance.” *Science*. https://doi.org/10.1126/science.257.5073.1064.

Nichol, Daniel, Joseph Rutter, Christopher Bryant, Peter Jeavons, Alexander Anderson, Robert Bonomo, and Jacob Scott. 2017. “Collateral Sensitivity Is Contingent on the Repeatability of Evolution.” *BioRxiv*. https://doi.org/10.1101/185892.

O’Driscoll, Tristan, and Christopher W. Crank. 2015. “Vancomycin-Resistant Enterococcal Infections: Epidemiology, Clinical Manifestations, and Optimal Management.” *Infection and Drug Resistance*. https://doi.org/10.2147/IDR.S54125.

Oliver, D. R., B. L. Brown, and D. B. Clewell. 1977. “Analysis of Plasmid Deoxyribonucleic Acid in a Cariogenic Strain of Streptococcus Faecalis: An Approach to Identifying Genetic Determinants on Cryptic Plasmids.” *Journal of Bacteriology*.

Oz, Tugce, Aysegul Guvenek, Sadik Yildiz, Enes Karaboga, Yusuf Talha Tamer, Nirva Mumcuyan, Vedat Burak Ozan, et al. 2014. “Strength of Selection Pressure Is an Important Parameter Contributing to the Complexity of Antibiotic Resistance Evolution.” *Molecular Biology and Evolution*. https://doi.org/10.1093/molbev/msu191.

Palmer, A C, and R Kishony. 2014. “Opposing Effects of Target Overexpression Reveal Drug Mechanisms.” *Nat Commun* 5: 4296. https://doi.org/10.1038/ncomms5296ncomms5296 [pii].

Palmer, Adam C., and Roy Kishony. 2013. “Understanding, Predicting and Manipulating the Genotypic Evolution of Antibiotic Resistance.” *Nature Reviews Genetics*. https://doi.org/10.1038/nrg3351.

Pawlotsky, Jean Michel. 2011. “Treatment Failure and Resistance with Direct-Acting Antiviral Drugs against Hepatitis C Virus.” *Hepatology*. https://doi.org/10.1002/hep.24262.

Pericas, J. M., C. Cervera, A. del Rio, A. Moreno, C. Garcia de la Maria, X. Castañeda, Y. Armero, et al. 2014. “Changes in the Treatment of Enterococcus Faecalis Infective Endocarditis in Spain in the Last 15 Years: From Ampicillin plus Gentamicin to Ampicillin plus Ceftriaxone.” *Clinical Microbiology and Infection*. https://doi.org/10.1111/1469-0691.12756.

Pillai S. K., Moellering R. C., Jr., Eliopoulos G. M. 2005. “Antimicrobial Combinations.” In *Antibiotics in Laboratory Medicine.*, edited by Lorian V., 5th Editio, 365–440. Philadelphia, Pa, USA: Lippincott Williams and Wilkins.

Prabaker, Kavitha, and Robert A. Weinstein. 2011. “Trends in Antimicrobial Resistance in Intensive Care Units in the United States.” *Current Opinion in Critical Care*. https://doi.org/10.1097/MCC.0b013e32834a4b03.

Rodriguez De Evgrafov, Mari, Heidi Gumpert, Christian Munck, Thomas T. Thomsen, and Morten O.A. Sommer. 2015. “Collateral Resistance and Sensitivity Modulate Evolution of High-Level Resistance to Drug Combination Treatment in Staphylococcus Aureus.”

Molecular Biology and Evolution. https://doi.org/10.1093/molbev/msv006.

Sahm, D. F., J. Kissinger, M. S. Gilmore, P. R. Murray, R. Mulder, J. Solliday, and B. Clarke. 1989. "In Vitro Susceptibility Studies of Vancomycin-Resistant Enterococcus Faecalis." *Antimicrobial Agents and Chemotherapy*. https://doi.org/10.1128/AAC.33.9.1588.

Sanders, C C, W E Sanders, R V Goering, and V Werner. 1984. "Selection of Multiple Antibiotic Resistance by Quinolones, Beta-Lactams, and Aminoglycosides with Special Reference to Cross-Resistance between Unrelated Drug Classes." *Antimicrobial Agents and Chemotherapy*. https://doi.org/10.1128/AAC.26.6.797.

Sghir, Abdelghani, Genevieve Gramet, Antonia Suau, Violaine Rochet, Philippe Pochart, and Joel Dore. 2000. "Quantification of Bacterial Groups within Human Fecal Flora by Oligonucleotide Probe Hybridization." *Applied and Environmental Microbiology*. https://doi.org/10.1128/AEM.66.5.2263-2266.2000.

Stewart, Philip S. 2002. "Mechanisms of Antibiotic Resistance in Bacterial Biofilms." *International Journal of Medical Microbiology*. https://doi.org/10.1078/1438-4221-00196.

Stewart, Philip S, and J William Costerton. 2001. "Antibiotic Resistance of Bacteria in Biofilms." *The Lancet*. https://doi.org/10.1016/S0140-6736(01)05321-1.

SZYBALSKI, W., and V. BRYSON. 1952. "Genetic Studies on Microbial Cross Resistance to Toxic Agents. I. Cross Resistance of Escherichia Coli to Fifteen Antibiotics." *Journal of Bacteriology*.

Tana, Michele M., Ghany, Marc G. 2013. "Hepatitis B Virus Treatment: Management of Antiviral Drug Resistance." *Clinical Liver Disease*. https://doi.org/http://dx.doi.org/10.1002/cld.162.

Toprak, Erdal, Adrian Veres, Sadik Yildiz, Juan M. Pedraza, Remy Chait, Johan Paulsson, and Roy Kishony. 2013. "Building a Morbidostat: An Automated Continuous-Culture Device for Studying Bacterial Drug Resistance under Dynamically Sustained Drug Inhibition." *Nature Protocols*. https://doi.org/10.1038/nprot.2013.021.

Tripodi, M. F., A. Locatelli, L. E. Adinolfi, A. Andreana, and R. Utili. 1998. "Successful Treatment with Ampicillin and Fluoroquinolones of Human Endocarditis Due to High-Level Gentamicin-Resistant Enterococci." *European Journal of Clinical Microbiology and Infectious Diseases*. https://doi.org/10.1007/s100960050171.

Ubeda, Carles, Ying Taur, Robert R. Jenq, Michele J. Equinda, Tammy Son, Miriam Samstein, Agnes Viale, et al. 2010. "Vancomycin-Resistant Enterococcus Domination of Intestinal Microbiota Is Enabled by Antibiotic Treatment in Mice and Precedes Bloodstream Invasion in Humans." *Journal of Clinical Investigation*. https://doi.org/10.1172/JCI43918.

Werner, G., T. M. Coque, A. M. Hammerum, R. Hope, W. Hryniewicz, A. Johnson, I. Klare, et al. 2008. "Emergence and Spread of Vancomycin Resistance among Enterococci in Europe." *Euro Surveillance : Bulletin Europ??En Sur Les Maladies Transmissibles =*

European Communicable Disease Bulletin. https://doi.org/19046 [pii].

WHO. 2014a. "Antimicrobial Resistance. Global Report on Surveillance." *World Health Organization*, 2014. https://doi.org/10.1007/s13312-014-0374-3.

———. 2014b. "Global Tuberculosis Report 2014." *WHO Report*. https://doi.org/10.1155/2014/187842.

Wood, K B, K C Wood, S Nishida, and P Cluzel. 2014. "Uncovering Scaling Laws to Infer Multidrug Response of Resistant Microbes and Cancer Cells." *Cell Rep* 6 (6): 1073–84. https://doi.org/10.1016/j.celrep.2014.02.007S2211-1247(14)00086-2 [pii].

World Health Organisation. 2013. "Consolidated Guidelines on the Use of Antiretroviral Drugs for Treating and Preventing HIV Infection: Recommendations for a Public Health Approach." *WHO Guidelines*. https://doi.org/978 92 4 150572 7.

World Health Organization (WHO). 2015. "Guidelines for the Treatment of Malaria Third Edition." *Transactions of the Royal Society of Tropical Medicine and Hygiene*. https://doi.org/10.1016/0035-9203(91)90261-V.

Wright, Gerard D. 2011. "Molecular Mechanisms of Antibiotic Resistance." *Chemical Communications (Cambridge, England)*. https://doi.org/10.1039/c0cc05111j.

Yeh, Pamela J, Matthew J Hegreness, Aviva Presser Aiden, and Roy Kishony. 2009. "Drug Interactions and the Evolution of Antibiotic Resistance." *Nature Reviews Microbiology* 7 (June): 460. http://dx.doi.org/10.1038/nrmicro2133.

Yeh, Pamela, Ariane I. Tschumi, and Roy Kishony. 2006. "Functional Classification of Drugs by Properties of Their Pairwise Interactions." *Nature Genetics*. https://doi.org/10.1038/ng1755.

Yu, Wen, Kelsey M. Hallinen, and Kevin B. Wood. 2018. "Interplay between Antibiotic Efficacy and Drug-Induced Lysis Underlies Enhanced Biofilm Formation at Subinhibitory Drug Concentrations." *Antimicrobial Agents and Chemotherapy*. https://doi.org/10.1128/AAC.01603-17.

Zumla, Alimuddin, Ibrahim Abubakar, Mario Raviglione, Michael Hoelscher, Lucica Ditiu, Timothy D. McHugh, S. Bertel Squire, et al. 2012. "Drug-Resistant Tuberculosis-Current Dilemmas, Unanswered Questions, Challenges, and Priority Needs." *Journal of Infectious Diseases*. https://doi.org/10.1093/infdis/jir858.